# 9 PŘÍLOHY

I. Vladimíra Hanková, **Eva Slováková**, Jiří Zedník, Jiří Vohlídal, Radoslava Sivková, Hynek Balcar, Arnošt Zukal, Jiří Brus, Jan Sedláček: Polyacetylene-Type Networks Prepared by Coordination Polymerization of Diethynylarenes: New Type of Microporous Organic Polymers, Macromol. Rapid Commun. **2012**, 33, 158 - 163.

II. **Eva Slováková**, Arnošt Zukal, Jiří Brus, Hynek Balcar, Libor Brabec, Dmitrij Bondarev a Jan Sedláček: Transition-Metal-Catalyzed Chain-Growth Polymerization of 1,4-Diethynylbenzene into Microporous Crosslinked Poly(phenylacetylene)s: the Effect of Reaction Conditions, *Macromol. Chem. Phys.* **2014**, *215*, 1855 - 1869.

III. **Eva Slováková**, Marjan Ješelnik, Ema Žagar, Jiří Zedník, Jan Sedláček, Sebastijan Kovačič: Chain-Growth Insertion Polymerization of 1,3-Diethynylbenzene High Internal Phase Emulsions into Reactive π-Conjugated Foams, *Macromolecules*, **2014**, *47*, 4864 - 4869.

IV. Arnošt Zukal, **Eva Slováková**, Hynek Balcar, Jan Sedláček: Polycyclotrimers of 1,4-Diethynylbenzene, 2,6-Diethynylnaphthalene, and 2,6-Diethynylanthracene: Preparation and Gas Adsorption Properties, *Macromol. Chem. Phys.* **2013**, *214*, 2016 - 2026.

I.

Polyacetylene-Type Networks Prepared by Coordination Polymerization of Diethynylarenes: New Type of Microporous Organic Polymers

Vladimíra Hanková, Eva Slováková, Jiří Zedník, Jiří Vohlídal,
Radoslava Sivkova, Hynek Balcar, Arnošt Zukal, Jiří Brus, Jan Sedláček*

Microporous organic polymers (MOP) of a new type have been synthesised in high yields by a simple coordination polymerization of 1,3-diethynylbenzene, 1,4-diethynylbenzene and 4,4′-diethynylbiphenyl catalysed by [Rh(cod)acac] and [Rh(nbd)acac] complexes. The new MOPs are non-swellable polyacetylene-type conjugated networks consisting of ethynylaryl-substituted polyene main chains that are crosslinked by arylene linkers. Prepared MOP samples have a mole fraction of branching units (by ^{13}C CP/MAS NMR) from 0.30 to 0.47 and exhibit the BET (Brunaer-Emmett-Teller) surface up to 809 m^2 g^{-1} and hydrogen uptake up to 0.69 wt% (77 K, H_2 pressure 750 torr).

S_{BET} up to 809 m^2/g
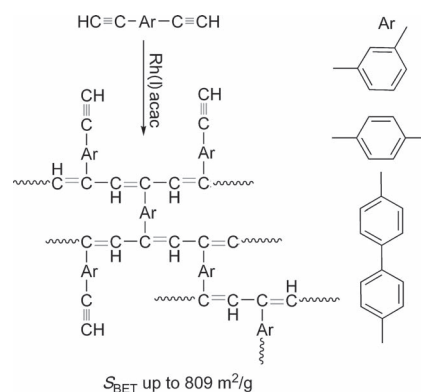
1. Introduction

Crosslinked microporous organic polymers (MOP) are intensively studied as materials with potential applications particularly in gas adsorption and storage.[1–12] Examples of MOPs of this type include hyper-crosslinked poly(styrene-co-divinylbenzene),[8,9] polyanilines,[13] polypyrroles,[14] poly(arylenevinylene)[15] and networks of aromatic rings.[11,16–18] Another types of crosslinked MOPs have been prepared from acetylene-type monomers.[19] Starting materials were either a mixture of di- and tri-ethynylarenes or a mixture of these ethynylarenes with (di- or tri-) iodo- or bromoarenes (average functionality of monomers, $f > 2$). MOPs of the poly(arylenebutadiynylene)[20] and poly(aryleneethynylene)[21–23] type were prepared from these mixtures via the Pd-catalysed homo- and cross-coupling. The specific surface area, $S_{BET} \approx 1000$ m^2 g^{-1} was mostly reported for these networks. An exceptionally high value ($S_{BET} = 1917$ m^2 g^{-1}) was reported by Holst et al.[24] for networks based on monomers with $f = 4$ containing an sp^3 central carbon [tetrakis(4-ethynylphenyl)methane and tetrakis(4-iodophenyl)methane]. Cooper et al.[2] studied poly(aryleneethynylene) networks in terms of their hydrogen storage capacity and revealed the hydrogen uptake up to 1.14 wt% (1.13 bar, 77 K).

An alternative path of transformation of ethynylarenes of higher functionality into MOPs might consist in coordination polymerization of these monomers catalysed by transition metal catalysts via methods known from preparation of linear poly(monosubstituted acetylene)s.[25,26] For example, coordination polymerization of a non-vicinal

V. Hanková, E. Slováková, Dr. J. Zedník, Prof. J. Vohlídal,
R. Sivkova, Prof. J. Sedláček
Department of Physical and Macromolecular Chemistry,
Faculty of Science, Charles University in Prague,
Hlavova 2030, CZ-128 40 Prague 2, Czech Republic
E-mail: jansedl@natur.cuni.cz
Dr. H. Balcar, Dr. A. Zukal
J. Heyrovský Institute of Physical Chemistry, v.v.i, Academy
of Sciences of the Czech Republic, Dolejškova
3, 182 23 Prague 8, Czech Republic
Dr. J. Brus
Institute of Macromolecular Chemistry, v.v.i., Academy
of Sciences of the Czech Republic, Heyrovský
Sq. 2, 16206 Prague 6, Czech Republic

diethynylbenzene may be assumed to yield a crosslinked polyacetylene-type poly(diethynylbenzene) that might represent an unsaturated analogue of poly(divinylbenzene). If a high extent of crosslinking is achieved, the microporous character of crosslinked polyacetylene-type polymers (contributed by a partly rigid character of the polyene main chains) seems to be promising. To the best of our knowledge, no report is available in the literature on this type of polymerization leading to MOP products. The polymerization of 1,4-diethynylbenzene described by Yang and co-workers was optimised for formation of soluble linear or partly branched poly[(4-ethynylphenyl)acetylene]s,[27] which were further studied as stimuli-responsive materials.[28] Russo and co-workers[29] described oxidative and catalytic polymerization of 4,4′-diethynylbiphenyl into insoluble polymers. However, the products porosity and adsorption properties have not been studied.

In this contribution, we report the first results on Rh-catalysed coordination polymerizations of non-vicinal diethynylarenes yielding networks that may be denoted as polyacetylene-type MOPs. The efficiency of newly prepared networks in hydrogen adsorption is discussed as well.

2. Experimental Section

2.1. Materials

Trimethylsilylacetylene, 4,4′-dibromobiphenyl, acetylacetonato-(cycloocta-1,5-diene)rhodium(I) [Rh(cod)acac], acetylacetonato-(norborna-2,5-diene)rhodium(I),[Rh(nbd)acac],bis(triphenylphosphine) palladium(II) dichloride [(PdCl$_2$(PPh$_3$)$_2$)], triphenylphosphine (PPh$_3$) and Cu$_2$I$_2$ (all by Sigma-Aldrich) were used as obtained. 1,3-Diethynylbenzene (1,3-DEB) and 1,4-diethynylbenzene (1,4-DEB) (both Sigma-Aldrich) were purified by vacuum distillation (1,3-DEB) and vacuum sublimation (1,4-DEB). Dichloromethane (Lachema, Czech Republic) was distilled from P$_2$O$_5$. 4,4′-Diethynylbiphenyl (4,4′-DEBPh) was prepared by Sonogashira coupling from trimethylsilylacetylene and 4,4′-dibromobiphenyl catalysed by [PdCl$_2$(PPh$_3$)$_2$]/Cu$_2$I$_2$/PPh$_3$ followed by deprotection of 4,4′-bis(trimethylsilylethynyl)biphenyl intermediate by tetrabutylammonium fluoride. The crude product was twice crystallized from *n*-hexane. ^{1}H and ^{13}C NMR spectral characteristics of prepared 4,4′-DEBPh were in agreement with literature.[21]

2.2. Techniques

For size exclusion chromatography (SEC) two devices were used: (i) Agilent Technologies 1100 Series apparatus with refractive index (RI) detector that provided apparent molecular-weight characteristics based on columns calibration with polystyrene (PS) standards. (ii) SEC/MALS apparatus equipped with Wyatt multi-angle light-scattering detector DAWN EOS and RI detector that provided absolute molecular-weight characteristics. Two PL-gel columns (Mixed B and Mixed C) and tetrahydrofuran (THF) as a mobile phase were used with both SEC devices.

All ^{13}C CP/MAS NMR spectra were measured at 11.7 T using a Bruker Avance 500 WB/US NMR spectrometer in a double-resonance 4-mm probehead at spinning frequency 12 kHz. The length of 90° (^{1}H) pulse was 2.5 μs, strength of spin-locking field B_1(^{1}H,[13]C) expressed in frequency units $\omega_1/2\pi = \gamma B_1$ was 64 kHz, the recycle delay was 6 s and cross-polarization contact time was 3 ms to reach quantitative results. During the acquisition of NMR signals heteronuclear TPPM (two-pulse phase-modulated) decoupling at $\omega_1/2\pi$ = 89.3 kHz was applied. Active cooling was used to compensate frictional heating of rotating samples.[30]

DR UV/vis spectra of polymers were recorded using a Perkin-Elmer Lambda 950 spectrometer.

Adsorption isotherms of nitrogen and hydrogen at 77 K were determined using an ASAP 2020 (Micromeritics) volumetric instrument equipped with three pressure transducers covering 133 Pa, 1.33 kPa and 133 kPa ranges. Polymer samples were outgassed as follows: Starting from room temperature the polymer was outgassed at 353 K (heating ramp of 0.5 K min⁻1) until the residual pressure of 1 Pa. After 1 h delay at 353 K, the temperature was further increased (heating ramp of 1 K min⁻1) up to 383 K. The sample was outgassed at this temperature under turbomolecular pump vacuum for 6 h. The BET surface area, S_{BET}, was determined by means of nitrogen adsorption data in relative pressure range from 0.05 to 0.25. The BET transform plots (see Supporting information, Figure S1) was linear in this pressure range, which includes the limits suggested previously.[31] for analysis of nitrogen adsorption on microporous polymers. The micropore volume V_{MI} was determined according to a previous report.[32].
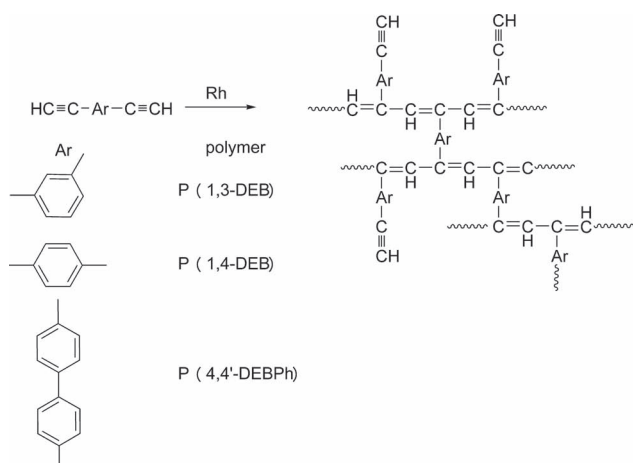
2.3. Polymerizations

All polymerizations were carried out in CH$_2$Cl$_2$ at room temperature. The initial concentrations were as follows: [Monomer]$_0$ = 0.6 mol L⁻¹, [Catalyst]$_0$ = 0.006 mol L⁻¹. All polymerizations proceeded as precipitation reactions. After 180 min, the reaction suspension was poured into the excess of CH$_2$Cl$_2$ and the solid polymer was washed by decantation in CH$_2$Cl$_2$ and then in methanol. Finally, the product was separated by filtration, dried in vacuo and the yield was determined gravimetrically.

3. Results and Discussion

3.1. Synthesis and Spectroscopic Characterization of Polymers

Mononuclear Rh(I) complexes, [Rh(nbd)acac] and [Rh(cod)acac] were used as polymerization catalysts. These catalysts (without a cocatalyst) are known to polymerize efficiently acetylenic monomers with one-terminal triple bond into linear high molecular-weight poly(monosubstituted acetylene)s.[33–36] Using these catalysts, three diethynylarenes (1,3-DEB, 1,4-DEB, 4,4′-DEBPh), that is, monomers with two equal terminal triple bonds, were polymerized in our study (see Scheme 1). The following list summarises the prepared polymers and their codes: (i) poly(1,3-diethynylbenzene) and poly(1,4-diethynylbenzene) prepared with [Rh(cod)acac] catalyst, codes: P(1,3-DEB)$_C$ and P(1,4-DEB)$_C$, respectively, (ii) poly(1,3-diethynylbenzene), poly(1,4-diethynylbenzene) and poly(4,4′-diethynylbiphenyl) prepared with

Materials
Views

www.MaterialsViews.com

Macromol. Rapid Commun. **2012**, *33*, 158–163

© 2012 WILEY-VCH Verlag GmbH & Co. KGaA, Weinheim

Macromolecular
Journals

159

Scheme 1. Synthesis of polyacetylene-type MOPs.

[Rh(nbd)acac] catalyst, codes: P(1,3-DEB)$_N$, P(1,4-DEB)$_N$ and P(4,4′-DEBPh)$_N$, respectively.

In all polymerizations, the slightly yellow solution of catalyst turned red after addition of a colourless monomer solution that indicated monomer transformation into conjugated polyacetylene-type polymer. Later (2–5 min), the onset of precipitation of a red-brown polymer was observed by naked eye. As the reaction continued the amount of voluminous polymer precipitate was increasing. In the case of P(1,4-DEB)$_N$ synthesis, we succeeded in SEC analysis of the soluble polymer before its precipitation. A withdrawn sample of the reaction mixture (reaction time 2–3 min) was immediately diluted with THF (1/100, V/V) and analysed by (i) SEC/MALS and (ii) SEC device using PS calibration of columns. Analyses provided following values of weight-average molecular weight, $\overline{M}_W$: an absolute value, $\overline{M}_W(\text{MALS}) = 3.1 \times 10^6$ and an apparent value, $\overline{M}_W(\text{PScal}) = 2.1 \times 10^5$. The relation $\overline{M}_W(\text{MALS}) \gg \overline{M}_W(\text{PScal})$ indicates that the analysed P(1,4-DEB)$_N$ was (even at the onset of its formation) highly branched or partly crosslinked. The product precipitation observed during the polymerization of all diethynylarenes thus evidently reflects the crosslinking of the polymers formed.
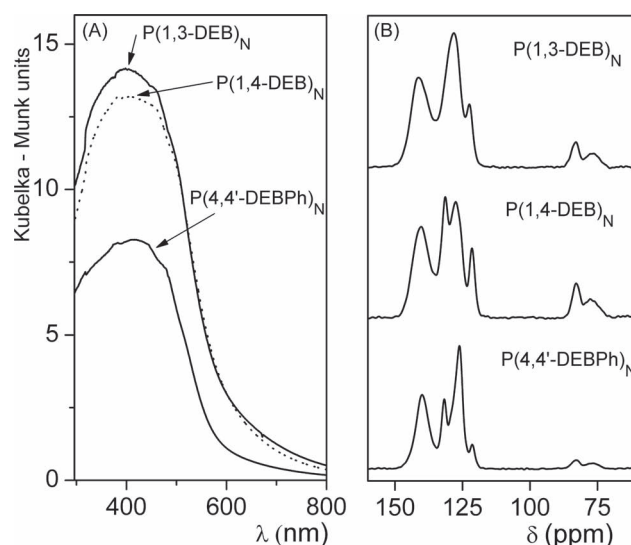

Figure 1. DR UV/vis spectra (panel A) and ^{13}C CP/MAS NMR spectra (panel B) of polymers prepared with [Rh(nbd)acac].

The isolated yields of polymers were from 80% to 90% (see Table 1). All polymers prepared were brown-red brittle solids insoluble and non-swellable in tested solvents (THF, CH_2Cl_2, $CHCl_3$ and benzene). Figure 1 shows the DR UV/vis spectra of polymers prepared with [Rh(nbd)acac]. Very similar DR UV/vis spectra resulted for polymers prepared with [Rh(cod)acac]. Spectra of all polymers showed a broad absorption band with maximum in the region from 370 to 420 nm and a low-energy absorption edge from 590 to 640 nm. We ascribed this band to π–π^* transition of partly conjugated main polymer chains according to the assignment of UV/vis bands of linear (substituted) polyacetylenes.[37,38] ^{13}C CP/MAS NMR spectra of all poly(diethynylarene)s contained (i) a broad, partly resolved signal in the region 115–150 ppm that corresponds to the resonance of aromatic carbons and carbons of the polymer main chains[39] and (ii) signals at about $\delta = 83$ and 76 ppm that correspond to carbons of non-transformed pendant ethynyls. Spectra of polymers prepared with [Rh(nbd)acac] are shown in Figure 1, the same pattern of spectra resulted for polymers prepared with [Rh(cod)acac]. The polymers prepared can be assumed

Table 1. Yield (*Y*), degree of branching (*DB*) (by ^{13}C CP/MAS NMR) and adsorption characteristics of poly(diethynylarene) networks. S_{BET} is the specific surface area obtained from the N_2 adsorption isotherm using BET approach, V_{MI} is the micropore volume, $a_{H2,750torr}$ is the volume of H_2 (in cm³ at STP (Standard Temperature and Pressure)) adsorbed on 1 g of a network (H_2 pressure = 750 torr).

Sample	*Y* [%]	*DB*	S_{BET} [m² g⁻¹]	V_{MI} [cm³ g⁻¹]	$a_{H2,750torr}$ [cm³(STP) g⁻¹]	$a_{H2,750torr}/S_{BET}$ [cm³(STP) m⁻²]
P(1,3-DEB)$_C$	90	0.39	498	0.151	49.5	0.099
P(1,4-DEB)$_C$	80	0.44	512	0.160	59.3	0.116
P(1,3-DEB)$_N$	83	0.46	653	0.206	66.9	0.102
P(1,4-DEB)$_N$	85	0.30	809	0.247	77.8	0.096
P(4,4′-DEBPh)$_N$	87	0.47	731	0.224	73.4	0.100

www.MaterialsViews.com

to consist of two kinds of monomeric units: (i) linear units in which only one ethynyl group was transformed into a segment of polymer main chain, whereas the second ethynyl remained non-transformed and (ii) branching units in which both ethynyl groups were changed into the segments of polymer main chains. The mole fraction of branching units can be considered as degree of branching of a polymer, DB. Values of DB were obtained from ^{13}C CP/MAS NMR data according to Equation (1).

$$DB = [1 - A_T/A_{ArD}(n_{Ar}/2 + 1)]/(A_T/A_{ArD} + 1). \qquad (1)$$

Symbol n_{Ar} stands for the number of aromatic carbon atoms per a monomeric unit, A_T is the integral intensity of signals of triple-bond carbons and A_{ArD} is the integral intensity of signals of aromatic and main chain double-bond carbons. As evident from Table 1, DB values from 0.30 to 0.47 resulted for polymers prepared. No systematic relation was found between the DB values and the type of catalysts and/or monomer applied for polymers preparation. ^{13}C CP/MAS NMR results support the idea that polymers prepared are the polyacetylene-type networks with ethynylaryl-substituted polyene main chains that are crosslinked via arylene linkers, as it is depicted in Scheme 1.

3.2. Nitrogen Adsorption Characteristics of Prepared Polymers

Nitrogen adsorption isotherms revealed microporous character of all poly(diethynylarene)s prepared. The isotherms on the polymers derived from 1,3-DEB and 1,4-DEB monomers exhibited typical flat hysteresis loop reminiscent of type H4 hysteresis of IUPAC classifications.

The isotherm on P(4,4′-DEBPh)$_N$ sample exhibited hysteresis loop of the type H3 of IUPAC classifications. The discussed difference in isotherms is evident from Figure 2 (panel A) where all the nitrogen isotherms are shown. Pore size distributions calculated from desorption branches of nitrogen isotherms using BJH (Barrett-Joyner-Halenda) algorithm are displayed in Supporting information (Figure S2). Samples P(1,3-DEB)$_C$, P(1,4-DEB)$_C$, P(1,3-DEB)$_N$ and P(1,4-DEB)$_N$ contain a minimal volume of very small pores, which corresponds to the step desorption of the end of hysteresis loop. The hysteresis loop of the isotherm on the sample P(4,4′-DEBPh)$_N$ indicates the presence of mesopores, which volume can be assessed roughly as ≈ 0.7 cm^3 g^{-1}. This finding may reflect a higher length of 4,4′-biphenylene crosslinks joining polyene chains of P(4,4′-DEBPh)$_N$. Hysteresis loops of isotherms on all samples are not closed. This phenomenon of so-called low-pressure hysteresis is typical for nitrogen adsorption on "soft" polymer adsorbents. The detailed discussion and possible explanation are given in ref.[31]. The texture parameters of polymers prepared are summarized in Table 1. The BET surface area, S_{BET}, ranged from 498 to 809 m^2 g^{-1} and for polymers derived from 1,3-DEB and 1,4-DEB it showed a slight correlation with the type of monomer and catalyst applied for synthesis: (i) polymers prepared with [Rh(nbd)acac] exhibited higher S_{BET} values in comparison with polymers prepared with [Rh(cod) acac], (ii) higher S_{BET} values resulted for polymers derived from 1,4-DEB in comparison with their counterparts derived from 1,3-DEB.

On the other hand, no straight correlation was found between S_{BET} and DB values. It indicates that besides DB, other factors may influence the specific surface area, for example, configurational structure of polyene main
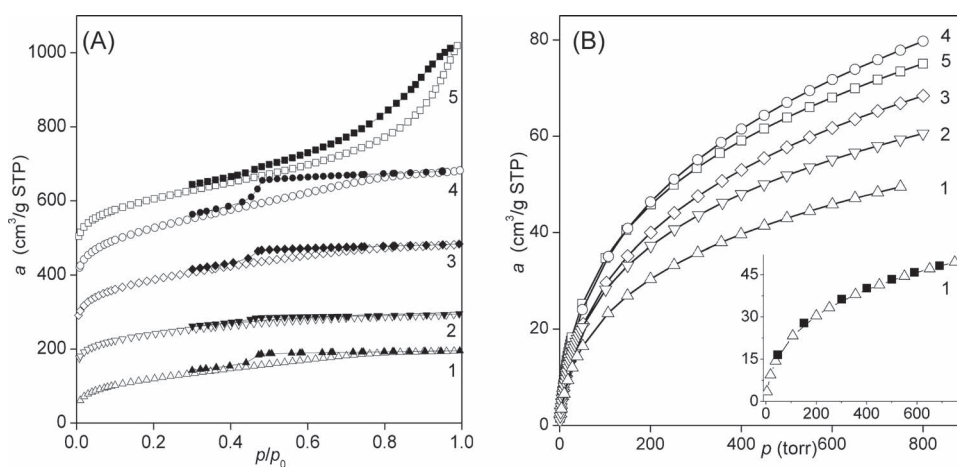

Figure 2. Nitrogen adsorption isotherms (panel A) and hydrogen adsorption isotherms (panel B) on samples P(1,3-DEB)$_C$ (curves 1), P(1,4-DEB)$_C$ (curves 2), P(1,3-DEB)$_N$ (curves 3), P(1,4-DEB)$_N$ (curves 4) and P(4,4′-DEBPh)$_N$ (curves 5). Solid points denote desorption. Nitrogen adsorption isotherms No. 2, 3, 4 and 5 are shifted vertically by 100 cm^3 g^{-1} STP each, the nitrogen adsorption isotherm No. 1 is not shifted. Inset in panel B shows representative points for hydrogen adsorption (empty points) and desorption (solid points) on P(1,3-DEB)$_C$.

chains of the networks. The insolubility of networks, however, makes the configuration of polyene main chains very difficult to be reliably revealed.

The above survey shows that the texture parameters of studied poly(diethynylarene)s are partly sensitive to the parameters of the synthesis. Research is in progress in our laboratory aimed to obtaining a further insight into the above outlined relations.

3.3. Hydrogen Adsorption on Prepared Polymers

Hydrogen adsorption isotherms are shown in Figure 2 (panel B). In contrast with nitrogen adsorption, the adsorption of hydrogen on all polymers was reversible (see the insert in Figure 2). Hydrogen adsorption capacities of polymers, $a_{H2,750torr}$, are summarised in Table 1. Symbol $a_{H2,750torr}$ stands for the volume of H_2 in cm^3 (at STP conditions) adsorbed on 1 g of polymer (adsorption conditions: temperature 77 K, H_2 pressure 750 torr). As evident from Table 1, values of $a_{H2,750torr}$ from 49.5 to 77.8 cm^3 g^{-1} (STP) were achieved that corresponded to hydrogen uptake from 0.44 to 0.69 wt%. The inspection of data in Table 1 showed that the ratio $a_{H2,750torr}/S_{BET}$ was nearly constant for all the polymers tested, that is, the hydrogen adsorption capacities were proportional to the surface area S_{BET}.

4. Conclusion

The efficiency of coordination polymerization for the transformation of non-vicinal diethynylarenes into MOPs has been demonstrated and MOPs of a new type, polyacetylene-type MOPs, have been prepared. Polyacetylene-type MOPs consisting of ethynylaryl-substituted polyene main chains crosslinked via arylene crosslinks may represent an easy accessible alternative to poly(aryleneethynylene)-type MOPs which are step growth polymerizations products. Prepared MOPs exhibit the S_{BET} area up to 809 m^2 g^{-1} and seem to be promising for adsorption and gas-storage applications. As the texture parameters of polyacetylene-type MOPs were found to be partly sensitive to the conditions of synthesis, a further optimisation of physical properties (hydrogen uptake, in particular) of these materials seems to be possible.

Supporting Information

Supporting Information is available from the Wiley Online Library or from the author.

[1]   N. B. McKeown, P. M. Budd, *Macromolecules* **2010**, *43*, 5163.
[2]   A. I. Cooper, *Adv. Mater.* **2009**, *21*, 1291.
[3]   A. Thomas, *Angew. Chem. Int. Ed.* **2010**, *49*, 8328.
[4]   J. X. Jiang, A. I. Cooper, Microporous organic polymers: design, synthesis, and function, in *Functional Metal-Organic Frameworks: Gas Storage, Separation and Catalysis, Book Series: Topics in Current Chemistry*, Vol. 293, Springer-Verlag, Berlin **2010**, p. 1.
[5]   S. Tedds, A. Walton, D. P. Broom, D. Book, *Faraday Discuss.* **2011**, *151*, 75.
[6]   P. M. Budd, A. Butler, J. Selbie, K. Mahmood, N. B. McKeown, B. Ghanem, K. Msayib, D. Book, A. Walton, *Phys. Chem. Chem. Phys.* **2007**, *9*, 1802.
[7]   J. Germain, J. M. J. Fréchet, F. Svec, *Small* **2009**, *5*, 1098.
[8]   J. Germain, J. Hradil, J. M. J. Fréchet, F. Svec, *Chem. Mater.* **2006**, *18*, 4430.
[9]   J. Y. Lee, C. D. Wood, D. Bradshaw, M. J. Rosseinsky, A. I. Cooper, *Chem. Commun.* **2006**, 2670.
[10] K. Zhang, B. Tieke, F. Vilela, P. J. Skabara, *Macromol. Rapid Commun.* **2011**, *32*, 825.
[11] K. V. Rao, S. Mohapatra, C. Kulkarni, T. K. Maji, S. J. George, *J. Mater. Chem.* **2011**, *21*, 12958.
[12] A. Thomas, P. Kuhn, J. Weber, M. M. Titirici, M. Antonietti, *Macromol. Rapid. Commun.* **2009**, *30*, 221.
[13] J. Germain, J. M. J. Fréchet, F. Svec, *J. Mater. Chem.* **2007**, *17*, 4989.
[14] J. Germain, J. M. J. Fréchet, F. Svec, *Chem. Commun.* **2009**, 1526.
[15] R. Dawson, F. Su, H. Niu, C. D. Wood, J. T. A. Jones, Y. Z. Khimyak, A. I. Cooper, *Macromolecules*, **2008**, *41*, 1591.
[16] J. Germain, F. Svec, J. M. J. Fréchet, *Chem. Mater.* **2008**, *20*, 7069.
[17] J. Schmidt, M. Werner, A. Thomas, *Macromolecules* **2009**, *42*, 4426.
[18] J. Smidt, J. Weber, J. D. Epping, M. Antonietti, A. Thomas, *Adv. Mat.*, **2009**, *21*, 702.
[19] J. Liu, J. W. Y. Lam, B. Z. Tang, *Chem. Rev.* **2009**, *109*, 5799.
[20] J. X. Jiang, F. Su, H. Niu, H. C. D. Wood, N. L. Campbell, Y. Z. Khimyak, A. I. Cooper, *Chem. Commun.* **2008**, 486.
[21] J. X. Jiang, F. Su, A. Trewin, C. D. Wood, H. Niu, T. A. Jones, Y. Z. Khimyak, A. I. Cooper, *J. Am. Chem. Soc.* **2008**, *130*, 7710.
[22] X. Jiang, F. Su, A. Trewin, C. D. Wood, N. L. Campbell, H. Niu, C. Dickinson, A. Y. Ganin, M. J. Rosseinsky, Y. Z. Khimyak, A. I. Cooper, *Angew. Chem. Int. Ed.* **2007**, *46*, 8574.
[23] W. Lu, D. Yuan, D. Zhao, C. I. Schilling, O. Plietzsch, T. Muller, S. Bräse, J. Guenther, J. Blümel, R. Krishna, Z. Li, H.-C. Zhou, *Chem. Mater.* **2010**, *22*, 5964.
[24] J. R. Holst, E. Stöckel, D. J. Adams, A. I. Cooper, *Macromolecules*, **2010**, *43*, 8531.
[25] M. Shiotsuki, F. Sanda, T. Masuda, *Polym. Chem.* **2011**, *2*, 1044.
[26] J. Sedláček, J. Vohlídal, *Collect. Czech. Chem. Commun.* **2003**, *68*, 1745.

[27] X. Zhan, M. Yang, Z. Lei, *J. Mol. Catal. A: Chem.* **2002**, *184*, 139.

[28] Y. Li, M. Yang, M. Ling, Y. Zhu, *Sens. Actuators B: Chem.* **2007**, *122*, 560.

[29] A. Bolasco, F. Chimenti, A. Frezza, A. Furlani, G. Infante, E. Muraglia, G. Ortaggi, G. Polzonetti, M. V. Russo, G. Sleiter, *Polymer*, **1992**, *33*, 3049.

[30] J. Brus, *Solid-State Nucl. Magn. Reson.* **2000**, *16*, 151.

[31] J. Weber, J. Schmidt, A. Thomas, W. Böhlmann, *Langmuir* **2010**, *26*, 15650.

[32] S. Lowell, J. E. Shields, M. A. Thomas, M. Thommes, in *Characterization of Porous Solids and Powders: Surface Area, Pore Size and Density*, Kluwer, Dordrecht, The Netherlands **2004**, 129.

[33] J. Svoboda, J. Sedláček, J. Zedník, G. Dvořáková, O. Trhlíková, D. Rédrová, H. Balcar, J. Vohlídal, *J. Polym. Sci., Part A: Polym. Chem.* **2008**, *46*, 2776.

[34] P. Mastrorilli, C. F. Nobile, V. Gallo, G. P. Suranna, G. Farinola, *J. Mol. Catal. A: Chem.* **2002**, *184*, 73.

[35] H. Hori, C. Six, W. Leitner, *Macromolecules* **1999**, *32*, 3178.

[36] O. Trhlíková, J. Zedník, J. Vohlídal, J. Sedláček, *Macromol. Chem. Phys.* **2011**, *212*, 1987.

[37] D. Bondarev, J. Zedník, I. Plutnarová, J. Vohlídal, J. Sedláček, *J. Polym. Sci., Part A: Polym. Chem.* **2010**, *48*, 4296.

[38] T. Masuda, S. M. Abdul Karim, R. Nomura, *J. Mol. Catal. A: Chem.* **2000**, *160*, 125.

[39] J. Sedláček, J. Vohlídal, S. Cabioch, O. Lavastre, P. Dixneuf, H. Balcar, M. Štícha, J. Pfleger, V. Blechta, *Macromol. Chem. Phys.* **1998**, *199*, 155.

Polyacetylene-Type Networks Prepared by Coordination Polymerization of Diethynylarenes: New Type of Microporous Organic Polymers

Vladimíra Hanková, Eva Slováková, Jiří Zedník, Jiří Vohlídal, Radoslava Sivkova, Hynek Balcar, Arnošt Zukal, Jiří Brus, Jan Sedláček[*]

_____

V. Hanková, E. Slováková, J. Zedník, J. Vohlídal, R. Sivkova, J. Sedláček
Department of Physical and Macromolecular Chemistry, Faculty of Science, Charles University in Prague, Hlavova 2030, CZ-128 40 Prague 2, Czech Republic

H. Balcar, A. Zukal
J. Heyrovský Institute of Physical Chemistry, v.v.i, Academy of Sciences of the Czech Republic, Dolejškova 3, 182 23 Prague 8, Czech Republic

J. Brus
Institute of Macromolecular Chemistry, v.v.i., Academy of Sciences of the Czech Republic, Heyrovský Sq. 2, 16206 Prague 6, Czech Republic
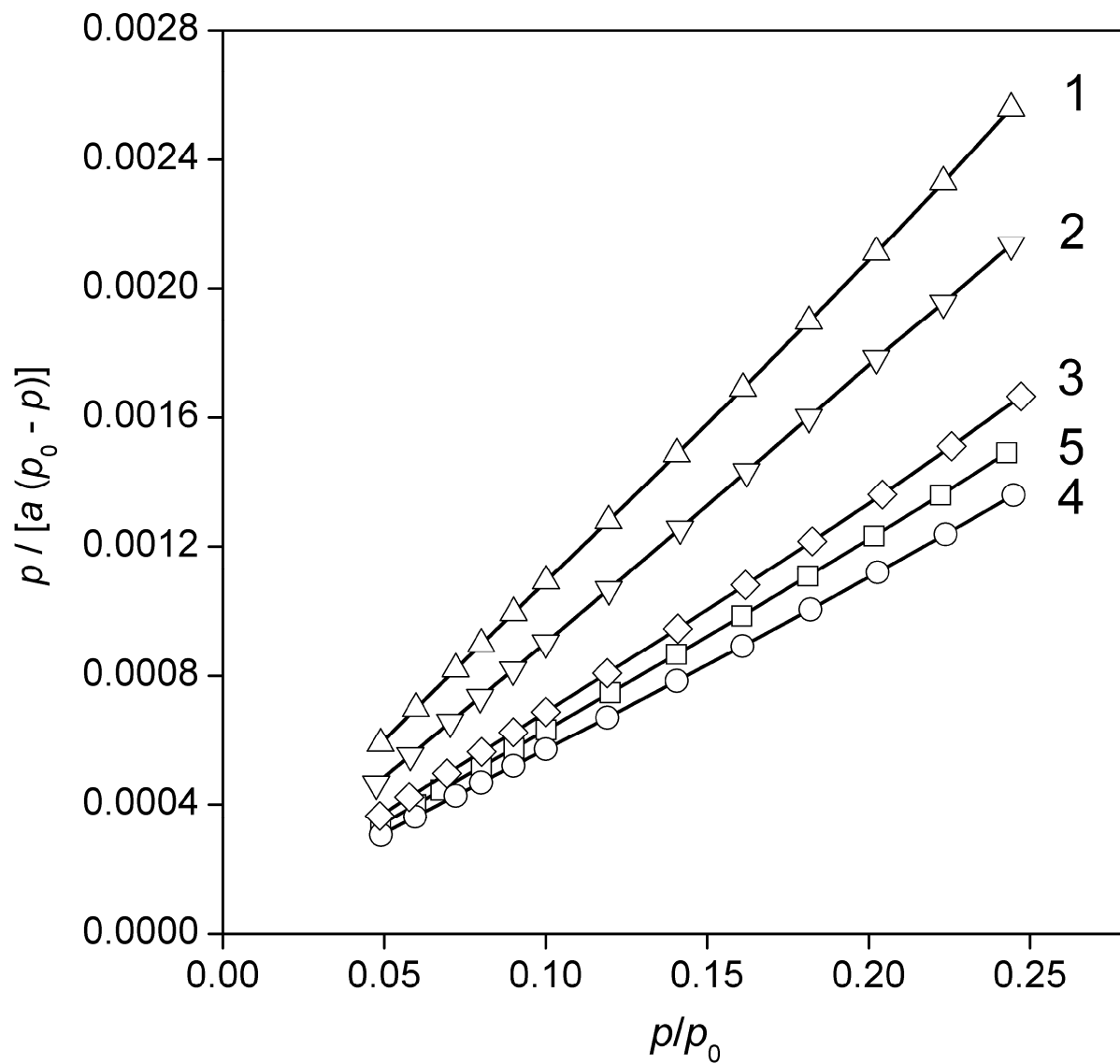
Figure S1. BET transform plots of the samples: P(1,3-DEB)$_C$ (curve 1), P(1,4-DEB)$_C$ (curve 2), P(1,3-DEB)$_N$ (curve 3), P(1,4-DEB)$_N$ (curve 4), and P(4,4′-DEBPh)$_N$ (curve 5).
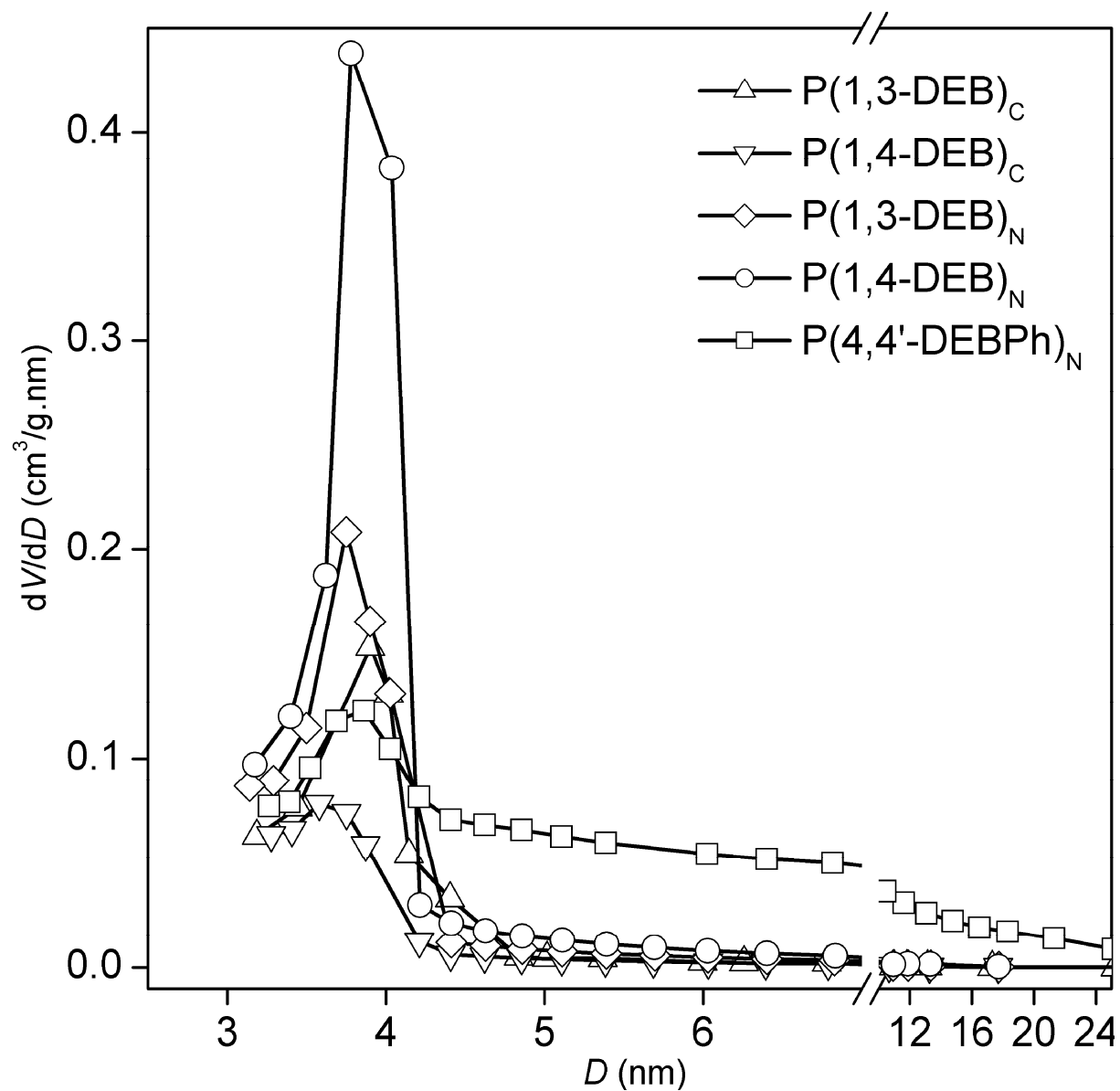
Figure S2. Pore size distributions of prepared samples. The spike on the end of distribution curves reflects an artifact caused by the spontaneous evaporation of nitrogen from very small pores.[32]

For ref.[32] see the list of references of the article.

II.

Eva Slováková, Arnošt Zukal, Jiří Brus, Hynek Balcar, Libor Brabec, Dmitrij Bondarev a Jan Sedláček: Transition-Metal-Catalyzed Chain-Growth Polymerization of 1,4-Diethynylbenzene into Microporous Crosslinked Poly(phenylacetylene)s: the Effect of Reaction Conditions, *Macromol. Chem. Phys*. **2014**, *215*, 1855 - 1869.

Transition-Metal-Catalyzed Chain-Growth Polymerization of 1,4-Diethynylbenzene into Microporous Crosslinked Poly(phenylacetylene)s: the Effect of Reaction Conditions

Eva Slováková, Arnošt Zukal, Jiří Brus, Hynek Balcar, Libor Brabec, Dmitrij Bondarev, Jan Sedláček*

Chain-growth polymerization of 1,4-diethynylbenzene into conjugated crosslinked polyacetylene-type poly(1,4-diethynylbenzene)s (PDEBs) is reported. While metathesis catalysts (WCl_6/Ph_4Sn, $MoCl_5$/Ph_4Sn, Mo Schrock carbene) fail in this polymerization, insertion Rh catalysts ([Rh(nbd)acac], [Rh(nbd)Cl]$_2$) provide microporous PDEBs in high yields. The Brunauer–Emmett–Teller (BET) surface, S_{BET}, of PDEBs prepared with [Rh(nbd)acac] increases, in dependence on the polymerization solvent, in the order: THF $\ll$ pentane < benzene < methanol < CH_2Cl_2. S_{BET} further increases with both increasing monomer concentration and increasing polymerization temperature and reaction time, reaching a highest value of 1469 m^2 g^{-1}. In addition to micropores, PDEBs contain mesopores. The mesopore volume and average mesopore diameter increase with the time and the temperature of the polymerization up to 2.52 cm^3 g^{-1} and 22 nm (72 h, 75 °C). The post-polymerization thermal treatment of PDEB (280 °C) results in formation of new crosslinks and modification of PDEB texture and sorption behavior manifested mainly by enhancement of H_2 adsorption capacity up to 4.55 mmol g^{-1} (77 K, 750 Torr).

$S_{BET} = 1469 \ m^2/g$
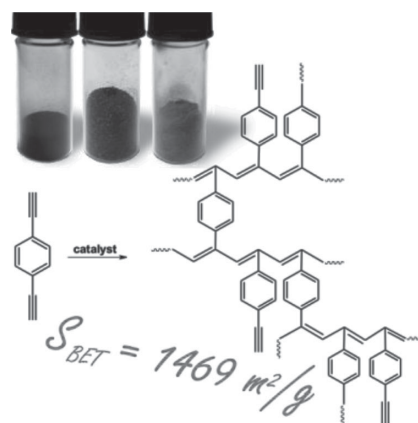
E. Slováková, Dr. D. Bondarev, Prof. J. Sedláček
Department of Physical and Macromolecular Chemistry, Faculty of Science, Charles University in Prague, Hlavova, 2030 CZ-128 43, Prague 2, Czech Republic
E-mail: jan.sedlacek@natur.cuni.cz
Dr. A. Zukal, Dr. H. Balcar, Dr. L. Brabec,
J. Heyrovský Institute of Physical Chemistry, v.v.i., Academy of Sciences of the Czech Republic, Dolejškova 3, CZ-182 23, Prague 8, Czech Republic
Dr. J. Brus
Institute of Macromolecular Chemistry, v.v.i., Academy of Sciences of the Czech Republic, Heyrovský Sq. 2 CZ-162 06, Prague 6, Czech Republic

1. Introduction

Porous polymers with pore sizes in the microporous range, reported often as microporous organic polymers (MOPs), have become materials of great and steadily increasing interest over the last decade.[1–5] The potential applications of MOPs range from: i) gas separation and reversible storage,[6–10] ii) catalysis,[11–14] and iii) energy transformation and storage[5,15,16] to iv) optoactive materials and sensors.[17–19] The microporosity of the majority of MOPs results from their extensive crosslinking that provides morphological rigidity to these polymers.[1–5] A wide spectrum

of synthetic paths to crosslinked MOPs is reported in the literature, mainly: polycondensations of multifunctional monomers,[20,21] FeCl$_3$-catalyzed hypercrosslinking of arene-containing prepolymers and/or monomers,[22,23] coupling reactions of multifunctional monomers,[8,24] trimerization reactions,[25,26] and others.

Acetylene monomers, ethynylarenes in particular, have been described many times as excellent starting materials for the synthesis of a variety of (mostly soluble) conjugated polymers and oligomers (see review by Tang and co-workers[27]). Step-growth polymerizations, cyclotrimerizations, and chain-growth polymerizations have been mostly used as the synthesis methods. Some of these reactions have recently been modified by increasing the functionality of monomer(s) applied for the synthesis, and several types of MOPs based on acetylene monomers have been prepared. Highly conjugated poly(arylenebutadiynylene)[28–30] and poly(arylene-ethynylene)[28,29,31,32] networks prepared via step-growth Pd-catalyzed couplings are the best known MOPs of this type. The starting materials for these networks were either a mixture of multiethynylarenes (MEAs) or a mixture of MEAs with (multibromo)arenes or (multiiodo)arenes (average functionality of monomers, $f > 2$). The Brunauer–Emmett–Teller (BET) specific surface area, (S_{BET}) about 1000 m^2 g^{-1} was prevailingly reported for these networks although exceptionally high S_{BET} values (1700–1900 m^2 g^{-1})[33,34] were revealed for networks prepared from tetrahedral monomers with $f = 4$. The reaction of MEAs with multiazidoarenes ("click" reaction) is another step-growth path to MOPs (S_{BET} up to 1200 m^2 g^{-1}).[10,33,35] The polycyclotrimerization of MEAs (f is from 2 to 4) was described as an efficient tool for the synthesis of polyarylene type MOPs (S_{BET} up to 1300 m^2 g^{-1}), in which the original arene cores of monomers were interconnected by benzenetriyl linkers formed via cyclotrimerization of three ethynyl groups of MEAs.[26,34,36]

Chain-growth polymerization of acetylenes containing one terminal ethynyl group, HC≡CR, into monosubstituted polyacetylenes, [—HC=CR—]$_n$, represents the most studied mode of the transformation of acetylenes into conjugated polymers.[27,37,38] Several hundreds of monomers have been polymerized in this way since 1970s.[37–40] The polymerizations are mostly performed as catalyzed reactions: either metathesis catalysts (Mo and W compounds)[41,42] or insertion catalysts (mainly Rh and Pd compounds)[27,43–45] are used. The type of the polymerization catalyst affects the configurational structure of the prepared polymers. While Rh catalysts produce highly regular head-to-tail polyacetylenes with a high content (nearly 100%) of *cis*-double bonds the catalysts based on W and Mo compounds provide less regular polymers with both *cis*- and *trans*-double bonds in the main chains.[27,37,41,46,47] Surprisingly, only several papers

report on the chain-growth polymerization of acetylenes aimed at the preparation of branched or crosslinked polyacetylenes that may, in principle, be achieved by a simple increase in the monomer functionality. Zhan and Yang[48] and Lei et al.[49] described homopolymerization of 1,4-diethynylbenzene (DEB) and copolymerization of DEB with phenylacetylene (PhA) catalyzed with Ni and Co catalysts. Dong and Ye[45] reported Pd-catalyzed copolymerization of PhA with various diynes. The reaction conditions of all these polymerizations were optimized so that the soluble branched polyacetylenes resulted as the products. Recently, our group reported two types of conjugated networks derived from substituted acetylenes by the chain growth polymerization.[50,51] The spontaneous polymerization of ethynylpyridines under quaternization with bis(bromomethyl)arenes provided ionic networks with the polyene main chains substituted with pyridyl and pyridiniumyl groups and crosslinked with —CH$_2$(arylene)CH$_2$— linkers.[50] The Rh-catalyzed polymerization of several diethynylarenes ($f = 2$) provided networks with the polyene main chains substituted with ethynylaryl groups and crosslinked with arylene linkers.[51] The diethynylarenes-based networks exhibited the MOP character with S_{BET} up to 800 m^2 g^{-1}. Results (reported as a rapid communication)[51] further showed that DEB was the most suitable monomer for the polyacetylene networks synthesis.

In this paper, we report the influence of the reaction conditions (the type of the catalyst, solvent, temperature, catalyst, and monomer concentrations) on the chain-growth polymerization of 1,4-diethynylbenzene (DEB) into poly(1,4-diethynylbenzene) (PDEB) networks. The study was focused on the possibility to affect the porosity and the sorption capacity of prepared PDEBs by a proper choice of the reaction conditions. In addition to it, the post-polymerization modification of these networks was studied with the same aim.

2. Experimental Section

2.1. Materials

Acetylacetonato(norborna-2,5-diene)rhodium(I) ([Rh(nbd)acac]), (norborna-2,5-diene)rhodium(I) chloride dimer, ([Rh(nbd)Cl]$_2$), WCl$_6$, MoCl$_5$, tetraphenyltin (Ph$_4$Sn), triethylamine (Et$_3$N), methanol, pentane (anhydrous) (all by Sigma–Aldrich), and 2,6-diisopropylphenylimido(neophylidene)molybdenum(VI)bis(*t*-butoxide) [Mo(=N—C$_6$H$_3$(*i*-Pr-2,6)$_2$)(=CHCMe$_2$Ph)(O-*t*-Bu)$_2$], (Mo Schrock carbene) (Strem) were used as obtained. DEB (TCI Europe) was purified by vacuum sublimation. Dichloromethane (Lachema, Czech Republic) was distilled from P$_2$O$_5$. Tetrahydrofuran (THF) (Sigma–Aldrich) was distilled from CaH$_2$ and CuI. Benzene (Sigma–Aldrich) used as a solvent in Rh-catalyzed polymerizations was distilled from P$_2$O$_5$. Purification of benzene

www.MaterialsViews.com

for the polymerizations with W and Mo catalysts is described elsewhere.[52]

2.2. Polymerization

The polymerizations with W- and Mo-based catalysts were performed in benzene under vacuum using the break-seal technique. The polymerizations with Rh-based catalysts were performed under argon in following solvents: benzene, CH_2Cl_2, THF, methanol, pentane. The solutions of the catalysts were prepared by dissolving a weighed amount of catalyst in 5 mL of a given solvent. If a cocatalyst was applied (Ph_4Sn, Et_3N), it was dissolved together with the catalyst and the resulting solution was reacted at room temperature for 15 min under stirring. The polymerizations were started by fast introduction of the solution of DEB in 5 mL of a given solvent into the solution of the catalyst under stirring. The initial concentration of DEB in the reaction mixtures ranged from 0.2 to 1.2 mol L^{-1}, the catalyst concentration was either 6 or 18 mmol L^{-1}. The reaction mixtures were reacted for either 3 h or 72 h at either room temperature or 75 °C. The reaction mixtures were sealed in a thick wall glass ampoule reactor in the case of polymerizations performed at 75 °C. The polymerizations were finished by diluting the reaction mixture (containing the solid polymer) with the solvent used for the polymerization in the volume ratio 1:10. The solid polymer was mechanically ground (if necessary) washed by decantation with the solvent used for the polymerization and finally dried in vacuum at room temperature to constant weight. The polymer yield was determined gravimetrically. The thermal modification of the polymers was done in a Büchi B-585 glass oven. About 200 mg of the polymer was heated in this apparatus for 3 h at 280 °C under vacuum.

2.3. Techniques

All the Fourier transform IR (FTIR) spectra were measured on a Nicolet Magna IR 760 using the diffuse reflection mode (DRIFTS). Samples were diluted with KBr.

All the ^{13}C cross-polarization magic-angle spinning (CP/MAS) NMR spectra of the solid polymers were measured at 11.7 T using a Bruker Avance III HD 500 US/WB NMR spectrometer (Karlsruhe, Germany, 2013). The finely powdered samples were placed into the 3.2-mm ZrO_2 rotors and the spinning frequency was always 20 kHz.

Diffuse reflectance (DR) UV–vis spectra of the solid polymers were recorded using a Perkin–Elmer Lambda 950 spectrometer. The polymers were diluted with $BaSO_4$ (1:10, w/w) before the measurements were carried out.

Thermogravimetric analysis (TGA) was performed at a TA Q500 apparatus under nitrogen atmosphere with heating rate 10 °C min^{-1} in the range from 40 to 800 °C. The samples were treated at 100 °C for 60 min under nitrogen flow prior to analysis to remove trapped moisture from the sample.

Micrographs of the surface of polymers were made on a scanning electron microscope JEOL JSM-5500LV. Samples were covered with a Pt layer ca. 15 nm thick by means of a sputter coater BAL-TEC SCD 050.

Adsorption/desorption isotherms of nitrogen and hydrogen at 77 K and carbon dioxide at 273 K were recorded using an ASAP

2020 (Micromeritics) volumetric instrument. The fresh samples were degassed starting at an ambient temperature up to 353 K (temperature ramp of 0.5 K min^{-1}) until the residual pressure of 1.33 Pa was attained. After further heating at 353 K for 1 h, the temperature was increased (temperature ramp of 1 K min^{-1}) until the temperature of 383 K was achieved. Degassing was continued at this temperature under the turbomolecular pump vacuum for 12 h.

3. Results and Discussion

3.1. Evaluation of the Texture Parameters of Prepared Porous Polymers

Based on the nitrogen isotherms, the texture parameters of porous polymers were calculated. As typical for these adsorbents, some nitrogen isotherms show a pronounced hysteresis upon desorption down to low equilibrium pressures. The recent discussion on this phenomenon is available in refs.[36,53] The hysteresis effect has implications on the determination of texture parameters. Relatively reliable information on the surface area and on the volume and distribution of mesopores can be obtained using the BET and BJH methods, respectively. As the origin of the hysteresis is not fully understood, no clear answer can be expected from different methods of micropore analysis.[53] In this contribution, the micropore volume was determined using the semi-empirical Horvath–Kavazoe method.

3.2. Poly(1,4-diethynylbenzene)s Prepared with Various Catalysts

1,4-Diethynylbenzene was polymerized in the chain-growth mode with Rh, Mo, and W catalysts (see Table 1) with the aim to prepare crosslinked PDEB according to Scheme 1. All the applied catalysts are known to be highly active in the polymerization of monofunctional arylacetylenes, PhA in particular, into (mostly soluble) linear high-molecular-weight poly(arylacetylene)s.[37,38,54] Conditions and results of DEB polymerizations are summarized in Table 1 where also the codes of the polymers prepared are given. Benzene was used as the solvent for the polymerizations with Mo- and W-based catalysts for the high compatibility of these catalysts with aromatic solvents.[38,39,55] The selection of CH_2Cl_2 for the polymerization with Rh-catalysts was based on our previous experience.[51,54] The polymerizations catalyzed with $[Rh(nbd)Cl]_2/Et_3N$ and $[Rh(nbd)acac]$ (Table 1 No. 1, 2) proceeded smoothly and gave PDEB in 77% and 85% yields, respectively, in 3 h. The reaction mixture turned red immediately after mixing DEB and Rh catalyst solutions that indicated instantaneous formation of the polymer. The onset of precipitation of the dark red PDEB was observed by naked eye several minutes

Table 1. Polymerization of DEB with insertion Rh-based catalysts (in CH_2Cl_2) and Mo- and W-based metathesis catalysts (in benzene). Catalyst concentration = 6 mmol L^{-1}, initial DEB concentration = 0.6 mol L^{-1}, room temperature. Y and X_{BU} stand for the yield of PDEB and the mole fraction of branching units in PDEB, respectively. Surface area S_{BET} and micropore volume V_{MI} were evaluated from the nitrogen adsorption isotherm.

No.	PDEB code	Catalyst	Reaction time [h]	Y [%]	X_{BU}	S_{BET} [m^2 g^{-1}]	V_{MI} [cm^3 g^{-1}]
1	PDEB1	[Rh(nbd)Cl]$_2$/ Et$_3$N	3	77	0.30	516	0.210
2	PDEB2	[Rh(nbd) acac]	3	85	0.30	809	0.323
3	PDEB3	WCl$_6$/Ph$_4$Sn	24	39	0.33	11	0
4		MoCl$_5$/Ph$_4$Sn	24	2	nd[b]	nd[b]	nd[b]
5		Mo-carbene[a]	24	11	nd[b]	nd[b]	nd[b]

[a]Schrock carbene, for the formula see the Experimental Section; [b]Not determined.

later. In the next reaction stage, a compact PDEB block was formed in the reaction vessel. The DEB polymerization with WCl$_6$/Ph$_4$Sn provided PDEB in a moderate yield only despite the prolongation of the reaction time to 24 h (see Table 1). PDEB was formed as a fine precipitate in this case. Only insoluble PDEBs were obtained as the final products in Rh- and W-catalyzed DEB polymerizations. This indicated the formation of the polymer networks. Both Mo catalysts tested (the ill-defined MoCl$_5$/Ph$_4$Sn catalyst and the well-defined Mo Schrock carbene) failed in the DEB polymerizations. The polymers prepared with Mo catalysts were insoluble in the reaction mixtures, however, they were formed in very low yields (Table 1).

Evidently, the Rh-based catalysts that polymerize monofunctional arylacetylenes in insertion propagation mode[27,43,56,57] were highly active also in the DEB

Scheme 1. Chain-growth polymerization of DEB with transition metal catalysts.

polymerization. On the other hand, the applied W and Mo catalysts that polymerize monofunctional arylacetylenes in metathesis propagation mode[41,58] exhibited low activity in the DEB polymerization. Some time ago, we reported that the metathesis polymerization of PhA (catalyzed by WOCl$_4$/Ph$_4$Sn) was affected by substrate inhibition[52] manifested by lowering the initial propagation rate due to a high monomer concentration in the reaction system. The explanation was proposed assuming a simultaneous coordination of two monomer molecules to one propagating W active species under formation of W species with a lowered propagation activity. The low PDEB yield achieved in DEB polymerization with WCl$_6$/Ph$_4$Sn catalyst (Table 1 No 3) can be elucidated similarly. The W-active species localized at the end of a growing PDEB macromolecule is surrounded by pendant ethynyl groups of this macromolecule so that the simultaneous coordination of two ethynyl groups to one W active species can easily proceed. This may impede the incorporation of DEB molecules into polymer chains. The low activity of Mo catalysts in the DEB polymerization may have the same reason since both Mo and W catalysts polymerize acetylenes in the metathesis mode.

PDEBs prepared with Rh and W catalysts (samples PDEB1, PDEB2, and PDEB3 from Table 1) were dark red brittle solids insoluble in tested solvents (THF, CH_2Cl_2, CHCl$_3$, and benzene). When dispersed in these solvents no swelling of polymer particles was observed by naked eye within 1 week. The ^{13}C CP/MAS NMR spectra of PDEB1, PDEB2, and PDEB3 are shown in Figure 1 together with the atom-numbering scheme. In general, ^{13}C CP/MAS NMR spectra of PDEBs contain signals at about $\delta = 83$ ppm and $\delta = 76$ ppm, which correspond to the resonance of sp carbons of nontransformed pendant ethynyl groups (carbons 7 and 8, respectively, in Figure 1) and a broad, partly resolved signal in the region 115–150 ppm that corresponds to the resonance of sp^2 carbons of aromatic rings
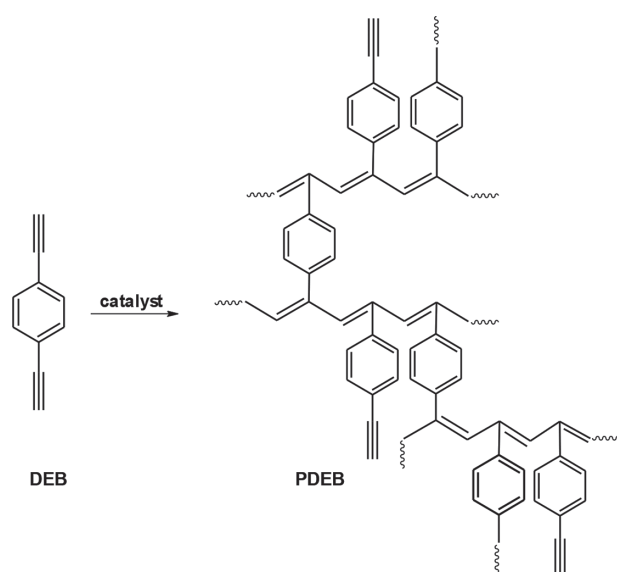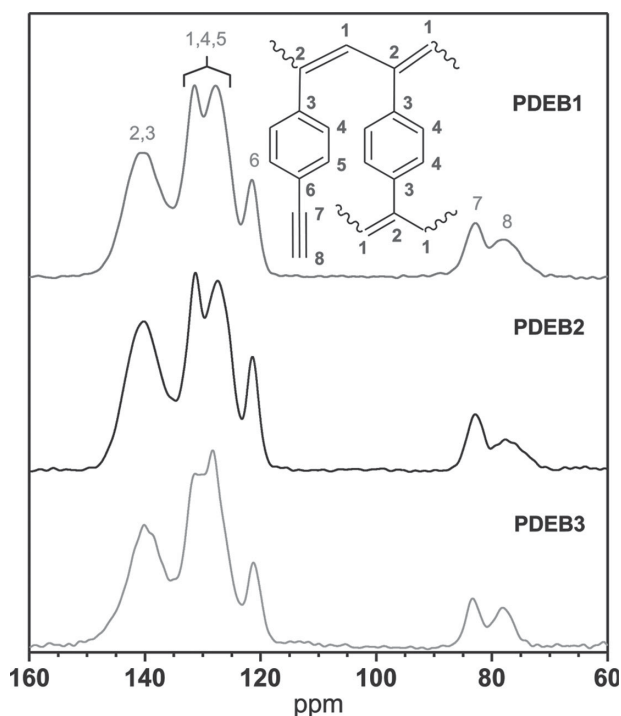
■ *Figure 1.* ^{13}C CP/MAS NMR spectra of polymers from Table 1.

and polymer main chains. For the detailed assignment of signals in this region, see Figure 1. The ^{13}C CP/MAS NMR spectroscopy showed that PDEB1, PDEB2, and PDEB3 contain two kinds of monomeric units: i) the linear units in which only one ethynyl group of DEB molecule was transformed into a segment of the polyene main chain while the second ethynyl group remained nontransformed and ii) branching units in which both ethynyl groups of DEB were changed into the segments of the polyene main chains. ^{13}C CP/MAS NMR results confirm that PDEB1, PDEB2, and PDEB3 are the polyacetylene-type networks with (4-ethynylphenyl)-substituted polyene main chains that are interconnected via the 1,4-phenylene linkers (Scheme 1). The mole fraction of branching units in PDEB networks, X_{BU}, was obtained from ^{13}C CP/MAS NMR data according to Equation (1) in which the symbols A_{sp} and A_{sp2} stand for the integral intensity of the signals of sp and sp^2 carbons, respectively:

$$X_{BU} = \left(A_{sp2} - 4 A_{sp}\right)/\left(A_{sp2} + A_{sp}\right) \tag{1}$$

As is evident from Table 1, similar values of X_{BU} (from 0.30 to 0.33) resulted for PDEB1, PDEB2, and PDEB3 regardless of the type of catalyst (W, Rh) used for the synthesis and the yield of the polymer achieved in the synthesis (from 39% to 85%). The high X_{BU} value of PDEB3 (W-based catalysis) is in accord with the above assumption on the high affinity of the W polymerization species

to surrounding pendant ethynyl groups of growing PDEB macromolecules.

Figure 2 shows FTIR spectra of PDEB1, PDEB2, and PDEB3. The presence of non-transformed pendant ethynyl groups in the polymers is clearly confirmed by the bands at about 3300 cm^{-1} ($v_{\equiv C-H}$) and 2110 cm^{-1} ($v_{C\equiv CH}$). The bands ascribable to phenylene units and main chain double bonds are present from 500 to 900 cm^{-1} and from 1500 to 1600 cm^{-1} regions. The FTIR spectra of PDEBs prepared with Rh and W catalysts are closely related to each other. Nevertheless, small differences are observed (see Figure 2): i) a shoulder at 790 cm^{-1} in the spectra of PDEB1 and PDEB2 that is missing in the spectrum of PDEB3, and ii) a shoulder at 1480 cm^{-1} in the spectrum of PDEB3 that is missing in the spectra of PDEB1 and PDEB2. The differences may be due to differences in the configuration of the main chain double bonds of particular samples. However, an assignment of the differences to a particular configuration can be made only tentatively, rather on the basis of reported correlation between the catalyst type and the configurational structure of the soluble linear poly(arylacetylene)s. It is well known that Rh-based catalysts polymerize monoethynylarenes into highly regular high-*cis*-poly(arylacetylene)s. The same monomers are polymerized with W-based catalysts into less regular polymers with both *cis*- and *trans*-double bonds in the main chains (*cis/trans*-polymers).[27,41,46] One may assume that Rh- and W-based catalysts preserve their specificity
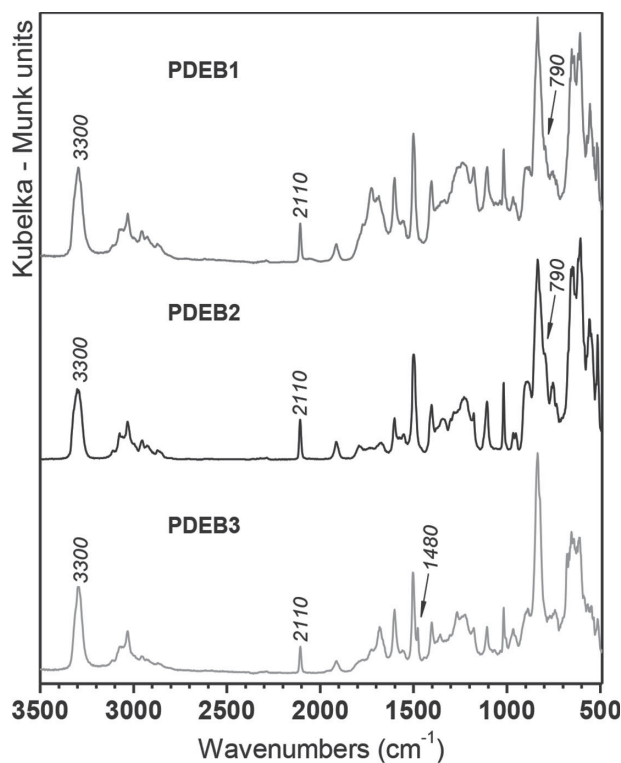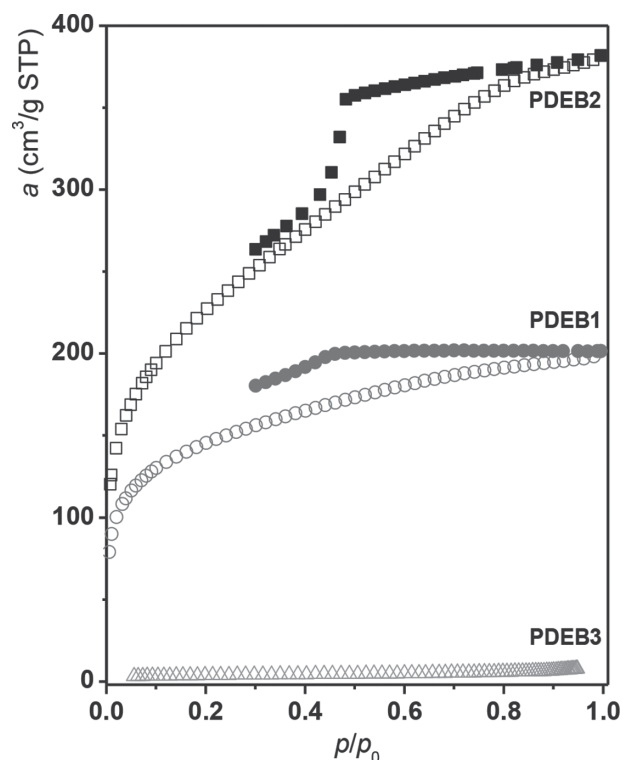

■ *Figure 2.* FTIR spectra of polymers from Table 1.

Figure 3. N$_2$ adsorption isotherms (77 K) on polymers from Table 1.

i) the pendant ethynyl can react with active end of other, covalently not connected PDEB chain (intermolecular crosslinking mode); ii) the pendant ethynyl can react with the active end of the same chain under the formation of a chain loop of various lengths (intramolecular cyclization mode); iii) the pendant ethynyl can be transformed into the polymerization active center (via initiation or transfer process) from which a polymer branch can grow. The intermolecular crosslinking (i.e., the interconnection of two chains by a short 1,4-phenylene strut) may be speculated as the most efficient contribution to the micropores formation.[59] The extent of the participation of the individual reaction modes of the transformation of pendant ethynyl groups can be governed by the type of the polymerization catalyst and by the configuration structure of the PDEB chains. Unfortunately, the particular modes by which the pendant ethynyl groups have been transformed during the PDEB formation are most probably undistinguishable by spectral analysis of the prepared PDEBs.

To conclude this chapter, we can state that from all the catalysts tested only the Rh-based catalysts provided PDEBs in high yields and with high specific surface areas. The most efficient Rh catalyst, [Rh(nbd)acac], was applied in further polymerization studies.

3.3. Poly(1,4-diethynylbenzene)s Prepared with [Rh(nbd)acac] Under Various Conditions

Table 2 contains the results of DEB polymerizations with [Rh(nbd)acac] performed in various solvents (CH$_2$Cl$_2$, benzene, THF, pentane, and methanol). CH$_2$Cl$_2$, benzene, and THF are known as good solvents for linear poly(phenylacetylene) (PPhA)[54,61] and were assumed to solvate well also the chain segments of PDEB networks. Pentane and methanol are nonsolvents of PPhA and thus they were assumed to solvate poorly the PDEB segments. The yields of PDEB achieved in CH$_2$Cl$_2$, benzene, and THF ranged from 78% to 85%. The onset of PDEB precipitation was observed several minutes after mixing DEB and catalyst solutions. When the polymerization was performed in methanol and pentane PDEB precipitated immediately after mixing DEB and catalyst solutions; however, the PDEB yield ranged from 44% to 53% only. The lower polymer yield achieved in methanol and pentane may reflect a restricted diffusion of the monomer molecules to the Rh polymerization species that are surrounded by poorly permeable growing PDEB chains.

All the polymerizations from Table 2 provided insoluble and non-swellable PDEBs. Polymers prepared in CH$_2$Cl$_2$, benzene, and THF (sample codes: PDEB2, PDEB4, and PDEB5, respectively) were dark red brittle solids. PDEBs prepared in pentane and methanol (sample codes PDEB6 and PDEB7, respectively) were yellow-orange powders.

with respect to the product configuration also in the DEB polymerization and that PDEB1 and PDEB2 prepared with Rh catalysts have higher *cis*-double-bond content than PDEB3 prepared with W catalyst.

Figure 3 shows the nitrogen adsorption isotherms on PDEB1, PDEB2, and PDEB3 (see the Experimental Section for details), corresponding texture parameters of polymers are summarized in Table 1. The presence of micropores and the BET surface area, S_{BET}, of 516 and 809 m^2 g^{-1} was revealed for PDEB1 and PDEB2, respectively. On the other hand, S_{BET} = 11 m^2 g^{-1} only resulted for PDEB3. As it is evident from Table 1, the S_{BET} values differed significantly despite the fact that X_{BU} values of PDEB1, PDEB2, and PDEB3 were almost the same.

The enormous difference between S_{BET} values of polymers prepared with either Rh catalysts (PDEB1, PDEB2) or W- catalyst (PDEB3) may be connected with the difference in configuration of Rh- and W-based PDEBs. Nevertheless, the texture of PDEBs may also be affected by variations in the architecture of PDEBs. At the early beginning of the DEB polymerization, the DEB molecules are incorporated into PDEB as monomeric units with pendant ethynyl groups. Subsequently, pendant ethynyl groups participate in polymerization. In analogy to the branching and crosslinking described for the chain-growth (co)polymerization of divinyl-type monomers in the literature,[59,60] one can assume several reaction modes for the transformation of the pendant ethynyl groups of the PDEB chains:

Table 2. Polymerization of DEB with [Rh(nbd)acac] in various solvents. Catalyst concentration = 6 mmol L^{-1}, initial DEB concentration = 0.6 mol L^{-1}, reaction time 3 h, room temperature. Y and X_{BU} stand for the yield of PDEB and the mole fraction of branching units in PDEB, respectively. Surface area S_{BET} and micropore volume V_{MI} were evaluated from the nitrogen adsorption isotherm.

No.	PDEB code	Solvent	Y [%]	X_{BU}	S_{BET} [m^2 g^{-1}]	V_{MI} [cm^3 g^{-1}]
1	PDEB2	CH$_2$Cl$_2$	85	0.30	809	0.323
2	PDEB4	Benzene	85	0.23	611	0.233
3	PDEB5	THF	78	0.26	<10	–
4	PDEB6	Pentane	44	0.32	286	0.113
5	PDEB7	Methanol	53	0.33	649	0.264

Figure 4 shows the DR UV–vis spectra of the polymers from Table 2. The spectra exhibit a broad absorption band with maximum at: 465 nm (PDEB4 and PDEB5), 435 nm (PDEB2 and PDEB7), and 385 nm (PDEB6), which reflects the π–π* transitions of the partly conjugated polymer main chains. The low energy edge of the absorption band lies in the range of 550–650 nm in the case of the spectra of PDEB6 and PDEB7. The absorption bands of the more conjugated samples PDEB2, PDEB4, and PDEB5 exhibit the low energy tail exceeding the wavelength of 800 nm.

The ^{13}C CP/MAS NMR and FTIR spectra of PDEBs from Table 2 are shown in Supporting Information (Figure S1 and S2, respectively). No influence of the polymerization solvent on the shape of ^{13}C CP/MAS NMR and FTIR spectra was found: FTIR spectra of all the samples from Table 2

correspond to FTIR spectrum of PDEB2 (see Figure 2), ^{13}C CP/MAS NMR of all the samples from Table 2 correspond to ^{13}C CP/MAS NMR spectrum of PDEB2 (see Figure 1). The X_{BU} values of PDEBs ranged from 0.23 to 0.33 (see Table 2). The high X_{BU} values resulted in methanol (X_{BU} = 0.33) and pentane (X_{BU} = 0.32) although only moderate PDEB yields were achieved in these solvents. This is in accord with the idea that the diffusion of the monomer molecules to the Rh polymerization species is restricted in the thermodynamically poor solvents for PDEB chains. This enhances the probability of pendant ethynyl groups of the PDEB monomeric units to be incorporated into the growing polymer chains. The characterization of samples from Table 2 by N$_2$ adsorption (see Figure 5 and Table 2) revealed presence of micropores in all the samples except for PDEB5. The micropore diameter distributions exhibited maxima centered between 1 and 1.3 nm. PDEB synthesized in THF (sample PDEB5) adsorbed only negligible amounts of N$_2$ (the same result was obtained for another PDEB prepared in THF under the same conditions). The S_{BET} values and the micropore volume of PDEBs increased in dependence on the polymerization solvent in the series: THF << pentane < benzene < methanol < CH$_2$Cl$_2$. The highest value, S_{BET} = 809 m^2 g^{-1}, resulted for PDEB2, which was synthesized in CH$_2$Cl$_2$. No correlation between S_{BET} and X_{BU} values is evident for PDEBs from Table 2. It is known from the literature[27,54] that the linear poly(arylacetylene)s prepared with Rh-based catalysts exhibit high-*cis*-configuration regardless of the type of the solvent used in the polymerization. In analogy to this, we assume that the configurational structure of PDEBs from Table 2 has not been influenced by the type of the polymerization solvent. This is supported by the fact that the shape of the FTIR spectra of PDEBs from Table 2 does not depend on the polymerization solvent (see Figure S2, Supporting Information). The type of polymerization solvent, however, could affect the architecture of PDEBs by affecting the participation of reaction modes by which the pendant ethynyl groups of DEB monomeric units are transformed (intermolecular crosslinking, intramolecular cyclization). Also the conformational structure of PDEBs could be affected
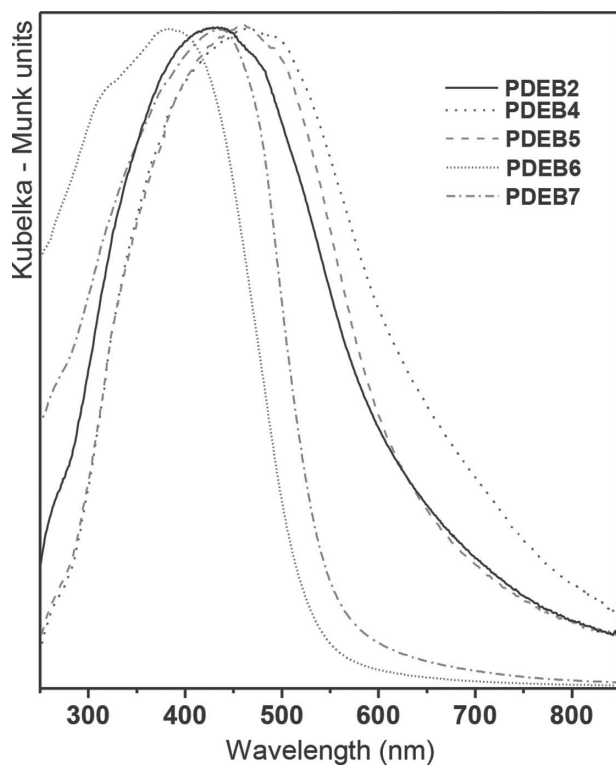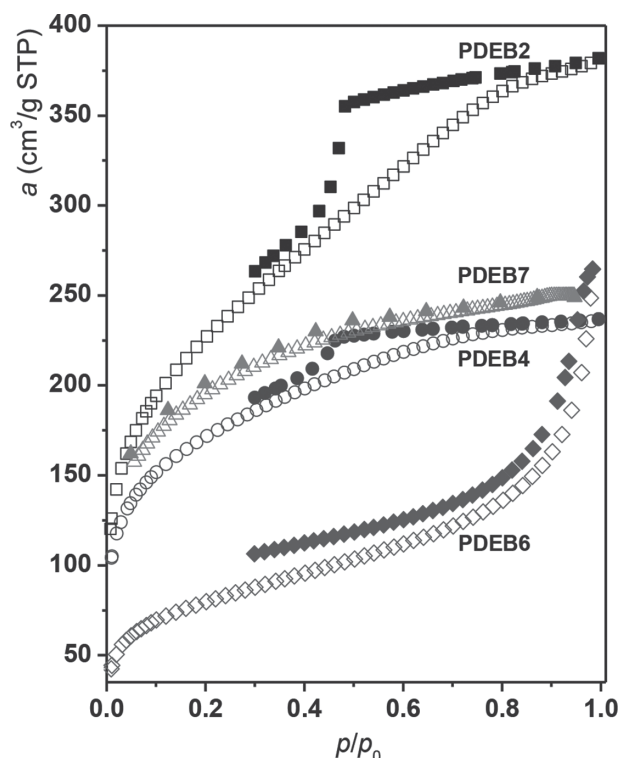

Figure 4. DR UV–vis spectra of prepared polymers from Table 2.

Figure 5. N_2 adsorption isotherms (77 K) on polymers from Table 2.

by the polymerization solvent[62] via the solvent impact on the packing of PDEB segments. We speculate that the influence of the polymerization solvent on PDEB texture reflects the influence of the solvent on architecture and/or conformational structure of PDEBs. Taking into account both the yields and S_{BET} values of PDEB (Table 2), it is evident that CH_2Cl_2 and benzene are superior solvents for the DEB polymerization with [Rh(nbd)acac].

The influence of the initial DEB concentration ([DEB]$_0$ = 0.2–1.2 mol L^{-1}) on the DEB polymerization and PDEBs characteristics was studied in experiments the results of which are given in Table 3. All the polymerizations were performed in CH_2Cl_2 under catalysis of [Rh(nbd)acac]. The ^{13}C CP/MAS NMR and FTIR spectra of PDEBs from Table 3 are given in Supporting Information (Figure S3 and S4, respectively). As evident from Table 3, the

parameter n_{DEB}/n_{Rh} (amount of DEB molecules inbuilt into PDEB per mole of catalyst) was increasing with increasing initial DEB concentration. Nevertheless, the highest (relative) yield of PDEB (85%) was achieved with medium [DEB]$_0$ = 0.6 mol L^{-1}. The X_{BU} parameter of PDEBs decreased from 0.36 to 0.14 with the increase of [DEB]$_0$ from 0.2 to 1.2 mol L^{-1}. Evidently, the probability of reaction of the pendant ethynyl groups of DEB monomeric units diminished if the reaction systems contained higher amount of the competing ethynyl groups present in monomer molecules. The N_2 adsorption isotherms on the PDEBs from Table 3 (see Figure 6) confirmed the microporous character of these polymers (micropore volume from 0.179 to 0.336 cm^3 g^{-1}). The S_{BET} values ranged from 410 m^2 g^{-1} (PDEB9, [DEB]$_0$ = 1.2 mol L^{-1}) to 867 m^2 g^{-1} (PDEB8, [DEB]$_0$ = 0.2 mol L^{-1}). Contrary to the sample series from Table 1 and Table 2, the PDEBs from Table 3 exhibited a good correlation between the X_{BU} and S_{BET} parameters: the S_{BET} values decreased with decreasing X_{BU}.

Table 4 contains the results of experiments dealing with the influence of the concentration of the catalyst, [Cat], and the reaction temperature and reaction time on the DEB polymerization and PDEBs characteristics. The polymerizations were performed with [Rh(nbd)acac] catalyst in CH_2Cl_2. The ^{13}C CP/MAS NMR and FTIR spectra of PDEBs from Table 4 are given in the Supporting Information (Figure S5 and S6, respectively). Comparison of the experiments performed at room temperature with various catalyst concentrations (No. 1, [Cat] = 6 mmol L^{-1}, No. 2, [Cat] = 18 mmol L^{-1}, see Table 4) showed an increase in the PDEB yield due to the increase in [Cat]. The analogous pair of experiments (Nos. 3 and 4, Table 4) performed at 75 °C showed the same effect of [Cat] values on the PDEB yields. The influence of the catalyst concentration on the X_{BU} values of prepared PDEBs was not straightforward as evident from Table 4, Nos. 1–4. On the other hand, the X_{BU} values of prepared PDEBs unambiguously rose with the increase in the reaction temperature [compare the experiments: i) No. 1 with No. 3 and ii) No. 2 with No. 4] and with reaction time (compare experiments Nos. 4 and 5). The elevated temperature most probably intensified movement of the PDEB chain segments that facilitated

Table 3. Polymerization of DEB with [Rh(nbd)acac] in CH_2Cl_2 at various initial DEB concentrations, [DEB]$_0$. Catalyst concentration = 6 mmol L^{-1}, reaction time 3 h, room temperature. Y and X_{BU} stand for the yield of PDEB and the mole fraction of branching units in PDEB, respectively. n_{DEB}/n_{Rh} represents the amount of DEB inbuilt into PDEB per mole of catalyst. Surface area S_{BET} and micropore volume V_{MI} were evaluated from the nitrogen adsorption isotherm.

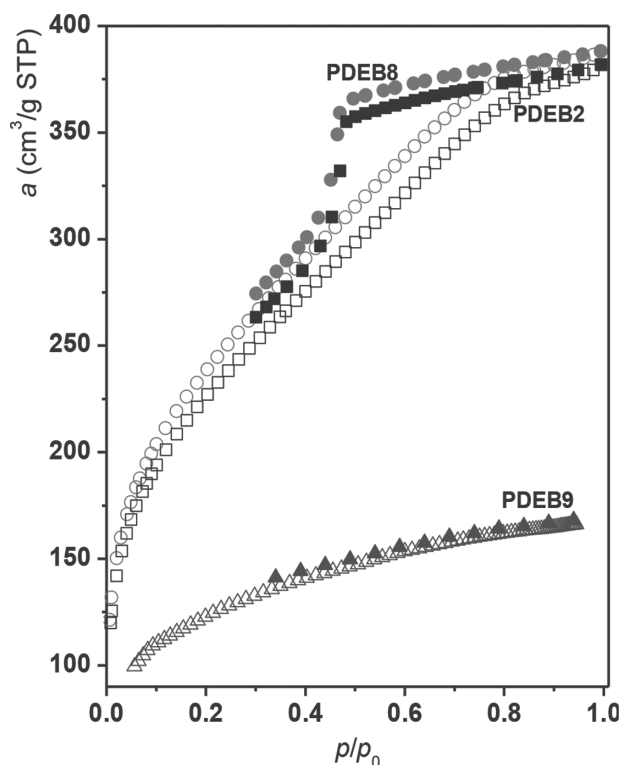| No.	PDEB code	[DEB]$_0$ [mol L^{-1}]	Y [%]	n_{DEB}/n_{Rh}	X_{BU}	S_{BET} [m^2 g^{-1}]	V_{MI} [cm^3 g^{-1}]
1	PDEB8	0.2	54	18	0.36	867	0.336
2	PDEB2	0.6	85	85	0.30	809	0.323
3	PDEB9	1.2	50	100	0.14	410	0.179

Figure 6. N$_2$ adsorption isotherms (77 K) on polymers from Table 3.

the incorporation of the pendant ethynyl groups of PDEB monomeric units into PDEB main chains.

The N$_2$ adsorption isotherms on samples from Table 4 are given in Figures 7 and 8. Figure 7 provides a comparison of N$_2$ adsorption isotherms on PDEBs prepared with [Cat] = 6 mmol L^{-1} at various temperature: PDEB2 (prepared at room temperature) and PDEB11 (prepared at 75 °C). The PDEB2 isotherm exhibited only a weak increase in the adsorption at $p/p_0 > 0.5$ and the maximum nitrogen adsorption capacity at 750 Torr, $a_{N2,750\ Torr}$, reached the value of 17.05 mmol g^{-1}. On the contrary, the isotherm on PDEB11 exhibited a strong increase in the

adsorption at $p/p_0 > 0.5$ that resulted in a higher $a_{N2,750\ Torr}$ value equal to 31.21 mmol g^{-1}. The effect of the reaction time on the PDEB behavior in the course of N$_2$ adsorption is evident from a comparison of isotherms on PDEB12 and PDEB 13 in Figure 8 ([Cat] = 18 mmol L^{-1}, reaction temperature 75 °C). The prolongation of the time of the synthesis from 3 h (PDEB12) to 72 h (PDEB13) resulted in a steeper increase in the amount of adsorbed N$_2$ at $p/p_0 > 0.5$ and the value of $a_{N2,750\ Torr}$ rose from 38.02 mmol g^{-1} (PDEB12) to 81.12 mmol g^{-1} (PDEB13). The S_{BET} values of polymers from Table 4 were sensitive particularly to the temperature and time of the synthesis. In dependence on these parameters, the S_{BET} values ranged from 809 cm^2 g^{-1} (PDEB2) to 1469 cm^2 g^{-1} (PDEB13).

The desorption branches of the isotherms on samples from Table 4 were treated using BJH algorithm to obtain the mesopore size distributions (see Figure 9). It should be noted that the spikes in the distribution curves for pore size lower than 5 nm are associated with spontaneous evaporation of metastable pore liquid. Therefore, they do not correspond to the true pore distribution. The BJH method revealed the presence of some mesopores in all the samples. The mesopore volume, V_{meso}, ranged from 0.319 (PDEB2) to 2.520 cm^3 g^{-1} (PDEB13). The mesopore size distributions exhibited distinct maxima only for PDEB11, PDEB12, and PDEB13 (diameters of 8, 13, and 22 nm, respectively). The mesopore diameters of PDEB2 and PDEB10 is assumed to be lower than 4 and 5 nm, respectively. Since the N$_2$ adsorption isotherms showed the presence of both micropores and mesopores in samples from Table 4 we can denote them as micro/mesoporous polymers. Various methods are known from the literature for influencing the diameter of the pores in the porous polymers: for example, the application of templates[63–65] or the variation of the length of the network crosslinks.[24,66] As evident from Table 4, the increase in mesopore volume and diameter in PDEBs was supported mainly by an increase of temperature and time of the PDEB synthesis. We speculate that mesopores in PDEBs

Table 4. Polymerization of DEB with [Rh(nbd)acac] at various catalyst concentrations, [Cat], and various temperatures, *T*. Initial DEB concentration = 0.6 mol L^{-1}. *Y* and X_{BU} stand for the yield of PDEB and the mole fraction of branching units in PDEB, respectively. S_{BET} is the surface area, $a_{N2,750\ Torr}$ is the amount of nitrogen adsorbed on 1 g of polymer at 750 Torr and 77 K, V_{MI} is the micropore volume, V_{meso} and D_{meso} are mesopore volume and the average mesopore diameter, respectively.

No.	PDEB code	[Cat] [mmol L^{-1}]	*T*	*Y* [%]	X_{BU}	S_{BET} [m^2 g^{-1}]	$a_{N2,750\ Torr}$ [mmol g^{-1}]	V_{MI} [cm^3 g^{-1}]	V_{meso} [cm^3 g^{-1}]	D_{meso} [nm]
1	PDEB2[a)	6	Room	85	0.30	809	17.05	0.323	0.319	<4
2	PDEB10[a)	18	Room	96	0.36	882	22.64	0.340	0.593	<5
3	PDEB11[a)	6	75 °C	88	0.54	979	31.21	0.378	0.860	8
4	PDEB12[a)	18	75 °C	100	0.44	975	38.02	0.373	1.119	13
5	PDEB13[b)	18	75 °C	100	0.64	1469	81.12	0.350	2.520	22

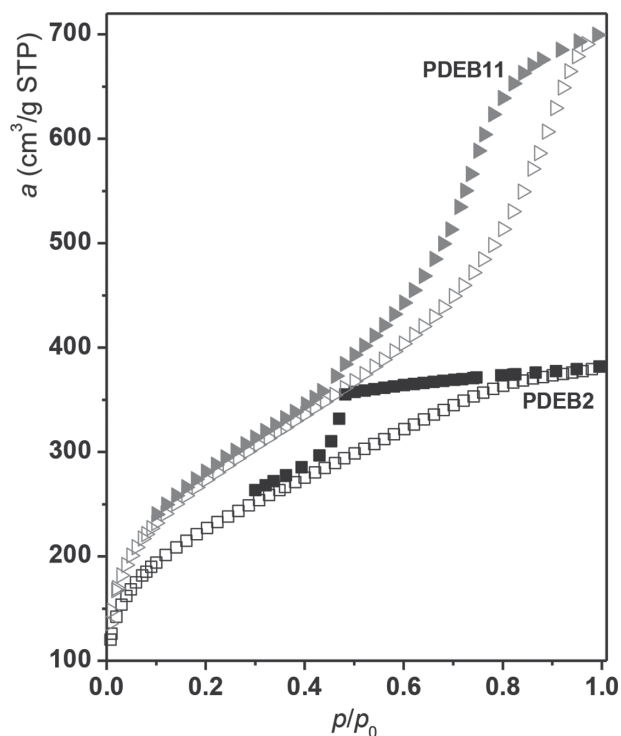[a)Reaction time 3 h; [b) Reaction time 72 h.

Figure 7. N$_2$ adsorption isotherms (77 K) on PDEB2 and PDEB11 from Table 4.

might result from a mutual knitting of small particles consisting of previously formed microporous PDEB network. The ethynyl groups of the surface segments of these
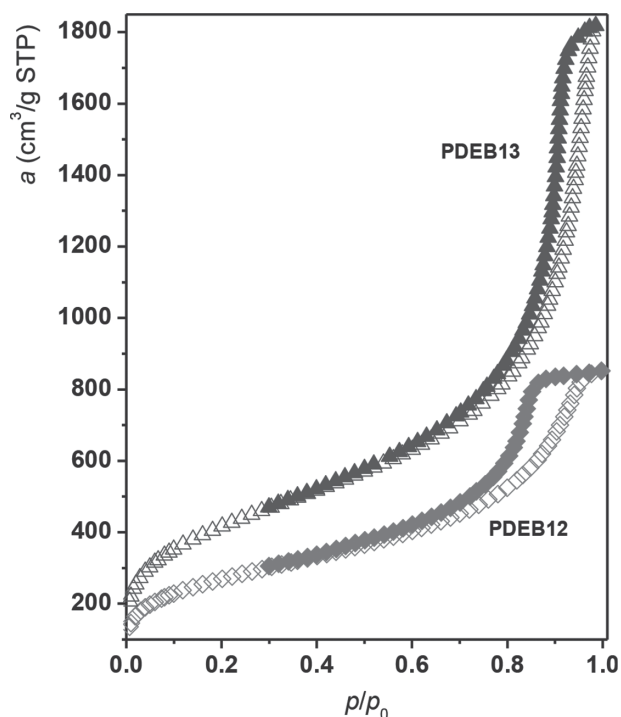

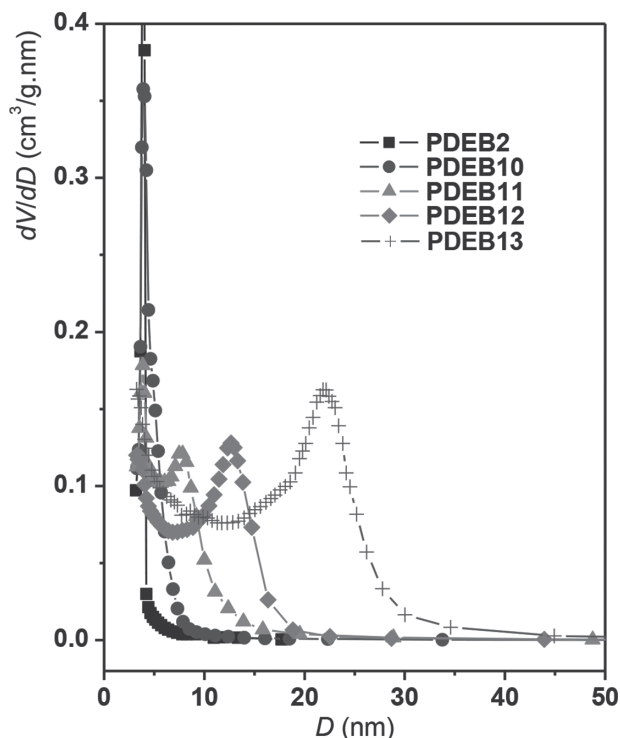*Figure 8.* N$_2$ adsorption isotherms (77 K) on PDEB12 and PDEB13 from Table 4.

Figure 9. Mesopore size distribution of polymers from Table 4. Calculated from the desorption branch of nitrogen isotherm (the BJH method was used).

particles and ethynyl groups of free DEB molecules may be involved in such polymerization knitting. The temperature increase may postpone the phase separation of the small PDEB particles and support the movement of their surface segments. Figure 10 shows SEM images of PDEB2 and PDEB12 samples, which differ in the mesopore volume and diameter (Table 4). As evident, these two samples differ also in their surface morphology; however, the extent of mesoporosity cannot be deduced from these images.

3.4. Thermal Modification of Poly(1,4-diethynylbenzene)s

All the PDEB samples from Table 1–4 contained non-reacted ethynyl groups in high concentration ranging from 2.9 mmol g^{-1} (sample PDEB13 Table 4) to 6.8 mmol g^{-1} (sample PDEB9 Table 3). The ethynyl groups represent the reactive sites of PDEBs that are promising for post-polymerization modifications of PDEB networks. In this paragraph, we report the results of a simple thermal postpolymerization modification. Sample PDEB2 from Table 4 was heated for 3 h at 280 °C in vacuum and thermally modified sample labeled as PDEB2M was prepared (see Experimental). An independent TGA analysis of PDEB2 (heating rate 10 °C min^{-1}) provided weight loss of 1.9% at 280 °C (see Figure S7, Supporting Information). The prolonged heating of PDEB2 at 280 °C (in TGA apparatus) resulted also in very low weight loss (2.2%
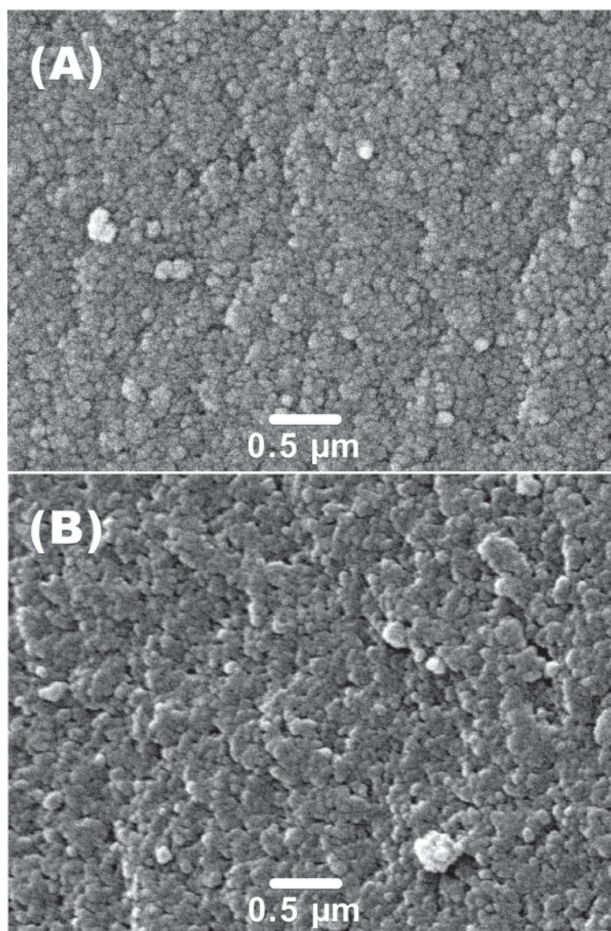
after 3 h and 2.8% after 6 h). Figure 11 shows ^{13}C CP/MAS NMR spectra of PDEB2 and PDEB2M. It is evident that the signals of the ethynyl groups in the network PDEB2 (at 76, 83, and 122 ppm) disappeared in the ^{13}C CP/MAS NMR spectrum of the thermally modified PDEB2M. Simultaneously, the thermal modification resulted in a broadening of the signals of sp^2 carbons in the spectrum of PDEB2M. The disappearance of ethynyl groups accompanying the modification of PDEB2 into PDEB2M was confirmed also by FTIR spectroscopy: FTIR spectrum of PDEB2M was free of bands at 2110 and 3300 cm^{-1} (see Figure 12). Recently, Chen and co-workers[67] reported the thermal curing of ethynyl-groups-containing oligomeric polyphenylenes prepared by catalytic cyclotrimerization of DEB and summarized possible reaction paths by which the ethynyl groups were transformed into the crosslinks of the polyphenylene prepolymers. Besides the cyclotrimerization of three terminal ethynyl groups yielding benzenetriyl crosslinks the coupling reactions of two ethynyl groups leading to butadiyne and buteneyne type temporary crosslinks were considered as most important. The butadiyne and buteneyne crosslinks were supposed to
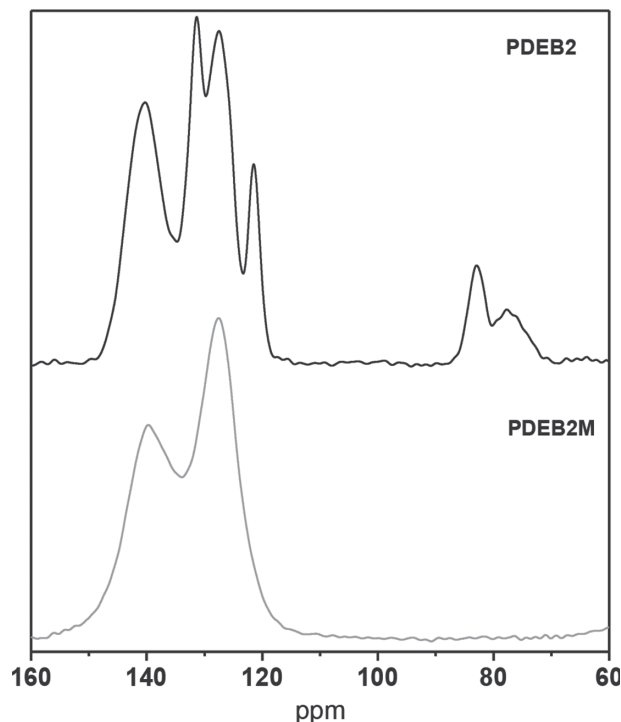
undergo subsequent thermal rearrangement and aromatization. We assume that the same reactions participated prevailingly in the thermal modification of PDEB2 into PDEB2M. Figure S8 (Supporting Information) shows the SEM image of PDEB2M. According to this image, the surface of this thermally modified sample was either smooth without visible particles or contained nanoparticles arranged with a high mass compactness. Thermally modified PDEB2M and its precursor PDEB2 were characterized by N$_2$ and H$_2$ adsorption at 77 K and by CO$_2$ adsorption at 273 K. Respective pairs of isotherms are given in Figure 13, S_{BET} values and adsorption capacities are summarized in Table 5. Figure 14 shows the micropore size distributions obtained from N$_2$ and CO$_2$ adsorption by Horvath–Kavazoe and DFT (density functional theory) methods, respectively. The N$_2$ adsorption provided information on micropores with diameter ≥1 nm while CO$_2$ adsorption revealed very small micropores with diameter <1 nm. Comparison of distribution curves based on N$_2$ adsorption shows the decrease of the diameter of (N$_2$ accessible) micropores due to the thermal modification of PDEB2 into PDEB2M. Pore size distribution based on CO$_2$ adsorption showed presence of some amount of small micropores (submicropores) in both PDEB2 and PDEB2M. The size distribution of submicropores exhibited a bimodal character with maxima at about 0.58 and 0.82 nm. The overall volume of submicropores was 0.028 cm^3 g^{-1} (PDEB2) and

Materials Views

www.MaterialsViews.com

Macromol. Chem. Phys. **2014**, *215*, 1855–1869
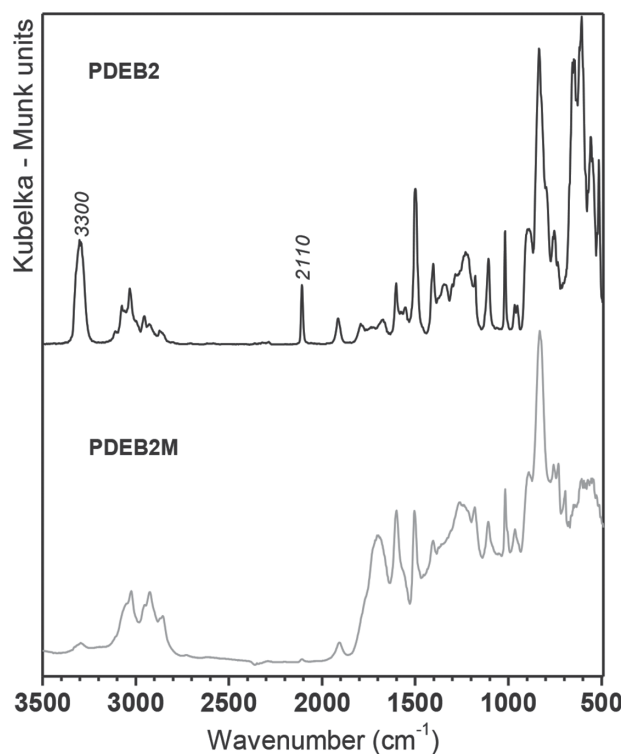© 2014 WILEY-VCH Verlag GmbH & Co. KGaA, Weinheim

Macromolecular Journals

1865

Figure 12. FTIR spectra of PDEB2 (sample before thermal modification) and PDEB2M (sample after thermal modification) from Table 5.

0.052 cm³ g⁻¹ (PDEB2M). Evidently, the thermal modification of the polymer resulted in a small increase in the submicropore volume. The findings based on Figure 14 are in accord with the assumption that the thermal modification of PDEB2 resulted very probably in an increase in the crosslinking density of the polymer.

Adsorption isotherm in Figure 13 and data From Table 5 show that the thermal modification of PDEB2 into PDEB2M resulted in decrease of both the S_{BET} value of the polymer and the amount of N_2 adsorbed on 1 g of the polymer at 750 Torr and 77 K, $a_{N2,750\ Torr}$. However, the H_2 and CO_2 adsorption capacities on parent and modified samples from Table 5 showed just the opposite trend. While the parent PDEB2 had the H_2 adsorption capacity, $a_{H2,750\ Torr} = 3.48$ mmol g⁻¹ (750 Torr, 77 K) and CO_2 adsorption capacity $a_{CO2,750\ Torr} = 1.32$ mmol g⁻¹ (750 Torr, 273 K), the thermally modified PDEB2M exhibited higher capacity values ($a_{H2,750\ Torr} = 4.55$ mmol g⁻¹, $a_{CO2,750\ Torr} = 1.78$ mmol g⁻¹). The comparison of H_2 and CO_2 adsorption isotherms in Figure 13 revealed that the modified sample PDEB2M exhibited a steeper initial increase in the amount of H_2 and CO_2 adsorbed than its parent counterpart PDEB2. The parallel decrease in the N_2 adsorption capacity and increase in the H_2 and CO_2 adsorption capacities observed due to the thermal modification of the polymer could partly reflect the decrease in micropore size caused by the
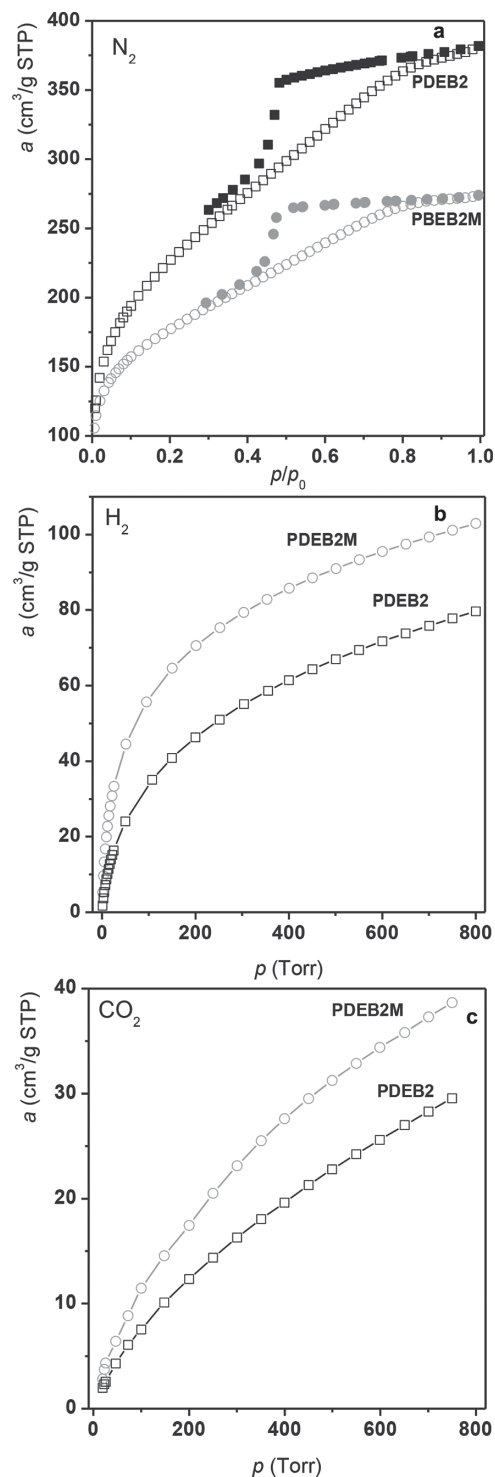
Figure 13. N_2 adsorption (a) and H_2 adsorption isotherms (b) (both at 77 K), and CO_2 adsorption isotherm (c) (273 K) for samples PDEB2 and PDEB2M from Table 5.

thermal treatment (Figure 14). The smaller pores of thermally modified PDEB2M might become worse accessible for N_2 molecules while they can still be easily accessible for smaller H_2 and CO_2 molecules.[68] The thermally modi-
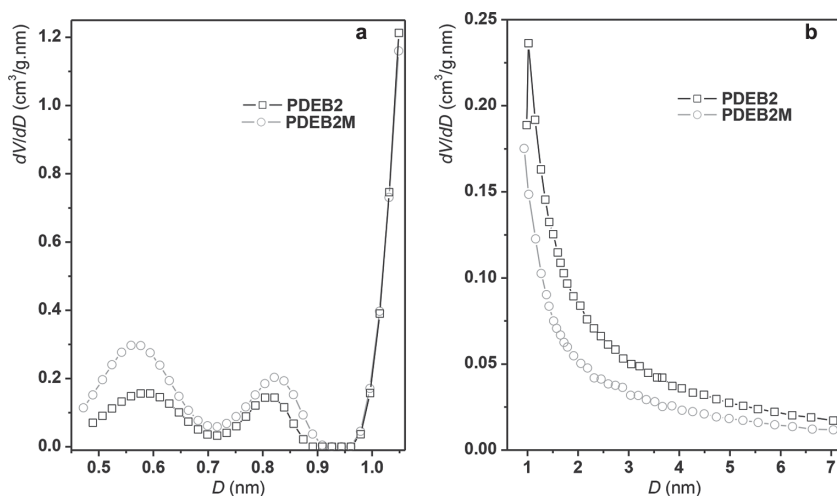
Figure 14. Pore size distribution of polymers PDEB2 and PDEM2M based on CO_2 (a) and N_2 (b) adsorption isotherms.

fied PDEB2M contains higher amount of aromatic constitutional segments (rich in delocalized electrons) than the parent PDEB2. This may be another reason for the observed increase in H_2 and CO_2 adsorption capacities due to the thermal modification of the polymer.

4. Conclusion

A series of W, Mo, and Rh catalysts has been used for the chain-growth polymerization of DEB into crosslinked polyacetylene-type PDEBs. Metathesis catalysts (WCl_6/Ph_4Sn, $MoCl_5$/Ph_4Sn, Mo Schrock carbene) gave low polymer yields only, despite the fact that they are highly active in the chain-growth polymerization of monoethynylarenes to linear polyacetylenes. On the other hand, the insertion Rh catalysts (particularly [Rh(nbd)acac] complex used in good solvents for PDEB segments) gave high PDEB yields.

The study of DEB polymerization with [Rh(nbd)acac] focused on the effects of the polymerization conditions on the structure and texture parameters of PDEB has revealed:

• The texture of PDEBs depends significantly on the solvent used for the polymerization. The S_{BET} values and the micropore volume of PDEBs increased in dependence on the polymerization solvent in the series: THF << pentane < benzene < methanol < CH_2Cl_2, reaching the highest S_{BET} = 809 m² g^{-1} (CH_2Cl_2). The impact of the polymerization solvent on the PDEB texture most probably reflects various influences of these solvents on the development of PDEB architecture and/or conformation in the course of polymerization.

• The S_{BET} values of PDEBs prepared were particularly improved by increasing the time of synthesis and the polymerization temperature from room temperature to 75 °C (S_{BET} up to 1469 m² g^{-1}). The S_{BET} increase was roughly correlated with the increase in the PDEB crosslinking extent. The polymerization temperature influenced also the pore size distribution: PDEB prepared at room temperature contained micropores and some mesopores with diameters <5 nm. PDEB prepared at 75 °C contained (besides micropores) mesopores with average pore diameter from 8 to 22 nm (mesopore volume up to 2.52 cm³ g^{-1}).

• Prepared PDEBs contain non-reacted ethynyl groups in high concentration (up to 6.8 mmol g^{-1}). We showed that thermal treatment of PDEB at 280 °C caused: i) total disappearance of pendant ethynyl groups under formation of new crosslinks most probably via cyclotrimerization, dimerization, and aromatization reactions and ii) subsequent modification of PDEB texture characteristics and sorption behavior. Particularly, the thermally modified PDEB exhibited higher H_2 and CO_2 adsorption capacities compared to the non-modified counterpart. This may reflect both the formation of new pores and an increase in the content of aromatic segments in PDEB due to the thermal modification.

The Rh-catalyzed chain-growth polymerization of DEB represents an easy path to the highly conjugated micro/mesoporous polymers the texture parameters of which can be controlled by reaction conditions. The nonreacted ethynyl groups in PDEBs can be utilized for further post-synthesis modifications of these polymers.

Table 5. Adsorption characteristics of PDEB2 and thermally modified PDEB2M. S_{BET} is the surface area determined from N_2 adsorption isotherm. $a_{N2,750\ Torr}$ and $a_{H2,750\ Torr}$ are the amounts of N_2 and H_2, respectively, adsorbed on 1 g of polymer at 750 Torr and 77 K. $a_{CO2,750\ Torr}$ is the amount of CO_2 adsorbed on 1 g of polymer at 750 Torr and 273 K.

PDEB code	S_{BET} [m² g^{-1}]	$a_{N2,750\ Torr}$ [mmol g^{-1}]	$a_{H2,750\ Torr}$ [mmol g^{-1}]	$a_{CO2,750\ Torr}$ [mmol g^{-1}]
PDEB2	809	17.05	3.48	1.32
PDEB2M	634	12.23	4.55	1.78

Makrials
Views
www.MaterialsViews.com

Macromol. Chem. Phys. **2014**, *215*, 1855–1869
© 2014 WILEY-VCH Verlag GmbH & Co. KGaA, Weinheim

Macromolecular
Journals

1867

Supporting Information

[1] D. Wu, F. Xu, B. Sun, R. Fu, H. He, K. Matyjaszewski, *Chem. Rev.* **2012**, *112*, 3959.
[2] A. Thomas, *Angew. Chem. Int. Ed.* **2010**, *49*, 8328.
[3] R. Dawson, A. I. Cooper, D. J. Adams, *Prog. Polym. Sci.* **2012**, *37*, 530.
[4] S. Xu, Y. Luo, B. Tan, *Macromol. Rapid Commun.* **2013**, *34*, 471.
[5] Z. Xiang, D. Cao, *J. Mater. Chem. A* **2013**, *1*, 2691.
[6] J. Germain, J. M. J. Fréchet, F. Švec, *Small* **2009**, *10*, 1098.
[7] N. B. McKeown, P. M. Budd, D. Book, *Macromol. Rapid Commun.* **2007**, *28*, 995.
[8] W. Lu, D. Yuan, D. Zhao, C. I. Schilling, O. Plietzsch, T. Muller, S. Bräse, J. Guenther, J. Blümel, R. Krishna, Z. Li, H.-C. Zhou, *Chem. Mater.* **2010**, *22*, 5964.
[9] R. Dawson, A. I. Cooper, D. J. Adams, *Polym. Int.* **2013**, *62*, 345.
[10] R. Dawson, E. Stöckel, J. R. Holst, D. J. Adams, A. I. Cooper, *Energy Environ. Sci.* **2011**, *4*, 4239.
[11] J.-X. Jiang, C. Wang, A. Laybourn, T. Hasell, R. Clowes, Y. Z. Khimyak, J. Xiao, S. J. Higgins, D. J. Adams, A. I. Cooper, *Angew. Chem. Int. Ed.* **2011**, *50*, 1072.
[12] E. Merino, E. Verde-Sesto, E. M. Maya, A. Corma, M. Iglesias, F. Sánchez, *Appl. Cat. A: Gen.* **2014**, *469*, 206.
[13] H. Kim, M. C. Cha, H. W. Park, J. Y. Chang, *J. Polym. Sci., Part A: Polym. Chem.* **2013**, *51*, 5291.
[14] P. Kaur, J. T. Hupp, S.-B. T. Nguyen, *ACS Catal.* **2011**, *1*, 819.
[15] A. Thomas, P. Kuhn, J. Weber, M.-M. Titirici, M. Antonietti, *Macromol. Rapid Commun.* **2009**, *30*, 221.
[16] L. Chen, Y. Honsho, S. Seki, D. Jiang, *J. Am. Chem. Soc.* **2010**, *132*, 6742.
[17] J. Brandt, J. Schmidt, A. Thomas, J. D. Epping, J. Weber, *Polym. Chem.* **2011**, *2*, 1950.
[18] J. Wei, X. Zhang, Y. Zhao, R. Li, *Macromol. Chem. Phys.* **2013**, *214*, 2232.
[19] S. Ren, R. Dawson, D. J. Adams, A. I. Cooper, *Polym. Chem.* **2013**, *4*, 5585.
[20] M. G. Rabbani, H.-M. El-Kaderi, *Chem. Mater.* **2012**, *24*, 1511.
[21] L. Liu, P.-Z. Li, L. Zhu, R. Zou, Y. Zhao, *Polymer* **2013**, *54*, 596.
[22] Y. Luo, S. Zhang, Y. Ma, W. Wang, B. Tan, *Polym. Chem.* **2013**, *4*, 1126.
[23] H. Lim, M. C. Cha, J. Y. Chang, *Macromol. Chem. Phys.* **2012**, *213*, 1385.
[24] J.-X. Jiang, F. Su, A. Trewin, C. D. Wood, H. Niu, T. A. Jones, Y. Z. Khimyak, A. I. Cooper, *J. Am. Chem. Soc.* **2008**, *130*, 7710.
[25] P. Kuhn, M. Antonietti, A. Thomas, *Angew. Chem. Int. Ed.* **2008**, *47*, 3450.
[26] S. Yuan, B. Dorney, D. White, S. Kirklin, P. Zapol, L. Yu, D.-J. Liu, *Chem. Commun.* **2010**, *46*, 4547.
[27] J. Liu, J. W. Y. Lam, B. Z. Tang, *Chem. Rev.* **2009**, *109*, 5799.
[28] Y. Xu, S. Jin, H. Xu, A. Nagaia, D. Jiang, *Chem. Soc. Rev.* **2013**, *42*, 8012.
[29] Q. Liu, Z. Tang, M. Wu, Z. Zhou, *Polym. Int.* **2014**, *63*, 381.
[30] J.-X. Jiang, F. Su, H. Niu, H. C. D. Wood, N. L. Campbell, Y. Z. Khimyak, A. I. Cooper, *Chem. Commun.* **2008**, 486.
[31] R. Dawson, A. Laybourn, R. Clowes, Y. Z. Khimyak, D. J. Adams, A. I. Cooper, *Macromolecules* **2009**, *42*, 8809.
[32] Y. Morisaki, M. Gon, Y. Chujo, *J. Polym. Sci., Part A: Polym. Chem.* **2013**, *51*, 2311.
[33] J. R. Holst, E. Stöckel, D. J. Adams, A. I. Cooper, *Macromolecules* **2010**, *43*, 8531.
[34] Z. Wang, S. Yuan, A. Mason, B. Reprogle, D.-J. Liu, L. Yu, *Macromolecules* **2012**, *45*, 7413.
[35] O. Plietzsch, C. I. Schilling, T. Grab, S. L. Grage, A. S. Ulrich, A. Comotti, P. Sozzani, T. Muller, S. Bräse, *New J. Chem.* **2011**, *35*, 1577.
[36] A. Zukal, E. Slováková, H. Balcar, J. Sedláček, *Macromol. Chem. Phys.* **2013**, *214*, 2016.
[37] M. Shiotsuki, F. Sanda, T. Masuda, *Polym. Chem.* **2011**, *2*, 1044.
[38] T. Masuda, *J. Polym. Sci., Part A: Polym. Chem.* **2007**, *45*, 165.
[39] T. Masuda, K. Hasegawa, T. Higashimura, *Macromolecules* **1974**, *7*, 728.
[40] R. Motoshige, Y. Mawatari, A. Motoshige, Y. Yoshida, T. Sasaki, H. Yoshimizu, T. Suzuki, Y. Tsujita, M. Tabata, *J. Polym. Sci., Part A: Polym. Chem.* **2014**, *52*, 752.
[41] T. Masuda, F. Sanda, in *Handbook of Metathesis, Vol. 3*, (Ed: R. H. Grubbs), Wiley-VCH, Weinheim, Germany, **2003**, Ch. 3.11, pp. 375.
[42] P. Topka, J. Sedláček, J. Zedník, J. Čejka, H. Balcar, *J. Polym. Sci., Part A: Polym. Chem.* **2008**, *46*, 2593.
[43] A. Furlani, C. Napoletano, M. V. Russo, W. J. Feast, *Polym. Bull.* **1986**, *16*, 311.
[44] J. Svoboda, M. Bláha, J. Sedláček, J. Vohlídal, H. Balcar, I. Mav-Golež, M. Žigon, *Acta Chim. Slov.* **2006**, *53*, 407.
[45] Z. Dong, Z. Ye, *Macromolecules* **2012**, *45*, 5020.
[46] D. Bondarev, J. Zedník, I. Plutnarova, J. Vohlídal, J. Sedláček, *J. Polym. Sci., Part A: Polym. Chem.* **2010**, *48*, 4296.
[47] J. Svoboda, J. Sedláček, J. Zedník, G. Dvořákova, O. Trhlíkova, D. Rédrová, H. Balcar, J. Vohlídal, *J. Polym. Sci., Part A: Polym. Chem.* **2008**, *46*, 2776.
[48] X. Zhan, M. Yang, *Eur. Polym. J.* **2001**, *37*, 1649.
[49] Z. Lei, M. Yang, X. Lin, *Polym. Int.* **1999**, *48*, 781.
[50] S. Petrášová, A. Zukal, J. Brus, H. Balcar, J. Pastva, J. Zedník, J. Sedláček, *Macromol. Chem. Phys.* **2013**, *214*, 2856.
[51] V. Hanková, E. Slováková, J. Zedník, J. Vohlídal, R. Sivkova, H. Balcar, A. Zukal, J. Brus, J. Sedláček, *Macromol. Rapid Commun.* **2012**, *33*, 158.
[52] J. Vohlídal, A. Holländer, M. Jančálková, J. Sedláček, I. Sargánková, *Collect. Czech. Chem. Commun.* **1991**, *56*, 351.
[53] J. Jeromenok, J. Weber, *Langmuir* **2013**, *29*, 12982.
[54] O. Trhlíková, J. Zedník, H. Balcar, J. Brus, J. Sedláček, *J. Mol. Catal. A: Chem.* **2013**, *378*, 57.
[55] J. Sedláček, J. Vohlídal, N. Patev, M. Pacovská, S. Cabioch, O. Lavastre, P. H. Dixneuf, H. Balcar, P. Matějka, *Macromol. Chem. Phys.* **1999**, *200*, 972.

[56] J. Sedláček, J. Vohlídal, *Collect. Czech. Chem. Commun.* **2003**, *68*, 1745.

[57] Z. Ke, S. Abe, T. Ueno, K. Morokuma, *J. Am. Chem. Soc.* **2011**, *133*, 7926.

[58] J. Vohlídal, J. Sedláček, N. Patev, O. Lavastre, P. H. Dixneuf, S. Cabioch, H. Balcar, J. Pfleger, V. Blechta, *Macromolecules* **1999**, *32*, 6439.

[59] K. Dušek, M. Dušková-Smrčková, *Progr. Polym. Sci.* **2000**, *25*, 1215.

[60] S. Hamzehlou, Y. Reyes, J. R. Leiza, *Macromolecules* **2013**, *46*, 9064.

[61] S. M. A. Karim, R. Nomura, T. Masuda, *J. Polym. Sci., Part A: Polym. Chem.* **2001**, *39*, 3130.

[62] D. Tan, W. Fan, W. Xiong, H. Sun, Y. Cheng, X. Liu, C. Meng, A. Li, W.-Q. Deng, *Macromol. Chem. Phys.* **2012**, *213*, 1435.

[63] J. Weber, A. Thomas, in *Nanoporous Materials Synthesis and Applications*, (Ed: Q. Xu), CRC Press, Boca Raton, FL, USA **2013**, p. 1.

[64] S. Kovačič, H. Kren, P. Krajnc, S. Koller, C. Slugovc, *Macromol. Rapid Commun.* **2013**, *34*, 581.

[65] M. S. Silverstein, *Polymer* **2014**, *55*, 304.

[66] K. Zhang, B. Tieke, F. Vilela, P. J. Skabara, *Macromol. Rapid Commun.* **2011**, *32*, 825.

[67] W.-C. Tseng, Y. Chen, G.-W. Chang, *Polym. Degrad. Stabil.* **2009**, *94*, 2149.

[68] S. Makhseed, J. Samuel, *J. Mater. Chem. A* **2013**, *1*, 13004.

Materials
Views
www.MaterialsViews.com

Macromol. Chem. Phys. **2014**, *215*, 1855–1869
© 2014 WILEY-VCH Verlag GmbH & Co. KGaA, Weinheim

Macromolecular
Journals

1869

Transition Metal Catalysed Chain-Growth Polymerization of 1,4-Diethynylbenzene into Microporous Cross-linked Poly(phenylacetylene)s: the Effect of Reaction Conditions.

Eva Slováková[1], Arnošt Zukal[2], Jiří Brus[3], Hynek Balcar[2], Libor Brabec[2], Dmitrij Bondarev[1], Jan Sedláček[1]

[1] Department of Physical and Macromolecular Chemistry, Faculty of Science, Charles University in Prague, Hlavova 2030, CZ-128 43 Prague 2, Czech Republic

[2] J. Heyrovský Institute of Physical Chemistry, v.v.i., Academy of Sciences of the Czech Republic, Dolejškova 3, 182 23 Prague 8, Czech Republic

[3] Institute of Macromolecular Chemistry, v.v.i., Academy of Sciences of the Czech Republic, Heyrovský Sq. 2, 16206 Prague 6, Czech Republic

Correspondence to: J. Sedláček (E - mail: jan.sedlacek@natur.cuni.cz)
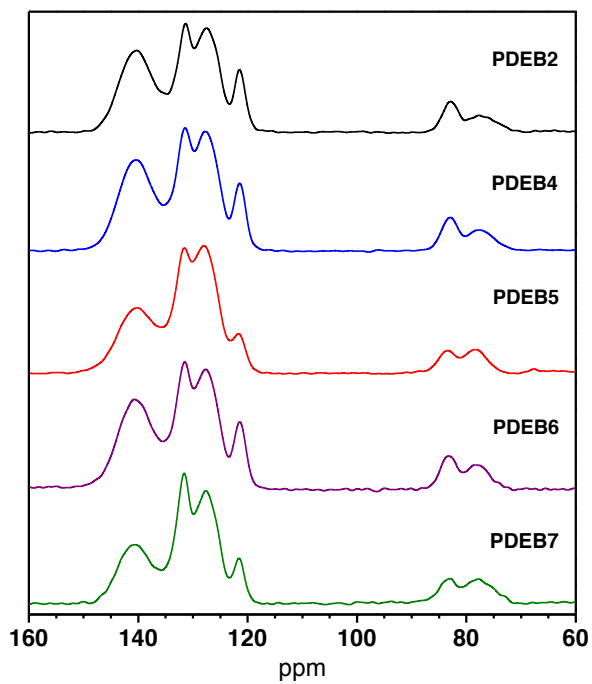
Figure S1 ^{13}C CP/MAS NMR of polymers from Table 2 in the main text.
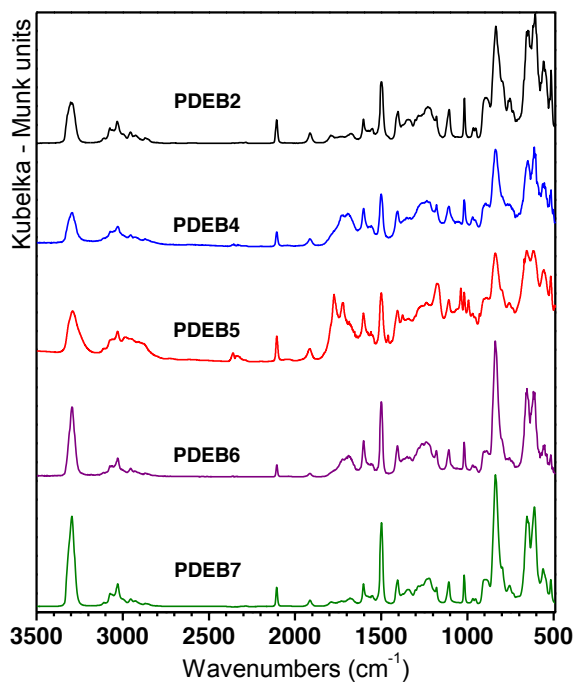
Figure S2 FTIR spectra of polymers from Table 2 in the main text.
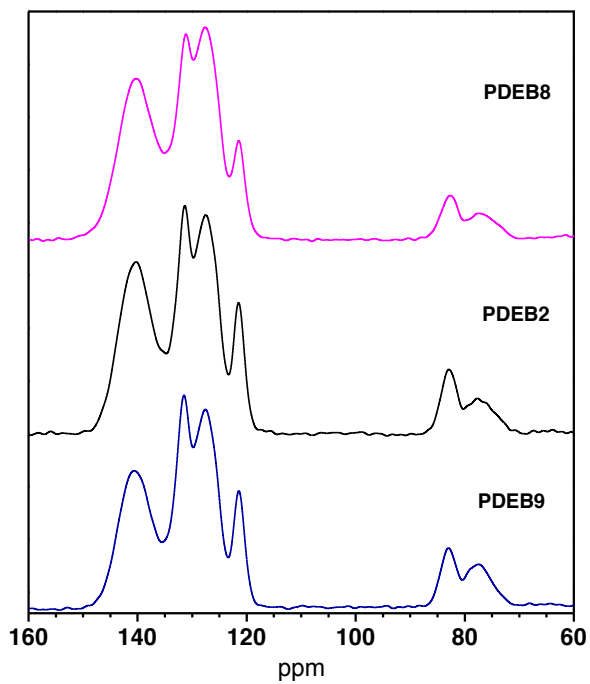
Figure S3 ^{13}C CP/MAS NMR of polymers from Table 3 in the main text.
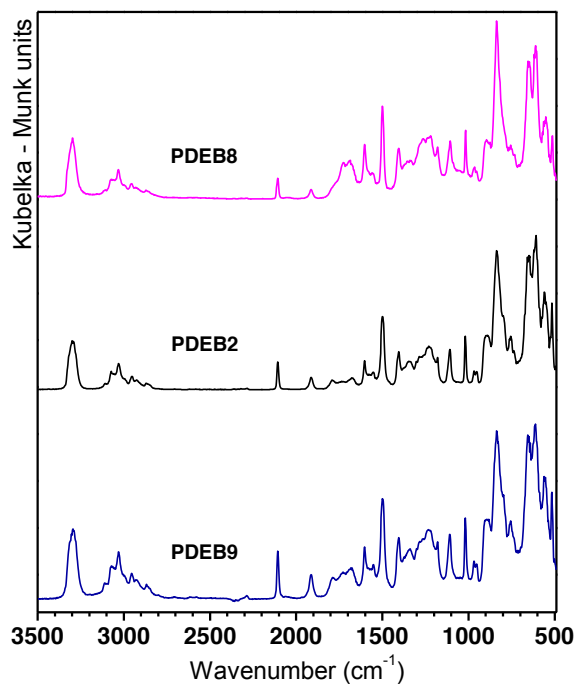
Figure S4 FTIR spectra of polymers from Table 3 in the main text.
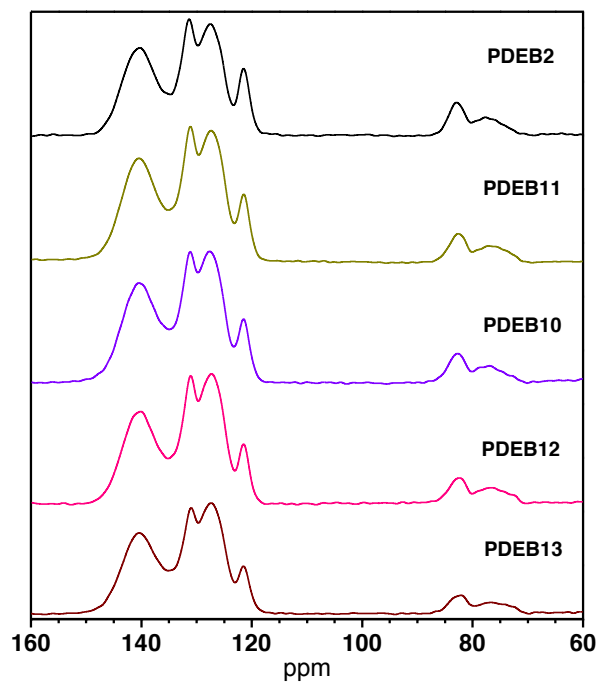
Figure S5 ^{13}C CP/MAS NMR spectra of polymers from Table 4 in the main text.
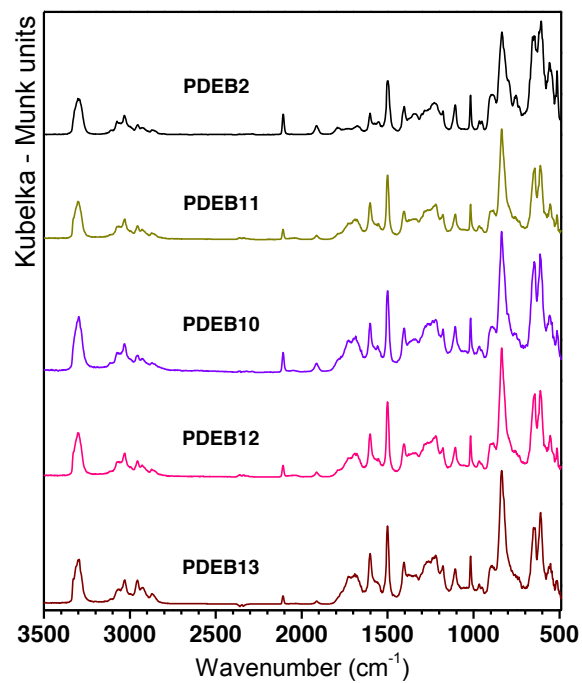
Figure S6 FTIR spectra of polymers from Table 4 in the main text.
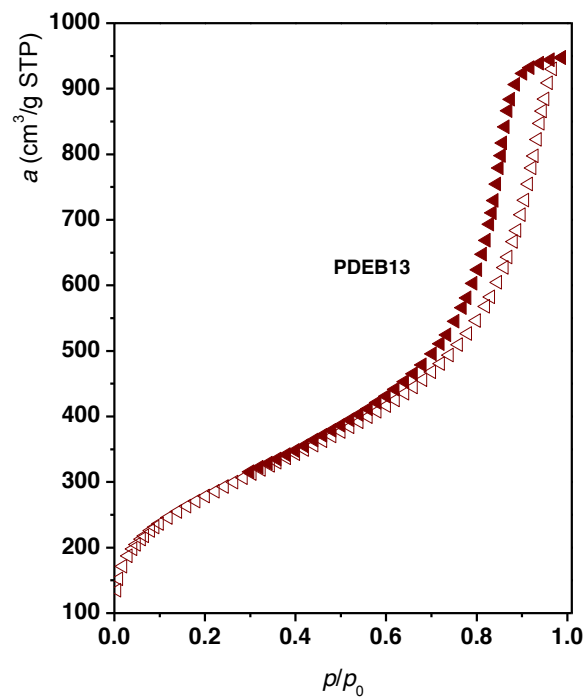
Figure S7 N_2 adsorption isotherms (77K) on polymer PDEB13 from Table 4 in the main text.
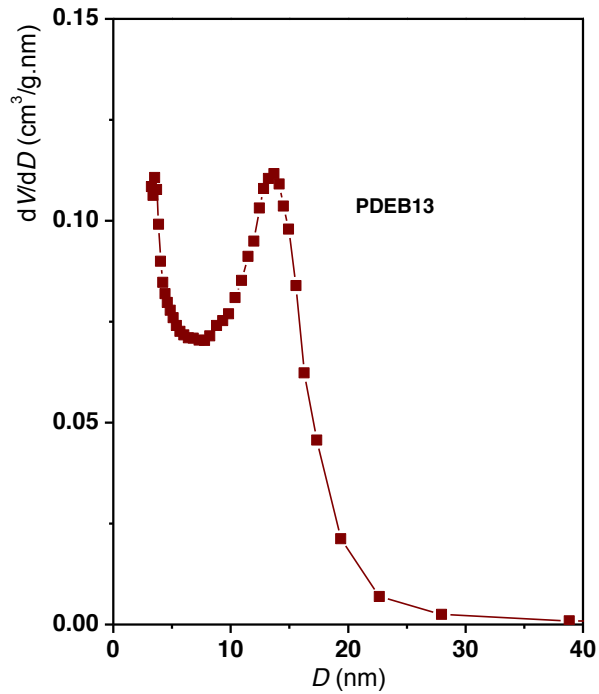
Figure S8 Pore size distribution of polymer PDEB13 from Table 4 in the main text. Calculated from the desorption branch of nitrogen isotherm (The BJH method was used).
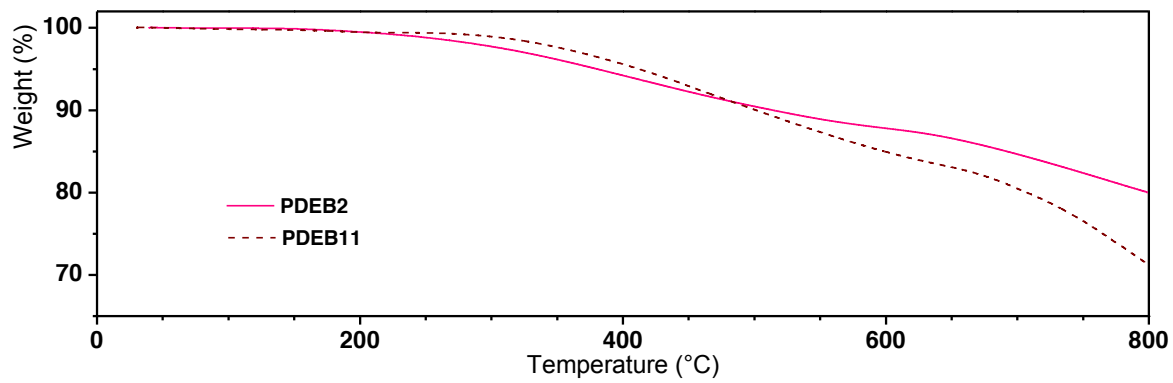
Figure S9 TGA curves (in nitrogen) for samples PDEB2 and PDEB11.
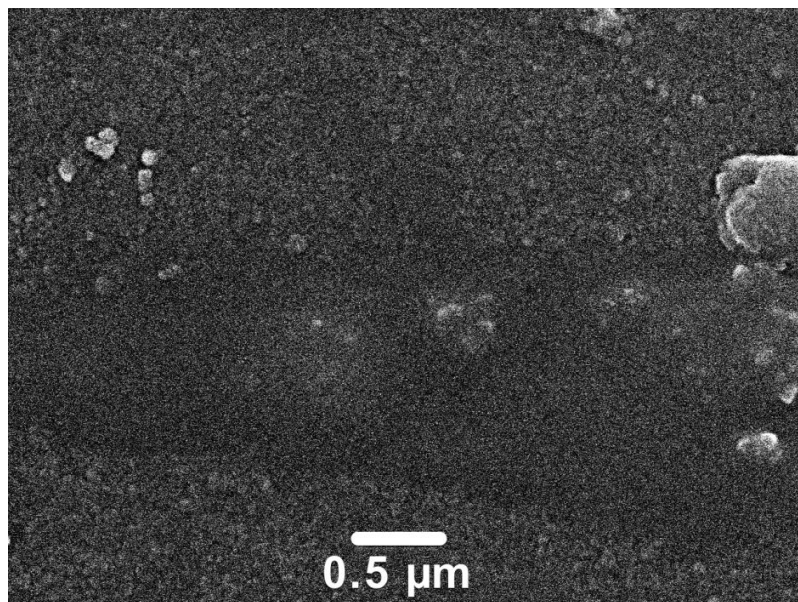
Figure S10 SEM image of PDEB2.
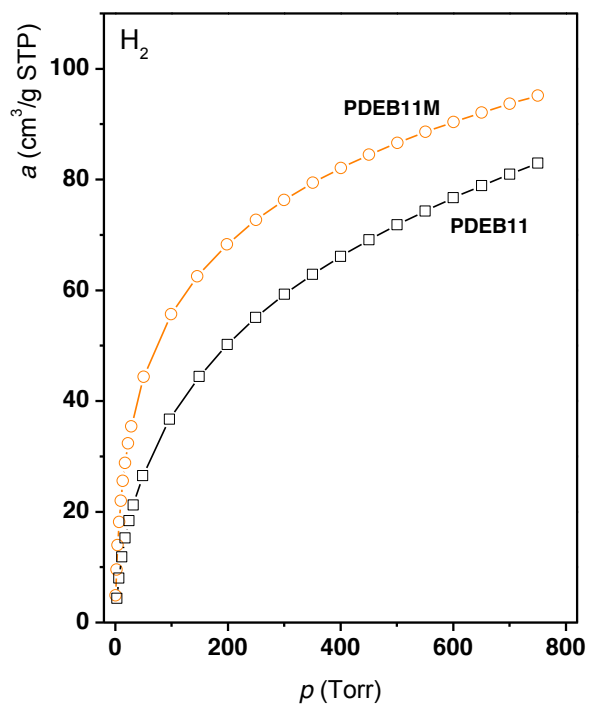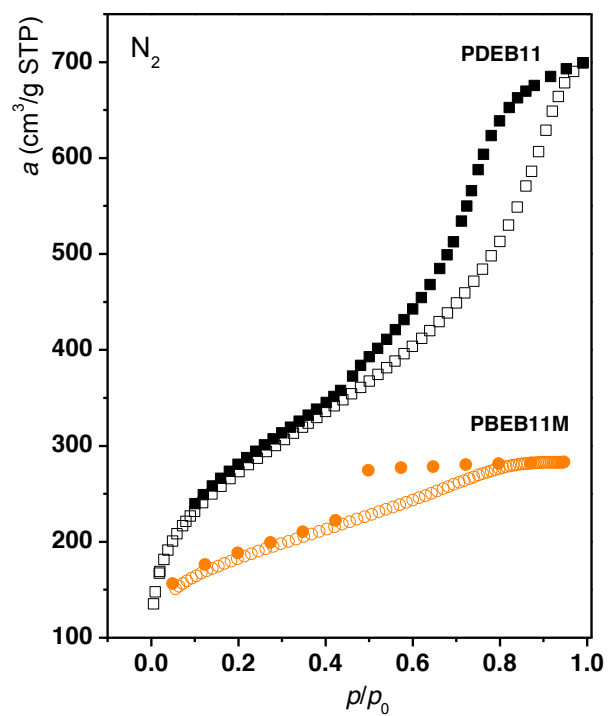
Figure S11 N_2 adsorption isotherms and H_2 adsorption isotherms (both at 77K) on samples PDEB11 and PDEB11M from Table 5 in the main text.

Figure S12 da/dp vs. p obtained from H_2 adsorption isotherms (77K) on samples PDEB11 and PDEB11M from Table 5.

III.

Chain-Growth Insertion Polymerization of 1,3-Diethynylbenzene High Internal Phase Emulsions into Reactive π-Conjugated Foams

Eva Slováková,[†] Marjan Ješelnik,[‡] Ema Žagar,[‡] Jiří Zedník,[†] Jan Sedláček,*[,†] and Sebastijan Kovačič*[,‡]

[†]Department of Physical and Macromolecular Chemistry, Faculty of Science, Charles University in Prague, Hlavova 9, 128 43 Praha 2, Czech Republic

[‡]Laboratory for Polymer Chemistry and Technology, National Institute of Chemistry, Hajdrihova 19, 1000 Ljubljana, Slovenia

Ⓢ Supporting Information

ABSTRACT: The π-conjugated micro/macroporous polyacetylene-type polyHIPE foams were synthesized for the first time by a chain-growth insertion polymerization of high internal phase emulsions (HIPEs). In the first step, the π-conjugated polyHIPE foams were prepared by polymerization of 1,3-diethynylbenzene HIPEs using [Rh(nbd)acac] complex as a catalyst. The π-conjugated polyHIPE foams consist of ethynylphenyl-substituted polyene main chains which are cross-linked by the 1,3-phenylene linkers. In the second step, the foams were chemically and thermally postmodified by applying the alkyne−azide cycloaddition reaction and the solvent free solid phase hyper-cross-linking at temperature of 280 °C. Thus, obtained polyacetylene-type polyHIPE foams exhibit hierarchically structured micro/macroporous morphology with sizes of the macropores and interconnecting pores of 3.4 ± 0.3 μm (or 4.8 ± 0.8 μm) and 0.96 μm (or 1.1 μm), respectively, wherein a substantial volume of micropores is also found within the macroporous walls as revealed by the calculations from the t-plots. The BET (Brunaer−Emmett−Teller) surface area of up to 110 and 380 m^2 g^{-1} was determined before and after solid phase hyper-cross-linking, respectively.
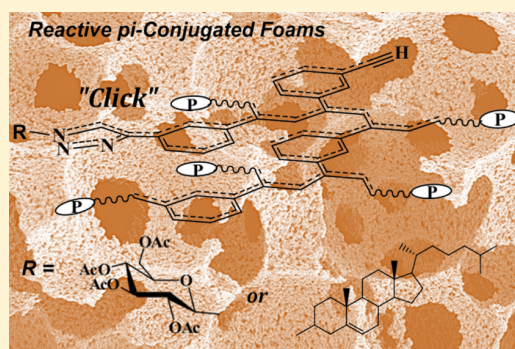
■ INTRODUCTION

The chain growth polymerization of ethynyl-containing monomers with transition-metal catalysts produces substituted polyacetylenes, i.e., conjugated polymers with alternating double and single bonds along the main chains.[1] This unique electronic structure endows substituted polyacetylenes with the properties (e.g., optical, magnetic, and luminisence properties),[2] which are very difficult to access with the corresponding vinyl polymers. Recently, the π-conjugated microporous polymers (CMPs)[3] have been attracted much attention owing to the high specific surface area, high extent of π-conjugation as well as pronounced and tunable microporosity. These materials have been widely studied in many application fields like gas separation,[4] reversible storage,[5] heterogeneous catalysis,[6] optoelectronics, and sensors.[7] Various step-growth polymerizations based on coupling and condenzation reactions have been used for the CMPs preparation.[3] Recently, the chain-growth polymerization of ethynyl-containing monomers has been demonstrated to be an effective tool for the CMPs preparation.[8] The major drawback of all microporous materials (including CMPs) and with this associated limited practical use of these materials is that they suffer from slow kinetics due to the mass transport limitations. Therefore, combining high surface area of CMPs with macroporous architecture of,, e.g., polyHIPEs[9] (*vide infra*) would greatly improve the hydrodynamic properties of CMPs and open up new application opportunities of such systems.

High internal phase emulsions (HIPEs), yielding the polyHIPEs after polymerization, are heterogeneous liquid−liquid mixtures characterized by a droplet (internal) phase volume fraction of at least 74% of the total emulsion volume.[10] Templating within the high internal phase emulsions (HIPEs) represents an interesting technique for the production of macroporous polymeric materials and has become very active research area.[11] Several polymerization mechanisms like free radical polymerization (FRP),[12] ATRP,[13] RAFT,[14] thiol−ene, and thiol−yne reactions,[15] as well as ROMP,[16] have been already used to solidify HIPEs. Recently, Zhang et al. reported the use of HIPE templating approach to combine the properties of polyHIPEs and CMPs, but the cavity-like structure of polyHIPEs and the high specific surface area of CMPs, representing the typical characteristics of these two types of materials, are missing. Nevertheless, thus obtained π-conjugated polyHIPEs were successfully applied as the heterogeneous photocatalysts.[17]

Herein, we propose for the first time rhodium catalyzed chain-growth insertion polymerization as a new tool for the preparation of reactive and well-defined three-dimensional (3D) micro/macroporous π-conjugated polyHIPE foams from the 1,3-diethynylbenzene (1,3-DEB) high internal phase

emulsions (HIPE). Furthermore, a potential of postmodification of nonreacted ethynyl groups either chemically via the azide "click" reaction or thermally via the aromatization reaction, is demonstrated.

■ EXPERIMENTAL SECTION

Materials and Synthesis. 1,3-Diethynylbenzene (1,3-DEB) (TCI Europe; amounts according to Table S1, Supporting Information) and surfactant Span80 (Sorbitan monooleate; MW = 428 g·mol⁻¹; Sigma-Aldrich) were placed in a 50 mL ampule and the mixture was stirred with an overhead stirrer at 400 rpm. The corresponding amount (*cf.* Table S1) of deionized water was added dropwise under constant stirring. After addition of water the mixture was further stirred for 1 h until a uniform emulsion was formed. Then, a solution of the catalyst (acetylacetonato)(bicyclo[2.2.1]hepta-2,5-diene)rhodium(I), [Rh-(nbd)acac] (Sigma-Aldrich; *cf.* Table S1) in dichloromethane (Lachema, Czech Republic) was added to the emulsion and the mixture was further stirred for 1 min. Subsequently, the emulsion was cured at room temperature for 3 h. The resulting solid polymer, poly(1,3-DEB), was repeatedly washed with CH_2Cl_2, separated by filtration, and dried in a vacuum oven at room temperature.

Characterization. The morphology investigations were performed by a scanning electron microscopy (SEM). The SEM images were taken on a Field emission electron microscope Ultra+ (Carl Zeiss) equipped with an energy dispersive spectrometer SDD X-Max 50 (Oxford Instruments). A piece of each sample was mounted on a carbon tab for better conductivity and the thin layer of gold was sputtered on the sample's surface prior scanning analysis (See details in the Supporting Information). The nitrogen adsorption measurements of polymer samples were performed on a Micromeritics TriStar 3000 surface area analyzer. The samples were outgassed at 90 °C under turbomolecular vacuum pump. The BET surface area was determined by means of nitrogen adsorption data in a relative pressure range from 0.05 to 0.25. In this pressure range the BET transform plots were linear. The ^{13}C CP/MAS NMR spectra were measured at 11.7 T using a Bruker Avance 500 WB/US NMR spectrometer with a double-resonance 4 mm probe head at a spinning frequency of 20 kHz. The Fourier transform IR (FTIR) spectra were measured on a Nicolet Magna IR 760 using the diffuse reflection mode (DRIFTS). Samples were diluted with KBr. The diffuse reflectance UV/vis (DR UV/vis) spectra of the solid polymers were recorded on a Perkin−Elmer Lambda 950 spectrometer. The polymers were diluted with $BaSO_4$ (1/10, w/w) before the measurements. The photoluminescence (PL) emission spectra of the solid polymers were measured on a Horiba Jobin Yvon Fluorolog 3 using a solid-state film holder (22.5 deg angle) and an excitation wavelength of 420 nm. Samples for the measurements were prepared as follows. Approximately 10 mg of finely powdered polymer was mixed with three drops of microscope glue (Entellan PB 5265, Euromex Microscopes, Holland). Then, the mixture was transferred to the fresh surface of the pyrolitic graphite slide (NT-MDT comp.).

■ RESULTS AND DISCUSSION

The HIPEs consisted of a mixture of 1,3-DEB (10 and 20 vol % of the whole emulsion volume) as a monomer and sorbitane monooleate (Span80; 23 vol % according to the monomer) as a surfactant. The internal (droplet) phase used was pure deionized water (90 and 80 vol % of the whole emulsion volume) (cf. Scheme 1 and Supporting Information, Table S1). A ratio between the continuous and the internal phase allowed, after the polymerization of the continuous phase of the HIPE, the preparation of polyHIPE foams with 90% (sample ES117) and 80% (sample ES119) porosity. All HIPEs were stirred for 1 h at 400 rpm and afterward, the initiator [Rh(nbd)acac] complex (1 mol % with respect to the monomer dissolved in dichloromethane) was added (cf. Supporting Information, Table S1). Curing the HIPEs at room temperature resulted

Scheme 1. Preparation Protocol of the π-Conjugated PolyHIPE Foams with Intrinsic Porosity
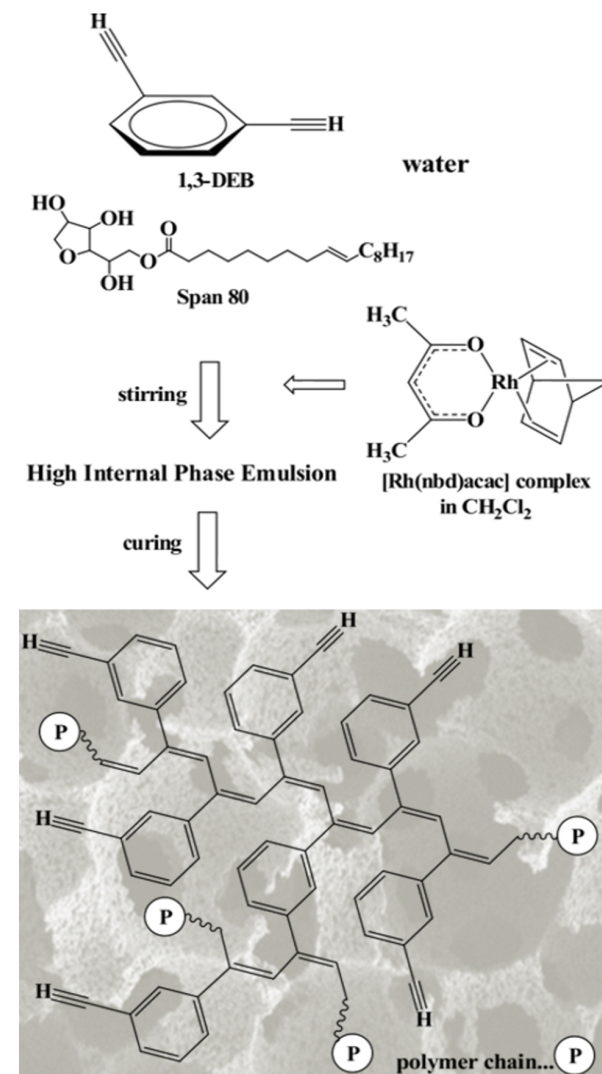
in solid polymeric materials, which were purified by decantation in dichloromethane, filtered, and dried under vacuum at room temperature until they reached a constant weight. All the prepared polymers were brown-red brittle monolithic pieces, insoluble and nonswellable in tested solvents (THF, CH_2Cl_2, $CHCl_3$, and benzene). Before the determination of polymerization yields, a few milligrams of each polymer was suspended in THF for 5 h at room temperature and the liquid phase (filtered off) analyzed by SEC (a column used was suitable for the oligomeric molecular-weight (MW) range). The chromatograms of the THF extracts of both ES117 and ES119 samples show the absence of the low MW compound(s) as well as the soluble polymer. The polymerization yields, calculated gravimetrically by setting the mass of the dried monoliths in relation to the mass of the 1,3-DEB monomer, are 66 and 53% for the samples ES117 and ES119, respectively. The rigid monolithic pieces were further characterized by scanning electron microscopy (SEM) to visualize and evaluate the foam morphology. The typical open cellular polyHIPE architecture is observed for both samples (cf. Figure 1). The mean cavity diameter determined by the SEM image analysis[18] (cf. Figure 1)
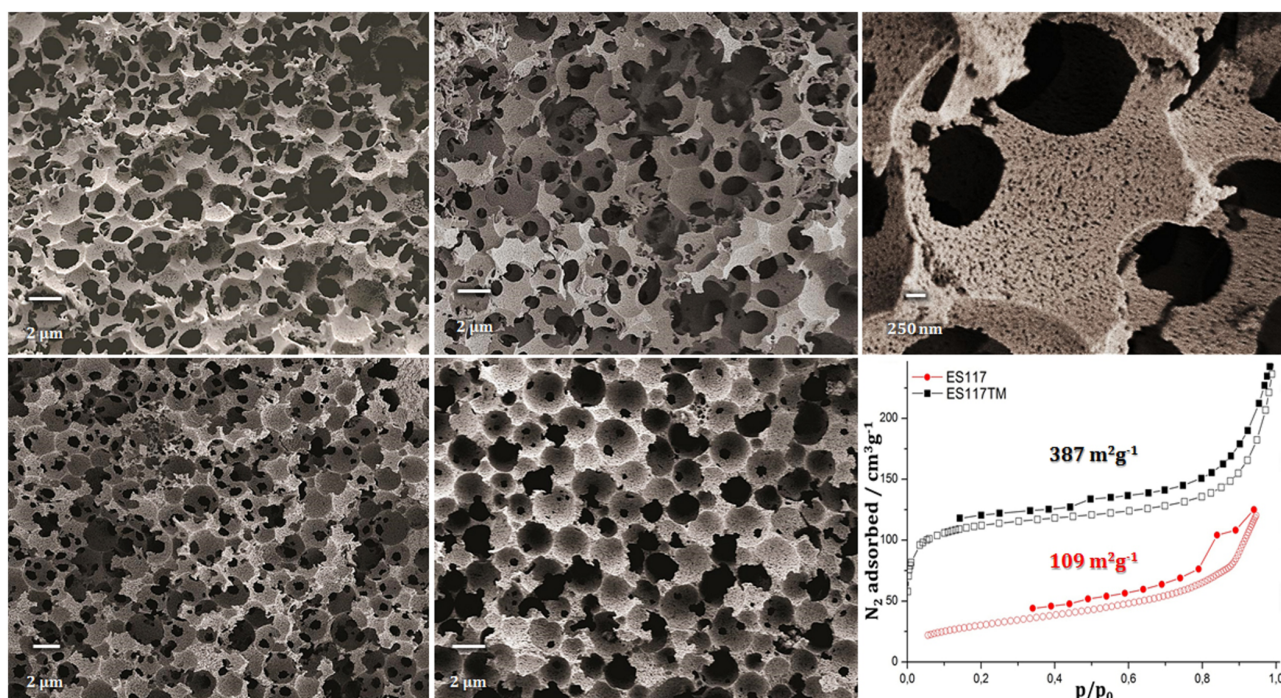
Figure 1. First row from left to right: SEM images of **ES119**, **ES117**, and **ES117** at higher magnification. Second row from left to right: SEM images of samples **ES119TM** (upon thermal modification), **ES119-CHOL** (upon chemical modification with CHOL), and N2 sorption isotherms (77 K) for samples **ES117** (black squares) and **ES117TM** (red circles). Key: empty points, adsorption; full points, desorption.

is 4.8 ± 0.8 and 3.4 ± 0.3 μm for the samples ES117 and ES119, respectively. The size of the interconnecting pores as determined from a mercury porosimetry data is 1.1 and 0.96 μm for the samples ES117 and ES119, respectively. The skeleton density as determined by a helium pycnometry is 1.21 and 1.17 g cm^{-3} for the samples ES117 and ES119, respectively (cf. Supporting Information Table S1). Of particular interest is the specific surface area of the novel polyacetylene-type π-conjugated polyHIPE foams. Generally, the polyHIPE foams prepared by polymerization of the HIPE emulsions tend to have rather low BET (Brunaer–Emmett–Teller) surface area (typically between 10–20 m^2 g^{-1}) due to low the amount of micro/mesopores, and only upon their additional treatment by hypercross-linking[19] or addition of inert porogens,[20] the surface area can be increased. In our case, an increase of the BET surface area from 15 (sample ES119) to 109 m^2 g^{-1} (sample ES117) can be ascribed to a syneresis effect, where the volume of CH_2Cl_2 used to dissolve the catalyst plays a role. Continuously growing polymer network inside discrete monomer-swollen micelles starts to precipitate in the form of gel-like nuclei that continue to grow and aggregate into the clusters through the process called syneresis.[21] Micro/mesopores are then formed as spaces inside these precipitated polymeric clusters. In order to prevent collapsing of polymeric clusters during drying, the polymer phase has to be sufficiently rigid. In our case, the rigidity of the polymer is provided by the polyene character of the main chains and the high extent of cross-linking. The presence of micro/mesopores in ES117 can be deduced from the shape of N_2 adsorption isotherms (cf. Figure 1 and S4). Moreover, the highly magnified SEM image (cf. Figure 1) shows small macropores (size between 70 and 100 nm) within the walls of cavities, which were formed as

spaces between agglomerated polymeric clusters that precipitate during syneresis.

In addition, the specific surface area was further increased by applying the so-called solid-state hyper-cross-linking approach, which is, as compared to the solution based hyper-cross-linking,[19] a solvent free approach that does not require a solvent to swell the polymer skeleton or a catalyst to trigger the postpolymerization cross-linking. In our approach, the remaining pendant ethynyl groups of the poly(1,3-DEB) skeleton were thermally reacted via the aromatization at 280 °C.[22] The thermally modified samples were labeled as ES117TM and ES119TM. The enlargement of the specific BET surface area from 15 to up to 184 m^2 g^{-1} for the sample ES119TM and from 109 to up to 387 m^2 g^{-1} for the sample ES117TM was observed from the data of nitrogen adsorption measurements (cf. Figure 1 and Supporting Information: Table S1 and Figure S4). After thermal modification an increase of skeletal density from 1.21 to 1.30 gcm^{-3} for the sample ES117 and from 1.17 to 1.36 gcm^{-3} for the sample ES119 was observed that reflects certain degree of hyper-cross-linking in the course of aromatization reaction. On the other hand, the macroporous architecture of the materials is totally preserved as indicate the SEM images of the thermally treated samples (cf. Figure 1 and Supporting Information Figure S3).

The chemical characterization of the newly obtained π-conjugated polyHIPEs comprised elemental analysis (EA), Fourier transform IR (FTIR), diffuse reflectance UV/vis (DR UV/vis) and photoluminescence (PL) spectroscopies as well as solid-state NMR spectroscopy (^{13}C CP/MAS NMR). Examination of the elemental composition of the ES119 sample gave the values of 90.96% C and 4.52% H that result in an empirical formula of $C_{10}H_{5.9}$ ($C_{10}H_6$ theoretically) and a C/H molar ratio of 1.677 (1.667 theoretically). The EA of the thermally

modified ES119TM sample revealed the values of 86.72% C and 3.77% H that result in the empirical formula of $C_{10}H_{5.2}$ and the C/H molar ratio of 1.917 (*cf.* Supporting Information, Table S3). The increase in C/H molar ratio is ascribed to aromatization of the sample in the course of thermal modification. The same can be concluded from the EA results of the sample pair ES117 and ES117TM (Supporting Information, Table S3). The ^{13}C CP/MAS NMR spectra of the ES117 and ES119 samples show a broad, partly resolved signal in the region 115−150 ppm that corresponds to the aromatic carbons and the carbons of the polyene main chains,[23] while the signals at about 83 and 76 ppm are due to the carbons of the nonreacted pendant ethynyl groups (cf. Figure 2).[8] The
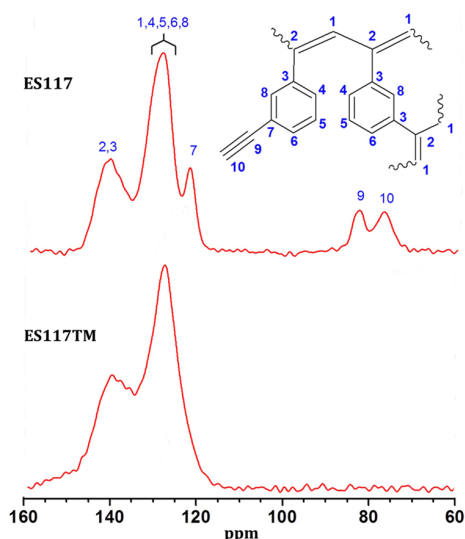
Figure 2. Enlarged ^{13}C CP/MAS NMR spectra of pristine ES117 (above) and thermally modified ES117TM (below) samples.

evaluation of the amount of free ethynyl groups from the ^{13}C CP/MAS NMR spectra of the ES117 and ES119 samples reveals the presence of about 5.1 mmol (ethynyl groups)/g, i.e. 0.64 of free ethynyl groups per one monomeric unit. Consequently, the degree of branching (DB) defined as DB

$= n_B/(n_L + n_B)$, where the n_B and n_L stand for the amounts of branched and linear monomeric units in polymer, respectively, is estimated to be 0.36 for both samples. In the ^{13}C CP/MAS NMR spectra of thermally modified ES117TM and ES119TM samples, no signals are observed in the region 76−83 and, thus, these results indicate complete or almost complete thermal transformation of the pendant ethynyl groups in parent samples (cf. Figure 2). The same conclusion results from the FTIR spectra of the thermally modified samples which particularly show an almost complete disappearance of the band at 3300 cm^{-1} ($\nu_{\equiv C-H}$) upon thermal modification of parent polymers (cf. Supporting Information: Figures S5 and S6). Because of fully conjugated nature of the polymer backbone, the DR UV/vis spectroscopy was performed and the spectra of both samples show a broad absorption band with the maximum in the region from 370 to 420 nm (cf. Figure 3). Upon samples' thermal modification the vis band tail red-shifted due to the enhanced extent of samples' conjugation (cf. Figure 3). When excited by the light of 420 nm wavelength both the parent and the thermally modified polymers exhibit photoluminescence manifested by a broad photoluminescence (PL) emission band with the maximum at 525 nm (parent polymers) and 530 nm (thermally modified polymers) (cf. Figure 3). Another way to postmodify the poly(1,3-DEB) backbone involved alkyne−azide cycloaddition ("click") reaction via the nonreacted pendant ethynyl groups. Mimicking a biological surface within the synthetic 3D scaffolds is an attractive prospect to prepare porous polymers as potential scaffolds for cell culturing.[24] For this purpose the 1-azido-2,3,4,6-tetra-*O*-acetyl-*β*-D-glucose (GLU) and the 3*β*-azido-5-cholestene (CHOL) were synthesized in accordance with the known synthetic procedure[25] and reacted with the remaining ethynyl groups of ES119 sample (cf. Scheme 2). A content of the GLU units in the ES119-GLU sample is 0.35 mmol/g and that of the CHOL units in the ES119-CHOL sample is 0.15 mmol/g as calculated based on the nitrogen content in the modified samples (see details in Supporting Information). Again, the polyHIPE architecture of chemically modified polymeric foams is totally preserved as reveal the SEM images of the ES119-GLU and ES119-CHOL samples (cf. Figure 1 and Supporting Information).
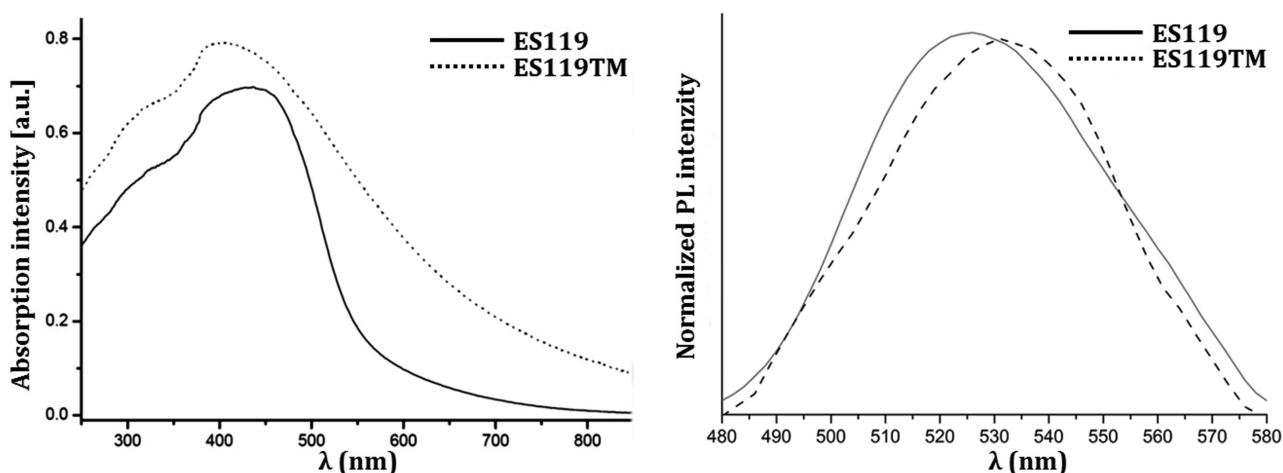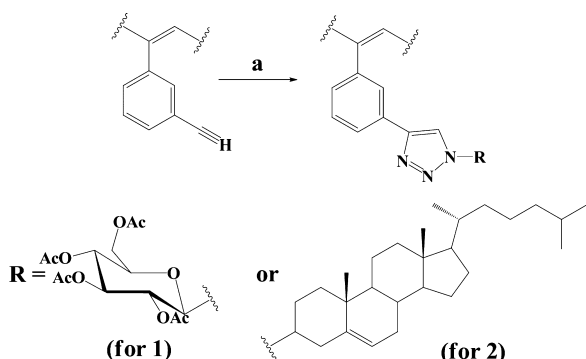

Figure 3. DR UV/vis spectra of pristine ES119 and thermally modified ES119TM samples (left) and photoluminescence (PL) spectra of pristine ES119 and thermally modified ES119TM samples (right).

Scheme 2. Chemical Modification Reactions: RN$_3$, Heating in (a) Toluene (for 1) or Xylene (for 2)

CONCLUSIONS

The chain-growth, rhodium catalyzed, insertion polymerization was applied for the preparation of fully conjugated and reactive polyacetylene-type polyHIPE foams with intrinsic microporosity. Thus, obtained polymeric foams show well-defined hierarchically structured micro/macroporous polyHIPE architecture with significantly higher specific surface area as compared to the standard polyHIPE foams, and high inherent reactivity. Latter was demonstrated by alkyne−azide cycloaddition of D-glucose azide and cholesteryl azide to the pendant ethynyl groups of the 1,3-DEB skeleton and by the solid phase hyper-cross-linking reaction. Chain-growth catalytic insertion polymerization (CIP) technique to solidify HIPEs can endow polyHIPE foams with unique electronic structure and properties that are very difficult to access with the corresponding vinyl monomers. Therefore, this chain-growth CIP has a great potential to extend the fields of advanced applications of this class of porous polymers in the future.

ASSOCIATED CONTENT

Ⓢ Supporting Information

Experimental details and additional SEM images, FTIR spectra, and N$_2$ sorption isotherm data. This material is available free of charge via the Internet at http://pubs.acs.org.

AUTHOR INFORMATION

Corresponding Authors

*(J.S.) E-mail: jan.sedlacek@natur.cuni.cz.
*(S.K.) E-mail: sebastijan.kovacic@ki.si.

Notes

The authors declare no competing financial interest.

ACKNOWLEDGMENTS

REFERENCES

(1) (a) Shiotsuki, M.; Sanda, F.; Masuda, T. *Polym. Chem.* **2011**, *2*, 1044. (b) Liu, J. Z.; Lam, J. W. Y.; Tang, B. Z. *Chem. Rev.* **2009**, *109*, 5799.

(2) (a) Grimsdale, A. C.; Chan, K. L.; Martin, R. E.; Jokisz, P. G.; Holmes, A. B. *Chem. Rev.* **2009**, *109*, 897. (b) Jose, B. A. S.; Akai, K. *Polym. Chem.* **2013**, *4*, 5144. (c) Li, W.; Huang, H.; Lia, Y.; Deng, J. *Polym. Chem.* **2014**, *5*, 1107. (d) Sivkova, R.; Vohlídal, J.; Bláha, M.; Svoboda, J.; Sedláček, J.; Zedník, J. *Macromol. Chem. Phys.* **2012**, *213*, 411.

(3) (a) Xu, Y.; Jin, S.; Xu, H.; Nagaia, A.; Juany, D. *Chem. Soc. Rev.* **2013**, *42*, 8012. (b) Liu, Q.; Tang, Z.; Wu, M.; Zhou, Z. *Polym. Int.* **2014**, *63*, 381.

(4) McKeown, N. B.; Budd, P. M.; Msayib, K. J.; Ghanem, B. S.; Kingston, H. J.; Tattershall, C. E.; Makhseed, S.; Reynolds, K. J.; Fritsch, D. *Chem.—Eur. J.* **2005**, *11*, 2610.

(5) Dawson, R.; Ratvijitvech, T.; Corker, M.; Laybourn, A.; Khimyak, Y. Z.; Cooper, A. I.; Adams, D. J. *Polym. Chem.* **2012**, *3*, 2034.

(6) (a) Palkovits, R.; Antonietti, M.; Kuhn, P.; Thomas, A.; Schuth, F. *Angew. Chem.* **2009**, *121*, 7042. (b) Dawson, R.; Adams, D. J.; Cooper, A. I. *Chem. Sci.* **2011**, *2*, 1173. (c) Stoeck, U.; Nickerl, G.; Burkhardt, U.; Senkovska, I.; Kaskel, S. *J. Am. Chem. Soc.* **2012**, *134*, 17335.

(7) (a) Chen, Y.; Honsho, S.; Seki, I.; Jiang, D. *J. Am. Chem. Soc.* **2010**, *132*, 6742. (b) Brandt, J.; Schmidt, J.; Thomas, A.; Epping, J. D.; Weber, J. *Polym. Chem.* **2011**, *2*, 1950.

(8) (a) Hanková, V.; Slováková, E.; Zedník, J.; Vohlídal, J.; Sivkova, R.; Balcar, H.; Zukal, A.; Brus, J.; Sedláček, J. *Macromol. Rapid Commun.* **2012**, *33*, 158. (b) Petrašová, S.; Zukal, A.; Brus, J.; Balcar, H.; Pastva, J.; Zedník, J.; Sedláček, J. *Macromol. Chem. Phys.* **2013**, *214*, 2856.

(9) "polyHIPE" is a Unilever trademark.

(10) Cameron, N. R.; Krajnc, P.; Silverstein, M. S. Colloidal Templating. In *Porous Polymers*; Silverstein, M. S., Cameron, N. R., Hillmyer, M. A.Eds.; Wiley & Sons: 2011.

(11) Silverstein, M. S. *Prog. Polym. Sci.* **2014**, *39*, 199.

(12) (a) Barbetta, A.; Dentini, M.; Leandri, L.; Ferraris, G.; Coletta, A.; Bernabei, M. *React. Funct. Polym.* **2009**, *69*, 724. (b) Audouin, F.; Fox, M.; Larragy, R.; Clarke, P.; Huang, J.; O'Connor, B.; Heise, A. *Macromolecules* **2012**, *45*, 6127−6135. (c) Wong, L. L. C.; Baiz Villafranca, P. M.; Menner, A.; Bismarck, A. *Langmuir* **2013**, *29*, 5952.

(13) Lamson, M.; Epsthein-Assor, Y.; Silverstein, M. S.; Matyjaszewski, K. *Polymer* **2013**, *54*, 4480.

(14) Luo, Y.; Wang, A.-N.; Gao, X. *Soft Matter* **2012**, *8*, 1824.

(15) (a) Lovelady, E.; Kimmins, S. D.; Wu, J.; Cameron, N. R. *Polym. Chem.* **2011**, *2*, 559. (b) Sergent, B.; Birota, M.; Deleuze, H. *React. Funct. Polym.* **2012**, *72*, 962.

(16) (a) Deleuze, H.; Faivre, R.; Herroguez, V. *Chem. Commun.* **2002**, 2822. (b) Kovačič, S.; Krajnc, P.; Slugovc, C. *Chem. Commun.* **2010**, *46*, 7504. (c) Kovačič, S.; Jeřabek, K.; Krajnc, P.; Slugovc, C. *Polym. Chem.* **2012**, *3*, 325. (d) Kovačič, S.; Matsko, N. B.; Jeřabek, K.; Krajnc, P.; Slugovc, C. *J. Mater. Chem. A* **2013**, *1*, 487. (e) Kovačič, S.; Kren, H.; Krajnc, P.; Koller, S.; Slugovc, C. *Macromol. Rapid Commun.* **2013**, *34*, 581. (f) Knall, A.-C.; Kovacic, S.; Hollauf, M.; Reishofer, D. P.; Saf, R.; Slugovc, C. *Chem. Commun.* **2013**, *49*, 7325. (g) Kovačič, S.; Matsko, N. B.; Ferk, G.; Slugovc, C. *J. Mater. Chem. A* **2013**, *1*, 7971. (h) Kovačič, S.; Preishuber-Pflugl, F.; Slugovc, C. *Macromol. Mater. Eng.* **2014**, *299*, 843.

(17) (a) Zhang, K. A. I.; Vobecka, Z.; Tauer, K.; Antonietti, M.; Vilela, F. *Chem. Commun.* **2013**, *49*, 11158. (b) Wang, Z. J.; Landfester, K.; Zhang, K. A. I. *Polym. Chem.* **2014**, *5*, 3559.

(18) Barbetta, A.; Cameron, N. R. *Macromolecules* **2004**, *37*, 3188.

(19) (a) Schwab, M. G.; Senkovska, I.; Rose, M.; Klein, N.; Koch, M.; Pahnke, J.; Jonschker, G.; Schmitz, B.; Hirscher, M.; Kaskel, S. *Soft Matter* **2009**, *5*, 1055. (b) Pulko, I.; Wall, J.; Krajnc, P.; Cameron, N. R. *Chem.—Eur. J.* **2010**, *16*, 2350.

(20) Barbetta, A.; Cameron, N. R. *Macromolecules* **2004**, *37*, 3202.

(21) (a) Gokmen, M. T.; Du Perez, F. E. *Prog. Polym. Sci.* **2012**, *37*, 365. (b) Sterchele, S.; Centomo, P.; Zecca, M.; Hanková, L.; Jeřábek, K. *Microporous Mesoporous Mater.* **2014**, *185*, 26.

(22) Tseng, W.-C.; Chen, Y.; Chang, G.-W. *Polym. Degrad. Stab.* **2009**, *94*, 2149.

(23) Sedláček, J.; Vohlídal, J.; Cabioch, S.; Lavastre, O.; Dixneuf, P.; Balcar, H.; Štícha, M.; Pfleger, J.; Blechta, V. *Macromol. Chem. Phys.* **1998**, *199*, 155.

(24) Hayward, A. S.; Eissa, A. M.; Maltman, D. J.; Sano, N.; Przyborski, S. A.; Cameron, N. R. *Biomacromolecules* **2013**, *14*, 4271.

(25) (a) Kumar, R.; Maulik, P. R.; Misra, A. K. *Glycoconjugate J.* **2008**, *25*, 595. (b) Sun, Q.; Cai, S.; Peterson, B. R. *Org. Lett.* **2009**, *11*, 567.

Chain-Growth Insertion Polymerization of 1,3-Diethynylbenzene in High Internal Phase Emulsions into Reactive Π-Conjugated Foams

Eva Slováková, Marjan Ješelnik, Ema Žagar, Jiří Zedník, Jan Sedláček, Sebastijan Kovačič

Supplementary Information
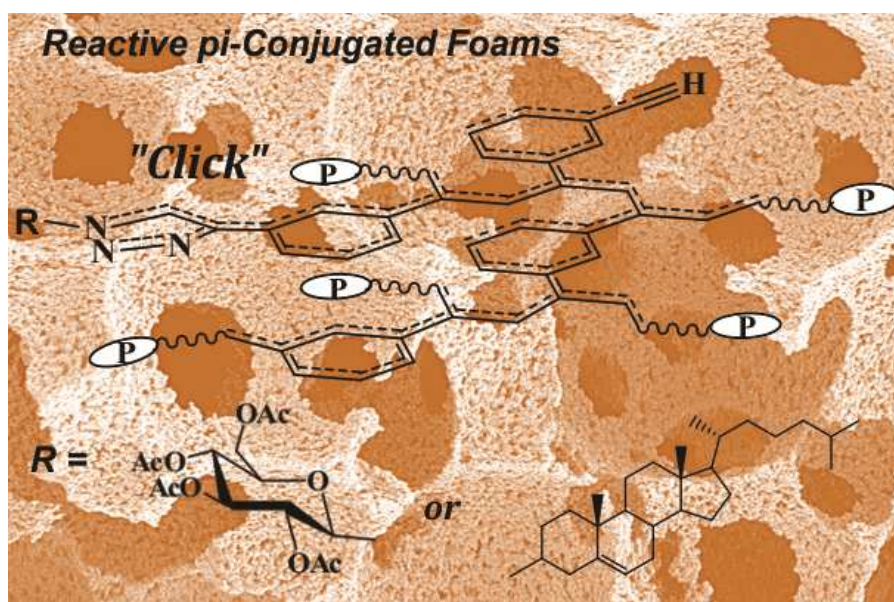
Table S1. Emulsions' composition

sample	V (1,3-DEB) [mL]	m (Rh) [mg]	V (CH$_2$Cl$_2$) [mL]	Surf. [mL]	V(H$_2$O) [mL]	E[a] [%]	Y.P.[b] [%]	S$_{BET}$ [m^{2}g^{-1}]	Skeleton density [gcm^{-3}][c]	V$_{micropores}$ [cm^3 g^{-1}][d]
ES117	2.00	44.3	1.5	0.6	17	90	66	109	1.210	0.0104
ES119	2.00	44.3	0.3	0.6	8	80	53	15	1.171	0.0017
ES117TM	Thermally modified sample ES117							387	1.300	0.1220
ES119TM	Thermally modified sample ES119							184	1.365	0.0114

[a] Theoretical porosity in per cent calculated from the volume ratio of water and 1,3-DEB
[b] Yield of polymer
[c] Determined by helium pycnometry
[d] Determined from the t-plot analyses according to Harkins and Jura[1]

1. Post-modification of poly(1,3-DEB)s

Thermal modification

Post-synthesis of poly(1,3-DEB)s was performed by thermal modification in a Bűchi B-585 glass oven. Approximately 200 mg of each polymer was heated at 280ºC in the glass oven for 3 h under vacuum.

Chemical modification

Preparation of ES119GLU sample

$C_{14}H_{19}N_3O_9$ (373,32)

toluene, reflux

$C_{10}H_6$ (126,15)

$C_{24}H_{25}N_3O_9$ (499,47)
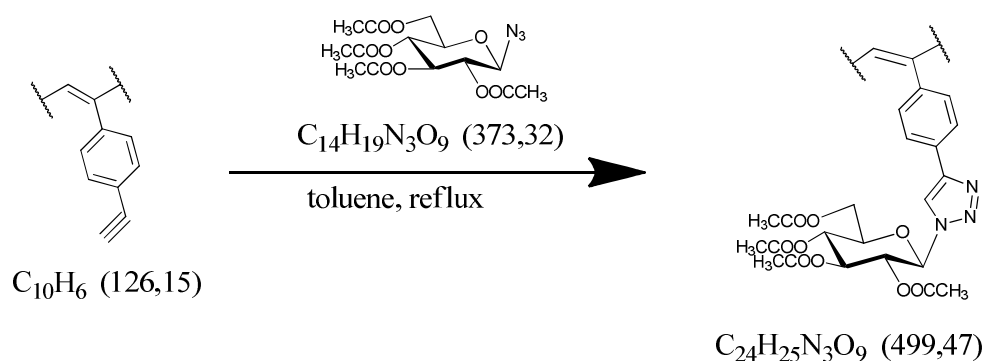
A suspension of 13 mg ES119 (ap. 0.07 mmol of ethynyl groups) and 37 mg of 1-azido-2,3,4,6-tetra-*O*-acetylglucose (GLU-N$_3$) (0.1 mmol, 1.4 eq) in 2 ml of toluene was mixed and heated under reflux for 60 h. The obtained reaction mixture was cooled to r.t., centrifuged (9000 rpm, 8 min) and separated. The precipitate was re-suspended in 2 ml of toluene, stirred

[1] Jura, G.; Harkins, W. D. *J. Am. Chem. Soc.*, **1944**, 66, 1356.

for 10 min and centrifuged. The product washing was repeated with THF (2 x 2 ml) and hexane (2 x 2 ml). The solid was dried under reduced pressure to obtain 11 mg of the final product.

The degree of polymer modification was determined based on the content of nitrogen (determined by elemental analysis) assuming the above reaction stoichiometry.

Preparation of ES119CHOL sample

$C_{10}H_6$ (126,15)　　$C_{27}H_{45}N_3$ (411,67)　xylene, reflux　　$C_{37}H_{51}N_3$ (537,82)
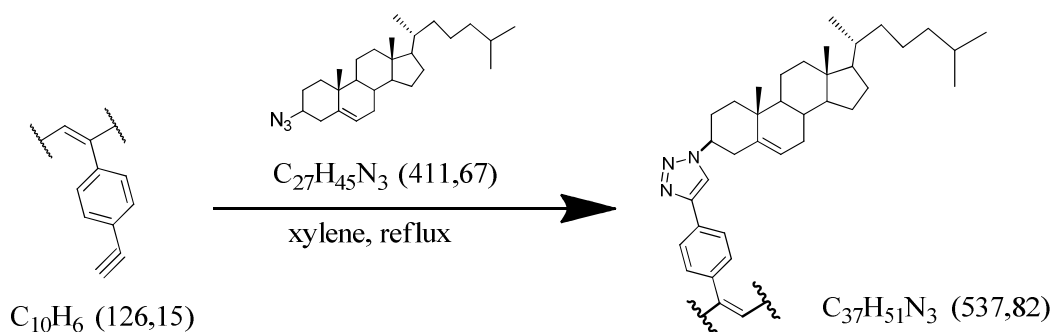
A suspension of 13 mg ES119 (ap. 0.07 mmol of ethynyl groups) and 41 mg 1-azido-cholesterol[2] (CHOL-N$_3$) (0.1 mmol, 1.4 eq) in 2 ml of xylene was heated under reflux for 30 h. The obtained reaction mixture was cooled to r.t., centrifuged (9000 rpm, 8 min) and separated. The precipitate was resuspended in 2 ml of toluene, stirred for 10 min and centrifuged. The product washing was repeated with THF (2 x 2 ml) and hexane (2 x 2 ml). The solid was dried under reduced pressure to obtain 13 mg of the final product.

Table S2. Degree of substitution and loading of chemically modified ES119s

	ES119-GLU	ES119-CHOL
Degree of sub. [%]	5[a]	2[b]
Calcd. N [%]	1.46	0.63
Found[c] N [%]	1.38	0.51
Loading[d]	0.35	0.15

[a]The best value was calculated for 5 % degree of substitution; calculated values for 4 % (1.19 %) and for 6 % (1.70 %), respectively, gave higher declination from theoretical value
[b]The best value was calculated for 2 % degree of substitution; calculated values for 1 % (0.32 %) and for 3 % (0.91 %), respectively, gave higher declination from theoretical value
[c]Full elemental analysis is available in Table S3
[d]mmol of glucose or cholesterol groups per gram of polymer

---

[2] Sun, Q.; Cai, S.; Peterson, B. R. *Org. Lett.*, **2009**, *11*(*3*), 567

2. Elemental Analysis (EA)

Elemental analyses of the polymers were performed at the Institute of Macromolecular Chemistry, Academy of Sciences of the Czech Republic.

Table S3. Elemental analysis data

Sample	C [w%]	H [w%]	N [w%]
ES119	90.96	4.52	-
ES119TM	86.71	3.77	-
ES119-GLU	79.71	6.48	1.38
ES119-CHOL	79.94	5.18	0.51
ES117	91.39	4.25	-
ES117TM	83.75	3.34	-

The finding that the total mass of C and H (by elemental analysis, EA) is below 100 % in the case of purely hydrocarbon polymers can be a consequence of (i) an incomplete combustion of the polymers during EA and/or (ii) (to a lesser extent) polymer contamination with (insoluble) Rh catalyst residue. Similar differences between the calculated and (by combustion EA) found elemental compositions have been reported for various hypercross-linked polymers that are rich in aromatic units and multiple bonds.[3]

3. Characterization

3.1. Scanning electron microscopy (SEM)

Morphology investigations were performed by a scanning electron microscopy. SEM images were taken on a Field emission electron microscope Ultra+ (Carl Zeiss) equipped with an energy dispersive spectrometer SDD X-Max 50 (Oxford Instruments). A piece of each sample was mounted on a carbon tab for better conductivity and a thin layer of gold was sputtered on sample surface prior scanning analysis. An average void size was determined from SEM micrographs analysis after scanning. Therefore, the mean and the standard deviations were drawn by manual measurements of diameters from a population of at least 40 voids. From SEM images analysis it is difficult to give a correct evaluation of the void size since the pores are inside the material and during the sample sectioning the cavities which appear are at

---

[3] (a) Jiang, J.-X.; Su, F.; Trewin, A.; Wood, C. D.; Campbell, N. L.; Niu, H.; Dickinson, C.; Ganin, A. Y.; Rosseinsky, M. J.; Khimyak, Y. Z.; Cooper, A. I. *Angew. Chem. Int. Ed.,* **2007**, 46, 8574–8578. (b) Holst, J. R.; Stöckel, E.; Adams, D. J.; Cooper, A. I. *Macromolecules*, **2010**, 43, 8531-8538.

random distance from the cavity centre. To get a better estimation of the real void diameter, it is necessary to introduce a statistical correction. Multiplication of the observed voids values from SEM images by a statistical factor of $2/3^{1/2}$ allows for a better estimation of the real cavity diameters.[4]
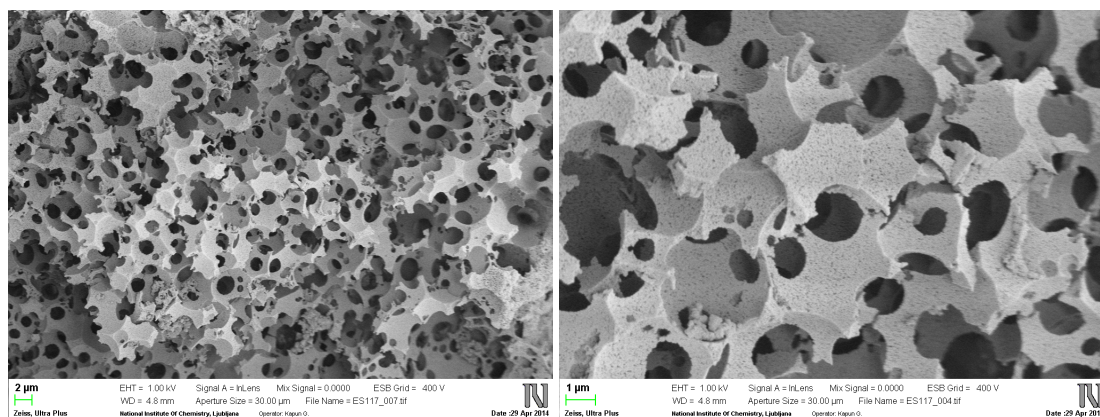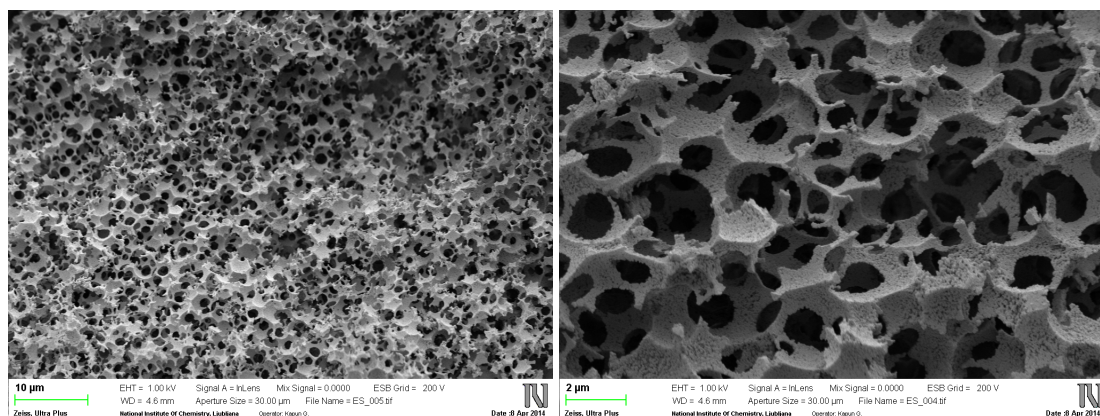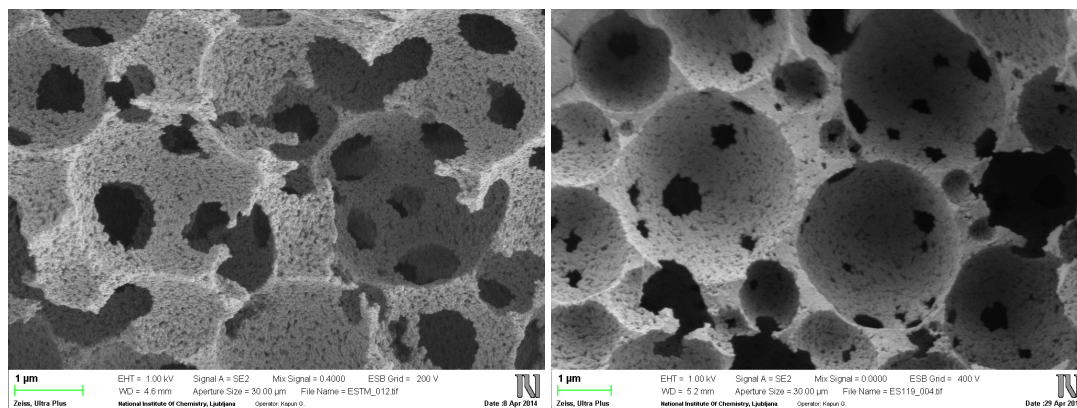

Figure S1. SEM images of sample ES117.

Figure S2. SEM images of sample ES119.

---

[4] A. Barbetta and N. R. Cameron, *Macromolecules*, 2004, **37**, 3188-3201

Figure S3. SEM images of thermally modified sample ES119TM (left) and chemically modified sample ES119CHOL (right).

3.2. BET (Brunaer-Emmett-Teller) surface area

Nitrogen adsorption measurements of polymer samples were performed on a Micromeritics TriStar 3000 surface area analyzer. The samples were outgassed at 90ºC under turbomolecular pump vacuum. The BET surface area was determined by means of nitrogen adsorption data in relative pressure range from 0.05 to 0.25. The BET transform plots were linear in this pressure range.
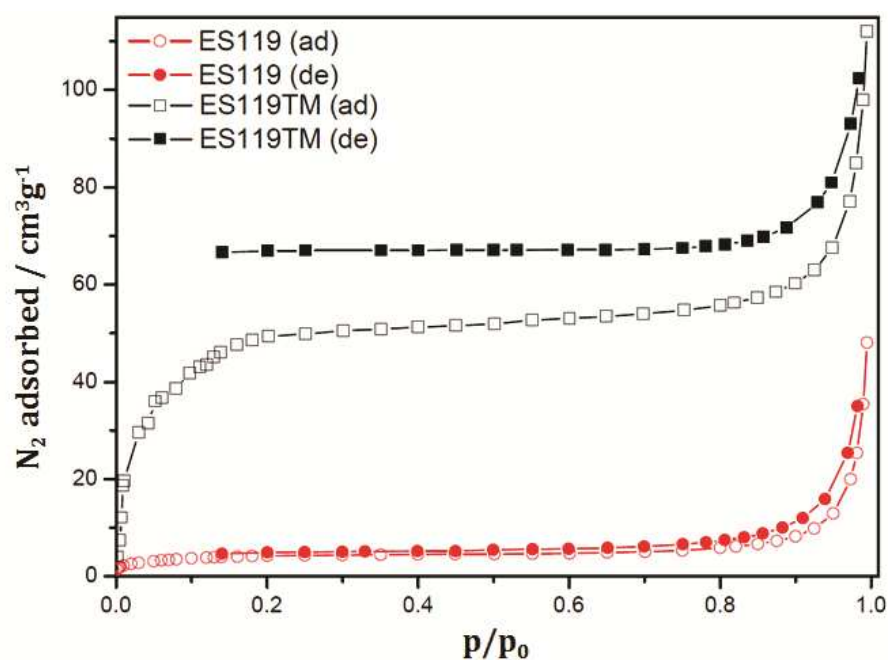
Figure S4. N_2 adsorption/desorption isotherms (77 °K) on ES119 and ES119TM samples.

3.3. Fourier Transform IR (FTIR) Spectroscopy

FTIR spectra were measured on a Nicolet Magna IR 760 using a diffuse reflection mode (DRIFTS). Samples were diluted with KBr.
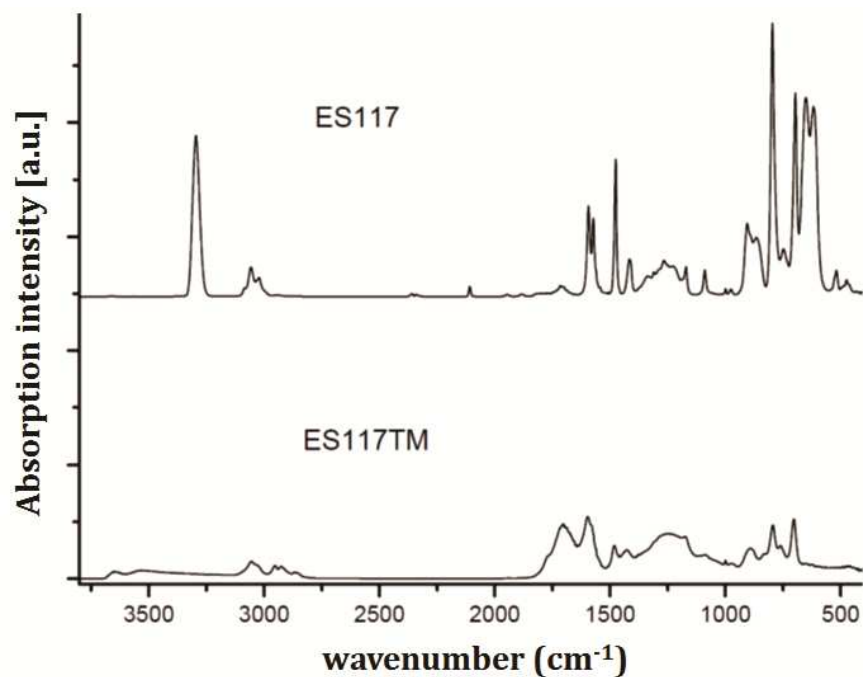
Figure S5. FTIR spectra of pristine ES117 and thermally modified ES117TM samples.
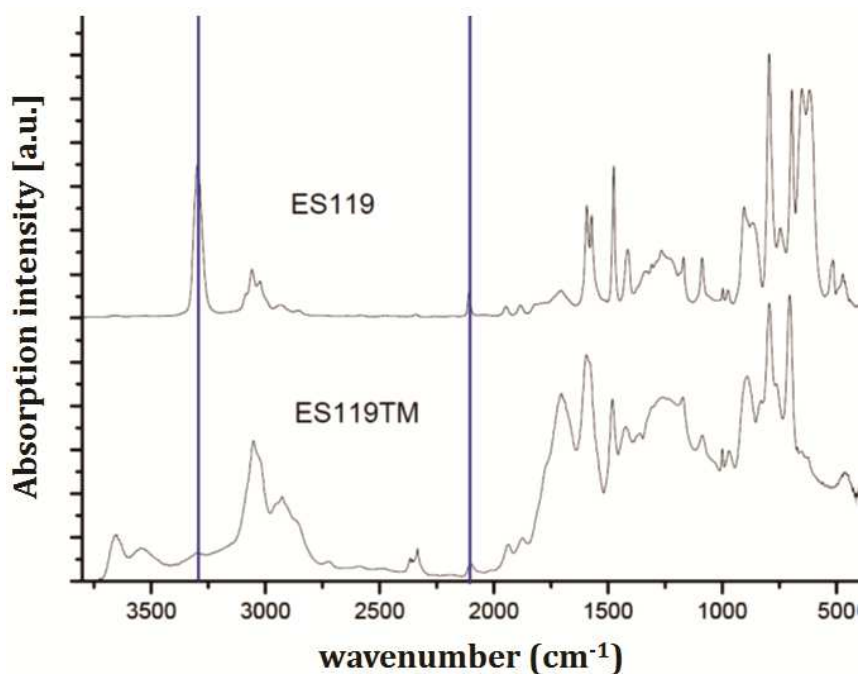
Figure S6. FTIR spectra of pristine ES119 and thermally modified ES119TM samples.
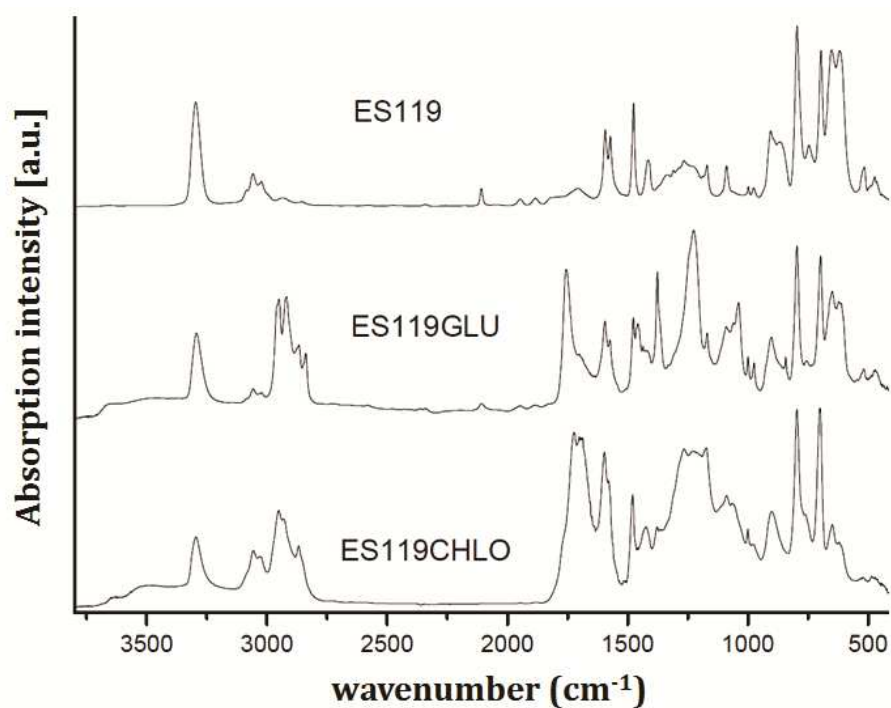
Figure S7. FTIR spectra of pristine ES119 and chemically modified ES119GLU and ES119CHOL samples.

3.4. Diffuse reflectance UV/vis spectroscopy (DR UV/vis)

Diffuse Reflectance UV/vis (DR UV/vis) spectra of solid polymers were recorded using a Perkin–Elmer Lambda 950 spectrometer. Before DR UV/vis measurements the polymers were diluted with $BaSO_4$ (1/10, w/w).

8

**Figure S8.** DR UV/vis spectra of pristine ES117 and thermally modified ES117TM samples.

IV.

Polycyclotrimers of 1,4-Diethynylbenzene, 2,6-Diethynylnaphthalene, and 2,6-Diethynylanthracene: Preparation and Gas Adsorption Properties

Arnošt Zukal,* Eva Slováková, Hynek Balcar, Jan Sedláček

Hyperbranched partly cross-linked polycyclotrimers of 1,4-diethynylbenzene, 2,6-diethynyl-naphthalene, and 2,6-diethynylanthracene, Pc(1,4-DEB), Pc(2,6-DEN), and Pc(2,6-DEA), respectively, are prepared using $TaCl_5/Ph_4Sn$ catalyst. Brunauer–Emmett–Teller (BET) surface area, microporosity, and maximum sorption capacity for H_2 and CO_2 decrease in the order of decreasing relative content of branching points in polycyclotrimers Pc(1,4-DEB) > Pc(2,6-DEN) > Pc(2,6-DEA), the highest values for Pc(1,4-DEB) being S_{BET} = 1299 m^2 g^{-1}, a_{H2} = 1.26 wt% (100 kPa, 77 K), and a_{CO2} = 10.8 wt% (100 kPa, 273 K). N_2 isotherms show that adsorption/desorption hysteresis occurs already at low equilibrium pressures. CO_2 isotherms show that the time allotted to the measurement influences both the maximum adsorption capacity and the hysteresis upon desorption.
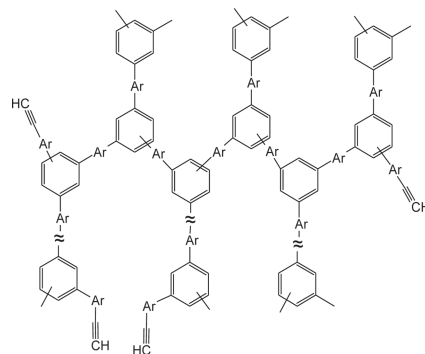
1. Introduction

Microporous organic polymers (MOPs) have become materials of great and steadily increasing interest over the last half a decade.[1] The main potential applications of MOPs range from (i) gas separation and reversible storage,[2–10] (ii) heterogeneous catalysis[11,12] to (iii) optoactive materials and sensors.[13–16] With respect to the importance of hydrogen storage, the ability of polymers to adsorb hydrogen was investigated and correlated with structure

parameters evaluated from nitrogen adsorption.[17–24] An exceptional uptake for hydrogen at low pressure was reported recently by several groups. Cooper and co-workers[25] prepared network based on tetrakis(4-bromo-phenyl)adamantane that exhibited H_2 uptake of 2.34 wt% (113 kPa, 77 K). Han and co-workers[26] reported microporous polycarbazole with hydrogen uptake of 2.80 wt% at 100 kPa and 77 K. Polyimide-based MOP of Makhseed and Samuel[21] showed H_2 storage capacity of 3.94 wt% at 1 MPa and 77 K.

If we adopt the source-based classification, we can delimit a subclass of MOPs derived from multifunctional ethynylarenes (MEA), that is, monomers containing usually from 2 to 4 terminal ethynyl groups attached to the arene(s) core of the molecule.[25,27–29] Polycyclotrimerization of MEAs represents a path leading to MOPs that have the structure of hyperbranched/cross-linked polyarylenes. The original arene cores of monomers are interconnected in polymers by benzenetriyl linkers formed via cyclotrimerization of three terminal ethynyl groups of MEAs. Liu and

Dr. A. Zukal, Dr. H. Balcar
J. Heyrovský Institute of Physical Chemistry, v.v.i, Academy of Sciences of the Czech Republic, Dolejškova 3, 182 23 Prague 8, Czech Republic
E-mail: arnost.zukal@jh-inst.cas.cz
E. Slováková, Prof. J. Sedláček
Department of Physical and Macromolecular Chemistry, Faculty of Science, Charles University in Prague, Hlavova, 2030, 128 40 Prague 2, Czech Republic

co-workers polycyclotrimerized 1,4-diethynylbenzene, 1,3,5-triethynylbenzene, 1,2,4,5-tetraethynylbenzene, and 4,4′-diethynylbiphenyl at 398 K under catalysis of $Co_2(CO)_8$. Quantitative yields of polycyclotrimers were achieved and polymers derived from bifunctional monomers were free of nonreacted ethynyl groups. The values of the surface area reached 1246 $m^2 g^{-1}$ (Yuan et al.[30]). Polycyclotrimerization with $Co_2(CO)_8$ was also used for the preparation of MOPs from [5,10,15,20-tetrakis(4-ethynylphenyl)porphyrin]-nickel(II), (Wang et al.[31]), from MEAs derived from 1,1′-binaphthyl building blocks[32] (the surface areas up to 1000 $m^2 g^{-1}$), and from tetrakis(4-ethynylphenyl)methane (Xie et al.[11] and Yuan et al.,[33] the surface areas from 1348 to 1547 $m^2 g^{-1}$).

Polycyclotrimerization has also been known as a powerful tool for the synthesis of soluble hyperbranched polymers, for example, polycyclotrimerization of 1,8-nonadiyne and 1,9-decadiyne[34] or co-polycyclotrimerization of diethynylarenes and alk-1-ynes.[35] These polycyclotrimerizations were catalyzed by TaCl$_5$/Ph$_4$Sn catalyst, which had been known from the pioneering works of Masuda et al. (see reviews[36,37]). It polymerized acetylenes with internal triple bond into linear high-molecular-weight polyacetylenes[38,39] and cyclotrimerized acetylenes with terminal triple bond (e.g., phenylacetylene) into the mixture of 1,3,5- and 1,2,4-trisubstituted benzenes.[40,41] Although many applications of TaCl$_5$/Ph$_4$Sn for acetylenes transformations have been described in the literature, to the best of our knowledge, no report is available on the application of TaCl$_5$/Ph$_4$Sn for the polycyclotrimerization of MEAs aimed at preparation of MOP products.

Generally, adsorption properties of MOPs are still not completely understood. The structure–porosity–adsorption properties relationship of MOPs was studied by using either single nitrogen adsorption at 77 K[42–44] or a combination of isotherms of various adsorptives, such as nitrogen, argon and hydrogen at 77 K, and carbon dioxide at 273–333 K.[45–48] Gas adsorption was also combined with small-angle X-ray scattering analysis[48] or ^{129}Xe NMR spectroscopy.[49] The use of small-angle X-ray scattering has confirmed that besides adsorption in micropores, pronounced elastic deformations of analyzed MOPs took place during increasing gas pressures.[20,49] For adsorption isotherms, in particular for isotherms of nitrogen, argon, or carbon dioxide recorded on various polymers an unusual type of adsorption/desorption behavior is typical. Adsorption and desorption branches of the hysteresis loop did not close and such irreversibility is observed at the lowest equilibrium pressures. This hysteresis can have various origins. In the so-called dual-mode adsorption,[50,51] the uptake of adsorptive molecules proceeds in two steps.[49] In the first step, the accessible pores are filled. In the second step, adsorptive molecules are dissolved in the polymer. The softness of the polymer matrix can lead to swelling effects and subsequently to adsorption irreversibility.[49] On the other hand, the adsorption irreversibility can be attributed to a slow kinetic of adsorption/desorption process. It was reported by Ritter et al.[45] and Ghanem et al.[52] that nitrogen adsorption on polymer can last several days.

In the present study, we report the synthesis and adsorption properties of a series of MOP-type polycyclotrimers derived from diethynylarenes differing in the number of the condensed benzene rings: 1,4-diethynylbenzene (1,4-DEB), 2,6-diethynylnaphthalene (2,6-DEN), and 2,6-diethynylanthracene (2,6-DEA). Polycyclotrimerization was performed using TaCl$_5$/Ph$_4$Sn catalyst. To investigate adsorption properties of these polymers, adsorption/desorption isotherms of nitrogen and hydrogen at 77 K and carbon dioxide in the temperature range 273–333 K were measured. In order to gain more insight into the adsorption/desorption behavior, scanning of hysteresis loops of nitrogen isotherms was performed. As kinetic effects in the adsorption on polymers cannot be excluded, the influence of the duration of the adsorption measurement on the adsorption properties of polymers was studied.

2. Experimental Section

2.1. Materials

TaCl$_5$ (99.8%; Sigma–Aldrich, Prague, Czech Republic), tetraphenyltin (Ph$_4$Sn) (Pierce Inorganics, Rotterdam, Netherland) were used as obtained. 1,4-DEB (96%; Sigma–Aldrich) was purified by vacuum sublimation. 2,6-DEN and 2,6-DEA were prepared by Sonogashira coupling of 2,6-dibromonaphthalene and 2,6-dibromoanthracene, respectively, with trimethylsilylacetylene catalyzed by [PdCl$_2$(PPh$_3$)$_2$]/Cu$_2$I$_2$/PPh$_3$ followed by deprotection of intermediates with tetrabutylammonium fluoride. ^{1}H and ^{13}C NMR spectral characteristics of prepared 2,6-DEN and 2,6-DEA were in agreement with literature.[53,54] Benzene (p.a., Lachema, Czech Republic) was distilled from P$_2$O$_5$ and degassed in vacuo.

2.2. Polycyclotrimers Preparation

All polycyclotrimerizations were carried out in benzene at room temperature using vacuum break-seals technique. Benzene solution of TaCl$_5$ was mixed with Ph$_4$Sn at room temperature. After 10 min, the solution of monomer was added. The initial concentrations of reaction component were: [monomer]$_0$ = 0.6 mol L^{-1}, [TaCl$_5$]$_0$ = 0.015 mol L^{-1}, [Ph$_4$Sn]$_0$ = 0.015 mol L^{-1}; volume of the reaction mixture was 5 mL. All polycyclotrimerizations proceeded as precipitation reactions. After 24 h, the reaction suspension was poured into the excess of benzene, the solid polymer was collected, washed with benzene and dried in vacuum at room temperature. The yield of polymer was determined gravimetrically.

www.MaterialsViews.com

Macromol. Chem. Phys. **2013**, *214*, 2016–2026

© 2013 WILEY-VCH Verlag GmbH & Co. KGaA, Weinheim

Macromolecular
Journals

2017

2.3. Methods

IR spectra were measured on a Nicolet Magna IR 760 using diffuse reflection mode (DRIFTS). Samples were diluted with KBr. ^{13}C CP/MAS NMR spectra were measured at 11.7 T using a Bruker Avance 500 WB/US NMR spectrometer. Details are given elsewhere.[55]

Scanning electron microscopy (SEM) was performed using a JEOL JSM-5500LV microscope at accelerating voltage of 9 kV.

Adsorption/desorption isotherms of nitrogen and hydrogen at 77 K and carbon dioxide at 273, 293, 313, and 333 K were recorded using an ASAP 2020 (Micromeritics, Norcross, Georgia, US) volumetric instrument. This instrument uses three pressure transducers (133 Pa, 1.33 kPa, and 133 kPa) that allow accurate adsorption isotherm measurement in a wide range of pressure. The Iso-Therm thermostat (e-Lab Services, Czech Republic) maintaining temperature of the sample with accuracy of ±0.01 K was used for the measurement of carbon dioxide adsorption.

The fresh samples were degassed starting at an ambient temperature up to 353 K (temperature ramp of 0.5 K min^{-1}) until the residual pressure of 1.33 Pa was attained. After further heating at 353 K for 1 h, the temperature was increased (temperature ramp of 1 K min^{-1}) until the temperature of 383 K was achieved. Degassing was continued at this temperature under the turbomolecular pump vacuum for 12 h. Before repeated adsorption measurement, the sample was degassed at 383 K (temperature ramp of 1 K min^{-1}) for 12 h under turbomolecular pump vacuum.

Adsorption isotherms of all adsorptives were recorded using different equilibration time intervals. (Equilibration time interval represents the number of seconds between successive pressure readings during equilibration.) As long equilibration intervals tend to lengthen whole measurement, the changes in these intervals have enabled us to acquire a dependence of adsorption properties on the length of measurement. To investigate nitrogen adsorption in more detail, desorption scanning curves were obtained by taking some points on the boundary adsorption branch and using these as the starting points for the measurement of desorption scans.

3. Results and Discussion

3.1. Synthesis of Polycyclotrimers and their General Properties

Diethynylarenes used as monomers in the present study, that is, 1,4-DEB, 2,6-DEN, and 2,6-DEA, contained two equal ethynyls, the positions of which on the arene rings were designed: i) to avoid mutual steric hindrance between ethynyls in a monomer molecule and ii) to minimize the steric shielding of the ethynyl groups by the arene cores of 2,6-DEN and 2,6-DEA monomers.
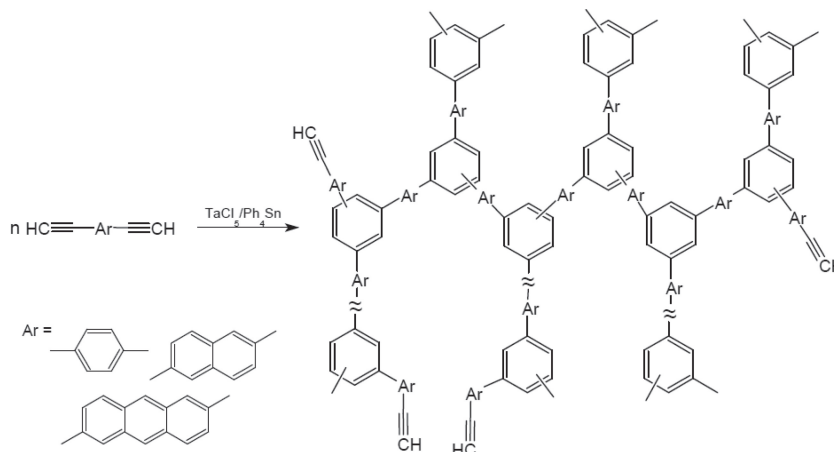
■ *Scheme 1.* Polycyclotrimerization of diethynylarenes.

These monomers were polycyclotrimerized (Scheme 1) with TaCl$_5$/Ph$_4$Sn catalyst system (1.25 mol% relative to triple bonds) at room temperature. The polymer yield is given in Table 1. Application of TaCl$_5$/Ph$_4$Sn catalyst system allowed to apply milder polycyclotrimerization conditions (see above) than those reported by Liu et al. for cyclotrimerizations catalyzed by Co$_2$(CO)$_8$ (6 mol% of catalyst relative to triple bonds, 398 K).[30] All polycyclotrimers prepared with TaCl$_5$/ Ph$_4$Sn were yellow-orange solids, insoluble (and also nonswellable) in THF, CH$_2$Cl$_2$, CHCl$_3$, and benzene. They were labeled as Pc(1,4-DEB), Pc(2,6-DEN), and Pc(2,6-DEA).

Pc(1,4-DEB), Pc(2,6-DEN), and Pc(2,6-DEA) were characterized by ^{13}C CP/MAS NMR and IR spectroscopies. Both ^{13}C CP/MAS NMR and IR spectra (Figure S1–S6, Supporting Information) are in accord with polymer structure proposed in Scheme 1. Certain amount of nontransformed terminal ethynyls still remaining in the structure of products was indicated by signals in the region of 70–85 ppm in ^{13}C CP/MAS NMR spectra[56] and by bands at about 3290 cm^{-1} ($\nu_{\equiv C-H}$) and at about 2100 cm^{-1} ($\nu_{C\equiv CH}$) in IR spectra. TaCl$_5$/Ph$_4$Sn applied as a catalyst for the simple cyclotrimerization of monoethynylated compounds always provided a mixture of 1,3,5- and 1,2,4-trisubstituted benzenes.[40,41] One can expect the same behavior of TaCl$_5$/Ph$_4$Sn also in the polycyclotrimerization of diethynylarenes. Thus, both benzene-1,3,5-triyl and

■ *Table 1.* Yield (*Y*) and parameters ξ of polycyclotrimers prepared.

Monomer	*Y* [%]	ξ[a] [%]
1,4-DEB	97	91
2,6-DEN	97	81
2,6-DEA	44	74

[a]ξ = conversion of terminal ethynyls.

benzene-1,2,4-triyl linkers are most probably present in the structure of polycyclotrimers as branching and/or cross-linking points. It is also in a good agreement with the substitution pattern of aromatic rings from IR in region 600–900 cm^{-1} as well as in the region 1660–2000 cm^{-1} (overtons and combination tone bands).

The quantification of ^{13}C CP/MAS NMR spectra provided the values of conversion of terminal ethynyls due to their incorporation into benzenetriyl linkers of polycyclotrimers (i.e., the conversion of sp carbons into sp^2 carbons). This conversion, ξ, was defined as follows: $\xi = (4 - N_{sp})/4$, where N_{sp} stands for the average number of nontransformed sp carbons per one monomeric moiety inbuilt into the polycyclotrimer. Values of ξ were calculated from ^{13}C CP/MAS NMR spectra according to Equation 1, where N_{ArM} is the number of aromatic carbons in one monomer molecule, A_{sp2} and A_{sp} are the integral intensities of signals of sp^2 and sp carbons, respectively, in the spectra of polycyclotrimers (see Supporting Information for the derivation of Equation 1).

$$\xi = (4A_{sp2} - A_{sp}N_{ArM})/(4A_{sp2} + 4A_{sp}) \qquad (1)$$

As evident from Table 1, the values of ξ decreased in the following order Pc(1,4-DEB) > Pc(2,6-DEN) > Pc(2,6-DEA) being 0.91 for Pc(1,4-DEB) and 0.74 for Pc(2,6-DEA).

Three modes of polycyclotrimers growing may be assumed. The intuitively simplest mode consists of the reaction of one ethynyl from a polycyclotrimer macromolecule with two ethynyls from two different monomer molecules (each diethynylarene molecule can "provide" only one ethynyl group for a particular cyclotrimerization step). This reaction mode (labeled as E_P2E_M) leads to the enlargement of the polycyclotrimer macromolecule only. The reaction of two ethynyls from a polycyclotrimer macromolecule(s) with one ethynyl from a monomer molecule represents the second reaction mode (labeled as $2E_PE_M$) by which both, the enlargement and the cross-linking of the polycyclotrimer macromolecule simultaneously proceed. The difference between E_P2E_M and $2E_PE_M$ modes is depicted in Scheme S1 in Supporting Information. The third reaction mode labeled as $3E_P$ (mutual reaction of three ethynyls from polycyclotrimer macromolecule(s) leading entirely to the cross-linking) is of the lowest probability from the steric reasons. Assuming that polycyclotrimers formation proceeds only via E_P2E_M mode, the highest value of ξ accessible in polycyclotrimerization of bifunctional monomers is equal to 0.75 (for degree of polymerization $\rightarrow \infty$, see Supporting Information, Table S1). Values of $\xi > 0.75$ found for Pc(1,4-DEB) and Pc(2,6-DEN) show that the cross-linking modes ($2E_PE_M$ and $3E_P$) participated at the formation of these polymers. The value of $\xi = 0.74$ found for Pc(2,6-DEA) may indicate either no or only a marginal contribution of the cross-linking modes on the Pc(2,6-DEA) formation.

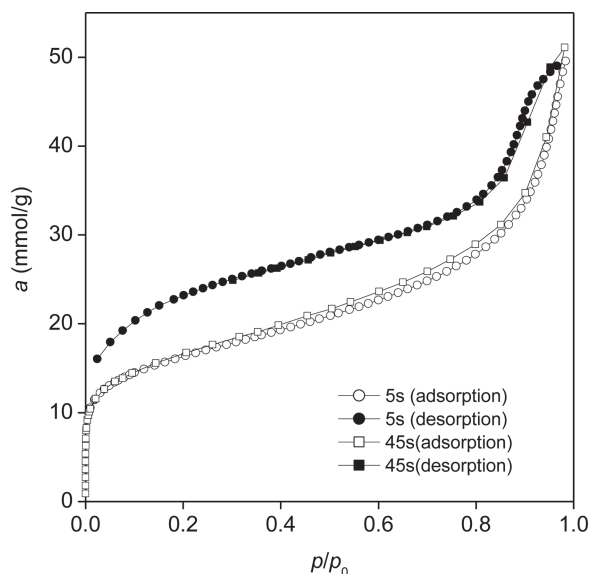**Figure 1.** Nitrogen isotherms on Pc(1,4-DEB) at 77 K collected using equilibration time intervals of 5 s and 45 s.

3.2. Adsorption of Nitrogen at 77 K

Nitrogen isotherms on Pc(1,4-DEB) and Pc(2,6-DEN) in Figure 1 and 2 are characterized by a hysteresis loop typical for many organic polymers. As frequently observed for these materials,[45,47] desorption branches of the isotherms do not show a low pressure limit of adsorption/desorption irreversibility which is for inorganic mesoporous materials close relative pressure $p/p_0 \approx 0.4$ (Lowell et al.[57]). In contrast to Pc(1,4-DEB) and Pc(2,6-DEN), nitrogen isotherm on the sample Pc(2,6-DEA) (Figure 3) is reminiscent of nitrogen
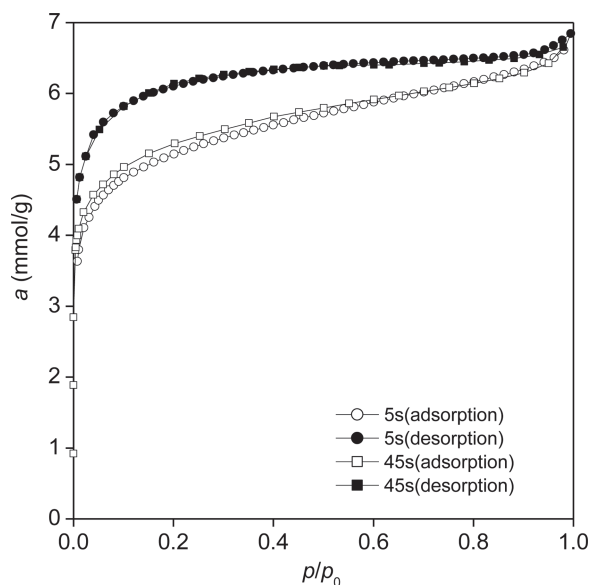
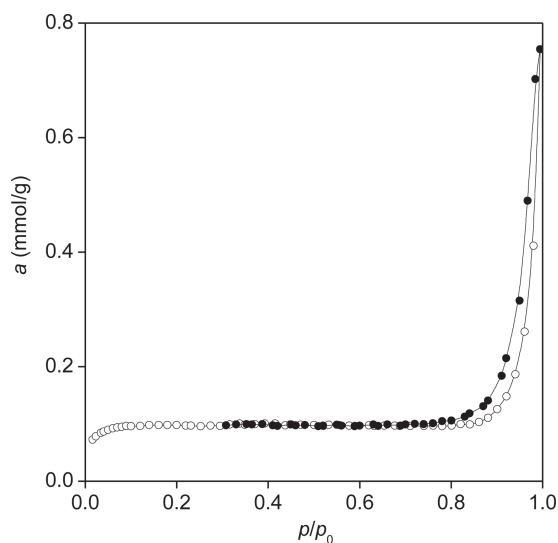**Figure 2.** Nitrogen isotherms on Pc(2,6-DEN) at 77 K collected using equilibration time intervals of 5 s and 45 s.

Materials
Views

www.MaterialsViews.com

Macromol. Chem. Phys. **2013**, *214*, 2016–2026
© 2013 WILEY-VCH Verlag GmbH & Co. KGaA, Weinheim

Macromolecular
Journals

2019

Figure 3. Nitrogen isotherm on Pc(2,6-DEA) at 77 K (solid symbols denote desorption.)

Figure 4. SEM image of the sample Pc(1.4-DEB).

isotherms on nonporous inorganic adsorbents. The steep increase in the region of relative pressures $p/p_0 > 0.9$ is due to capillary condensation in the interparticle space.

In order to characterize textural parameters of polycyclotrimers, the BET surface area was calculated from adsorption branch of the isotherm in the range of relative pressures 0.05–0.25 (Table 2). Relatively high values of the surface areas of samples Pc(1,4-DEB) and Pc(2,6-DEN) were found. In particular, the sample Pc(1,4-DEB) exhibited surface area typical for MOPs.[17] The surface area of sample Pc(2,6-DEA) calculated from the reversible part of the isotherm in the same range of relative pressures, was nearly negligible (Table 2) and most likely corresponded to the external area of particles. For this reason, Pc(2,6-DEA) was not examined in all details as Pc(1,4-DEB) and Pc(2,6-DEN).

The nitrogen isotherms reveal that the sample Pc(1,4-DEB) contains the largest amount of mesopores in comparison with polymers Pc(2,6-DEN) and Pc(2,6-DEA). Typical SEM image of the sample Pc(1,4-DEB) in Figure 4 shows approximately spherical particles 0.1–0.2 μm in diameter. The broad mesopore distribution of this sample calculated from the desorption branch of hysteresis loop in the range from 10 to 50 nm is presented
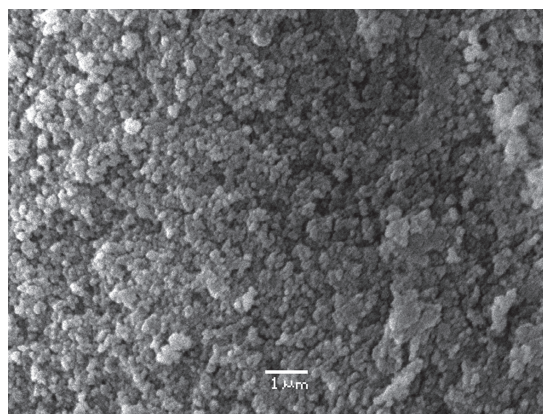
in Supporting Information (Figure S7, Supporting Information). With respect to the SEM image, we can assume that most of mesopores is formed as interstitial voids in between particles.

Different adsorption properties of polymers under study were characterized not only by the BET surface area but also by maximum adsorption capacity (Table 3). N_2 adsorption capacity was found to decrease in the same order as BET surface area, that is, in the order Pc(1,4-DEB) > Pc(2,6-DEN) > Pc(2,6-DEA). In the case of sample Pc(1,4-DEB), the nitrogen adsorption at relative pressure p/p_0 = 0.98 attained 51.0 mmol g^{-1} namely owing to the significant increase of adsorption at $p/p_0 > 0.5$. By contrast, maximum adsorption capacity of the sample Pc(2,6-DEN) was only 6.6 mmol g^{-1}. Decreasing adsorption capacity of polycyclotrimers might reflect the decreasing density of the branching points in the polymer framework. Moreover, the possible π–π stacking interaction of large anthracene cores may contribute to the compactness of Pc(2,6-DEA) sample.

It should be noted that starting from 1,4-diethynyl-benzene a microporous polymer denoted POP-1 was prepared by means of dicobalt octacarbonyl as a catalyst.[30] POP-1 material exhibited BET surface area of 1031 m^2 g^{-1} and micropore volume of 0.378 cm^3 g^{-1}. These structure parameters are comparable with those of the sample Pc(1,4-DEB). However, the nitrogen adsorption capacity 51.0 mmol g^{-1} of Pc(1,4-DEB), which is more than twice

Table 2. Physicochemical properties of polycyclotrimers.

Sample code	S_{BET}[a] [m^2 g^{-1}]	k_H[b] [mmol N_2 g^{-1}]	a_m[b] [mmol N_2 g^{-1}]	b[b]	V_{MI}[c] [cm^3 g^{-1}]
Pc(1,4-DEB)	1299	14.59	13.557	215	0.472
Pc(2,6-DEN)	418	1.51	5.013	155	0.175
Pc(2,6-DEA)	9	–	–	–	–

[a]S_{BET}, BET surface area; [b]k_H, a_m, b, constants of the Equation 2; [c]V_{MI}, micropore volume.

◼ *Table 3.* Adsorption capacities of polycyclotrimers.

Sample code	$a_{max,N2}$[a] [mmol N_2 g^{-1}]	$a_{max,H2}$[a] [wt%]	$a_{max,CO2,273K}$[b] [mmol CO_2 g^{-1}]	$a_{max,CO2,293K}$[b,c] [mmol CO_2 g^{-1}]	$a_{max,CO2,333K}$[b,c] [mmol CO_2 g^{-1}]
Pc(1,4-DEB)	51.0	1.26	2.45	1.49/1.63	0.55/0.82
Pc(2,6-DEN)	6.6	0.74	1.70	1.26/1.33	0.29/1.04
Pc(2,6-DEA)	0.75	≈0	0.30	—	—

[a]$a_{max,N2}$ and $a_{max,H2}$, amounts of nitrogen and hydrogen adsorbed at 100 kPa and 77 K; [b]$a_{max,CO2,273K}$, $a_{max,CO2,293K}$, and $a_{max,CO2,333K}$, amount of carbon dioxide adsorbed at 100 kPa and 273, 293, or 333 K; [c]The data refer to equilibration time intervals of 5 s/300 s.

as high as the maximum adsorption capacity of POP-1, indicates substantial differences in the structure of both polymers.

With the aim to evaluate whether the length of the equilibration time intervals applied for adsorption measurements affect the results, we measured the nitrogen isotherms on samples Pc(1,4-DEB) and Pc(2,6-DEN) two times. The usual practice of adsorption measurements supposes that equilibration is reached when the pressure change per equilibration time interval is less than 0.01% of the average pressure during the interval. Adsorption isotherms recorded using standard equilibration time interval of 5 s and isotherms with equilibration time interval of 45 s are shown in Figure 1 and 2. The overall time of the isotherms measurement and average time of equilibration per point in Table 4 illustrate considerable lengthening adsorption measurements if equilibration time interval of 45 s is applied. The small differences between nitrogen isotherms recorded using various equilibration time intervals (Figure 1 and 2) are obviously due to long term temperature and pressure drifts. As displayed isotherms reveal that the time of measurement practically does not play any role, there is no need to consider kinetic effects of nitrogen adsorption on polycyclotrimers under investigation.

In order to obtain more insight into adsorption/desorption hysteresis observed on polymers Pc(1,4-DEB) and Pc(2,6-DEN), we acquired the desorption scanning hysteresis loops. Starting points of desorption scans correspond to the series of equilibrium pressures p/p_0 of 0.05, 0.10, 0.20, …, 0.90, 0.95 for the sample Pc(1,4-DEB); and 0.05, 0.20, 0.40, 0.60, 0.80 for the sample Pc(2,6-DEN). Scans are displayed in Figure 5 and 6 for the whole region of equilibrium pressures; magnified scans in the region of pressures $p/p_0 < 0.1$ are shown in Supporting information (Figure S8 and S9, Supporting Information). Foregoing adsorption branches of all scans, which are not displayed for clarity, are perfectly identical. It follows from it that upon nitrogen desorption the original framework of polymers was restored.

The observation of desorption scans shows that they form a family of non-intersecting curves, which tend to come into confluence at equilibrium pressure $p/p_0 < 0.01$. In accordance with the dual-mode adsorption model,[50,51] it can be assumed that the nitrogen adsorption on MOPs exhibiting irreversible adsorption behavior is a result of reversible filling of permanent micropores and the dissolving of nitrogen molecules into the polymeric framework that may induce elastic deformations of the polymer. The formation of non-permanent micropores is also possible. As suggested by Weber et al.[49], the dissolving of nitrogen molecules in the polymer framework can be responsible for the observed hysteresis. We suppose that desorption of nitrogen molecules, which

◼ *Table 4.* Influence of the equilibration time interval on the length of adsorption measurement.

Sample code	Nitrogen			Hydrogen			Carbon dioxide		
	Δ[a] [s]	τ_{N2}[b] [min]	$\tau_{1,N2}$[c] [min]	Δ[a] [s]	τ_{H2}[b] [min]	$\tau_{1,H2}$[c] [min]	Δ[a] [s]	τ_{CO2}[d] [min]	$\tau_{1,CO2}$[c] [min]
Pc(1,4-DEB)	5	1484	12	5	735	21	5	159	4
Pc(1,4-DEB)	45	4959	97	45	1925	55	60	956	27
Pc(1,4-DEB)	—	—	—	—	—	—	300	3985	121
Pc(2,6-DEN)	5	447	5	5	503	13	5	229	5
Pc(2,6-DEN)	45	3559	66	45	970	26	60	924	24
Pc(2,6-DEN)	—	—	—	—	—	—	300	2739	83

[a]Δ, equilibration time interval; [b]τ_{N2} and τ_{H2}, time of the nitrogen and hydrogen measurement at 77 K; [c]$\tau_{1,N2}$, $\tau_{1,H2}$, and $\tau_{1,CO2}$, average time of equilibration per point; [d]τ_{CO2}, time of the carbon dioxide isotherm measurement at 333 K.

www.MaterialsViews.com

Macromol. Chem. Phys. **2013**, *214*, 2016–2026

© 2013 WILEY-VCH Verlag GmbH & Co. KGaA, Weinheim
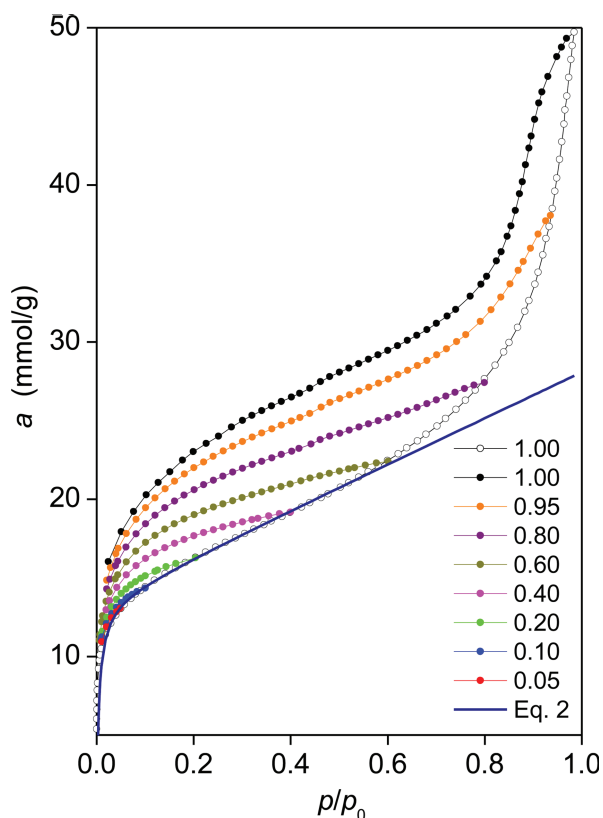
Macromolecular
Journals

2021

Figure 5. Nitrogen isotherm at 77 K and desorption scans (solid points) for Pc(1,4-DEB). Foregoing adsorption branches are omitted for clarity. The inset gives the pressures corresponding to the starting points of desorption scans. The curve in Royal blue is calculated using Equation 2.

Figure 6. Nitrogen isotherm at 77 K and desorption scans (solid points) for Pc(2,6-DEN). Foregoing adsorption branches are omitted for clarity. The inset gives the pressures corresponding to the starting points of desorption scans. The curve in Royal blue is calculated using Equation 2.

become trapped in the polymer framework, is more difficult than their penetration into the polymer framework during adsorption. Therefore, desorption takes place at lower equilibrium pressures than adsorption.

Irreversibility of gas adsorption on polymers represents phenomenon, which raises doubts about the applicability of standard procedures for the analysis of porous flexible materials.[47] The BET, BJH, or *t*-plot methods were suggested for inert solid adsorbents. If they are applied on MOPs, the meaning of obtained porosity characteristics may be problematic. However, these characteristics can provide some qualitative information suitable for comparison of various MOPs of the same or similar type.

The scans in low pressure region reveal that the dissolving of nitrogen molecules in polymer framework occurs from the beginning of adsorption process simultaneously with the micropore filling. Therefore, we applied the simple form of the dual-mode sorption model for the description of adsorption branches of the nitrogen isotherms. The total amount adsorbed *a* can be expressed as the sum of the Henry adsorption contribution a_H occurring owing to the dissolving of nitrogen molecules into the polymer and Langmuir adsorption contribution a_L due
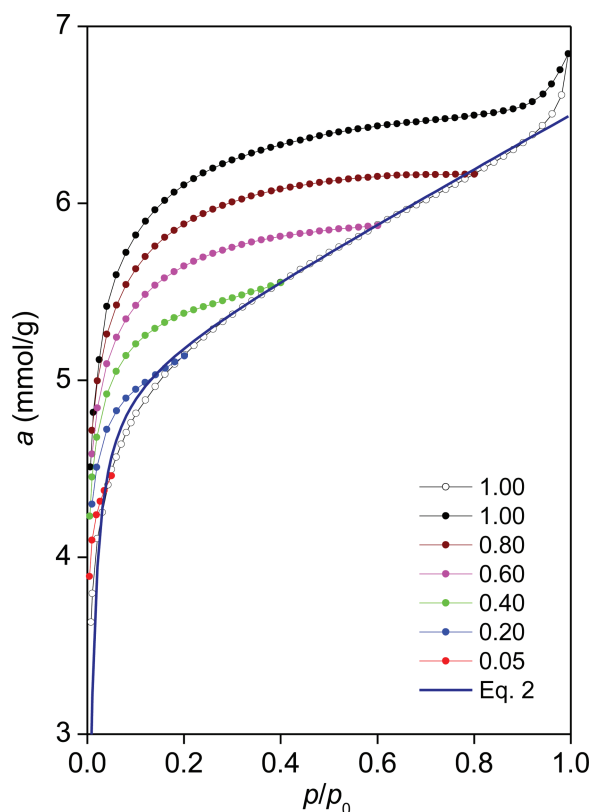
to filling of permanent micropores of polymer; see Equation 2, where $h = p/p_0$ is relative pressure, k_H is the Henry's solubility coefficient, a_m is the Langmuir saturation constant, and b is the Langmuir affinity constant:

$$a = a_H + a_L = k_H h + a_m[bh/(1 + bh)] \qquad (2)$$

According to Equation 2, the adsorption branch should be linear after filling permanent micropores. As shown in Figure 6, the adsorption branch of the isotherm on Pc(1,4-DEB) is linear only in the region of relative pressure $0.3 < p/p_0 < 0.5$. In contrast to the polymer Pc(1,4-DEB), adsorption branch of the isotherm on the sample Pc(2,6-DEN) is linear in the range of relative pressure from 0.3 to 0.9 (Figure 6).

The data for $p/p_0 < 0.5$ [sample Pc(1,4-DEB)] or $p/p_0 < 0.9$ [sample Pc(2,6-DEN)] were used to assess parameters k_H, a_m, and b; their values obtained using the method of least squares are given in Table 2. Adsorption branches of isotherms calculated using these parameters are displayed in Figure 5 and 6. This comparison shows that there are only small deviations of calculated curves from the experimental points in the pressure regions used for the evaluation of constants k_H, a_m, and b.
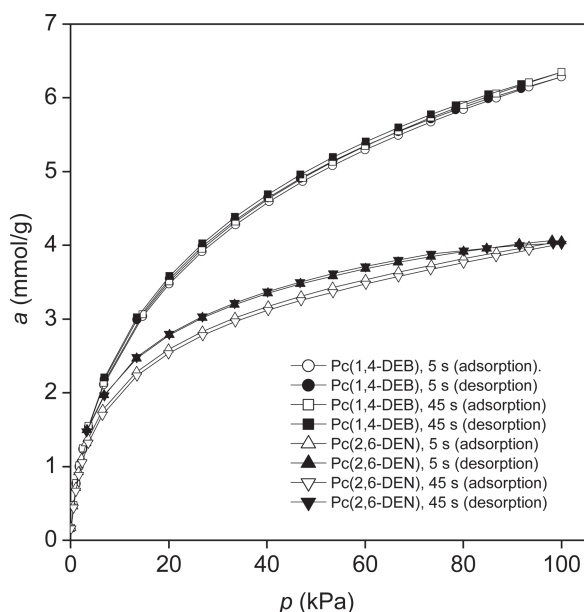
www.MaterialsViews.com

Figure 7. Hydrogen isotherms on Pc(1,4-DEB) and Pc(2,6-DEN) at 77 K collected using equilibration time intervals of 5 and 45 s.

The values of parameters k_H, a_m, and b illustrate substantial differences between polymers Pc(1,4-DEB) and Pc(2,6-DEN). The capacity of permanent micropores, that is, the constant a_m, is markedly higher for the polymer Pc(1,4-DEB) than that for the polymer Pc(2,6-DEN). Corresponding volumes of permanent micropores calculated by a formula $V_{MI} = a_m v_{mol}$ (v_{mol} denotes molar volume of liquid nitrogen) are given in Table 2. The high micropore volume of Pc(1,4-DEB) is in accord with the high BET surface area and may correspond to the high density of branching points in this polycyclotrimer. The Henry's coefficients k_H reveal that due to a higher volume of permanent micropores nitrogen molecules penetrate into the framework of the Pc(1,4-DEB) much more easily in comparison with Pc(2,6-DEN).

At relative pressures $p/p_0 > 0.5$, the adsorption branch of the isotherm on Pc(1,4-DEB) is characterized by the convex shape with a steep increase when $p/p_0 \to 1$. A similar less pronounced increase is apparent on the adsorption branch of the isotherm on Pc(1,6-DEN) at relative pressures $p/p_0 > 0.9$. We assume that two factors can contribute to this phenomenon: i) an extensive dissolving of nitrogen in the framework of Pc(1,4-DEB) by which new non-permanent pores can be formed, and ii) a capillary condensation of nitrogen among polymer particles.

3.3. Adsorption of Hydrogen at 77 K

Hydrogen adsorption/desorption isotherms were measured using the same equilibration time intervals as applied for N_2 adsorption measurement. The overall time

of isotherm measurement and average time of equilibration per point are listed in Table 4.

The isotherms shown in Figure 7 reveal that the time of hydrogen adsorption measurement plays negligible role. The isotherm on the sample Pc(1,4-DEB) is practically reversible, the isotherm on the sample Pc(2,6-DEN) shows narrow hysteresis down to low equilibrium pressures. Maximum uptake capacities at pressure of 100 kPa derived from isotherms and expressed in weight percentage are listed in Table 3. The maximum hydrogen capacity of sample Pc(1,4-DEB) attaining 1.26 wt% is lower than the best capacities of 2.22–2.80 wt% given for the same or similar experimental conditions by Chen and co-workers[23,26] and Makhseed et al.[24] (see Section 1). However, capacity reported for Pc(1,4-DEB) belongs among the good published results for organic polymers.[30] Capacity found for Pc(2,6-DEN) is considerably lower than that for Pc(1,4-DEB), and capacity of Pc(2,6-DEA) is negligible.

3.4. Adsorption of Carbon Dioxide at 273–333 K

In the first step of the investigation, all the measurements were performed using standard equilibrium time interval of 5 s. Carbon dioxide adsorption/desorption isotherms on Pc(1,4-DEB) and Pc(2,6-DEN) displayed in Figure 8 and 9 were recorded at 273, 293, 313, and 333 K. With respect to a small adsorption ability, the maximum adsorption capacity of the sample Pc(2,6-DEA) was determined only at 273 K. It follows from the adsorption data that the adsorption capacity determined at 100 kPa and 273 K decreased in the order Pc(1,4-DEB) > Pc(2,6-DEN) > Pc(2,6-DEA) being 2.45 mmol g^{-1} (10.8 wt%) for Pc(1,4-DEB) and 0.30 mmol g^{-1}
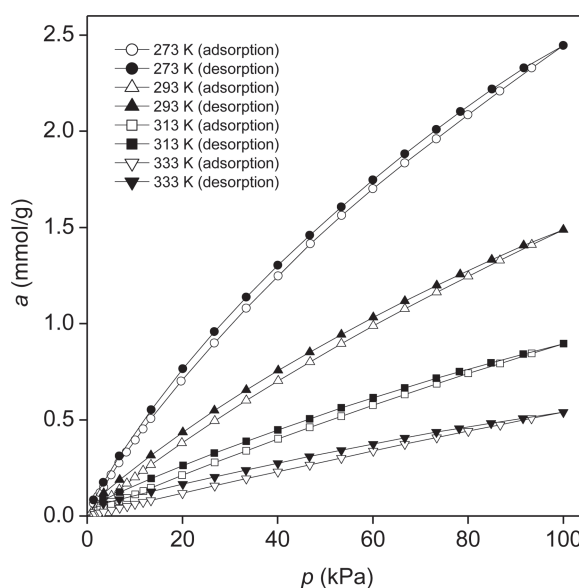

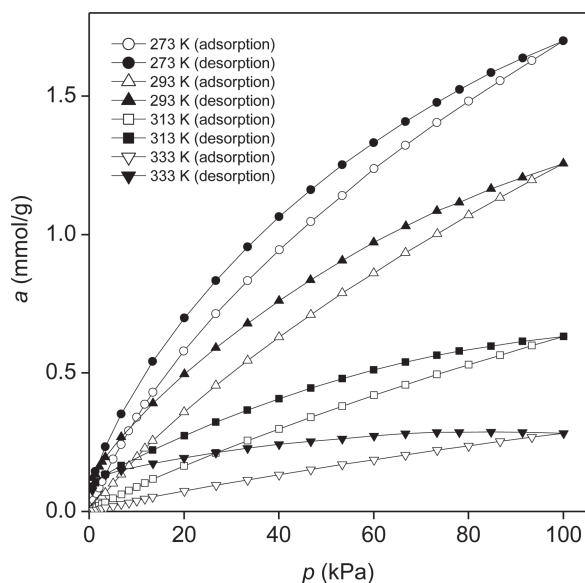**Figure 8.** CO_2 isotherms recorded on Pc(1,4-DEB) at 273, 293, 313, and 333 K.

Materials
Views
www.MaterialsViews.com

Macromol. Chem. Phys. **2013**, *214*, 2016–2026
© 2013 WILEY-VCH Verlag GmbH & Co. KGaA, Weinheim

Macromolecular
Journals

2023

Figure 9. CO_2 isotherms recorded on Pc(2,6-DEN) at 273, 293, 313, and 333 K.

Figure 10. CO_2 isotherms on Pc(1,4-DEB) at 333 K collected using equilibration time intervals of 5, 60, and 300 s.

(1.3 wt%) for Pc(2,6-DEA) (see Table 3). This decrease corresponds to the decrease of BET surface area and sorption capacity for nitrogen.

Temperature dependence of adsorption isotherms enabled us to evaluate isosteric heats, which provide information about the adsorbate–adsorbent interactions. As all isotherms show hysteresis down to low equilibrium pressures, the isosteric adsorption heats Q_{st} were calculated from adsorption branches according to the Clausius–Clapeyron equation

$$[\partial (\ln p)/\partial (1/T)]_a = -Q_{st}/R \tag{3}$$

where p is equilibrium pressure, T absolute temperature, and R universal gas constant. The values of Q_{st} evaluated for sample Pc(1,4-DEB) slightly decreased from 25.1 kJ mol^{-1} for the lowest amount adsorbed to 24.3 kJ mol^{-1} for CO_2 adsorption of 1.5 mmol g^{-1}. For the sample Pc(2,6-DEN), Q_{st} decreased from 27.3 to 26.5 kJ mol^{-1}. Contrary to this, isosteric adsorption heats of CO_2 on microporous inorganic adsorbents (such as zeolites) attain as much as 45–55 kJ mol^{-1} (Grajciar et al.[58]). Thus, it appears that isosteric adsorption heats indicate a weak interaction of CO_2 molecules with polycyclotrimers framework, which almost does not depend on the amount adsorbed.

In the second step of the investigation, carbon dioxide isotherms at temperatures 293 and 333 K were measured under equilibration time intervals of 60 and 300 s. Table 4 gives the overall times of the isotherm measurement and average times of equilibration per point for equilibrium time intervals of 5, 60, and 300 s. In contrast to the adsorption of nitrogen and hydrogen, the lengthening of measurement time had a striking effect
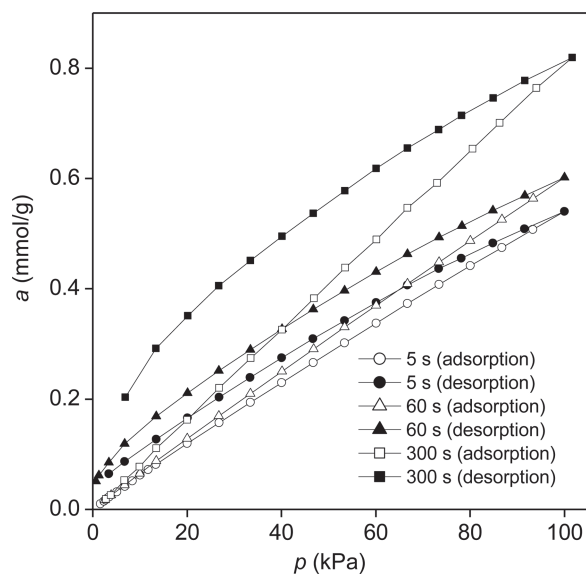
on the carbon dioxide adsorption. Isotherms at 333 K in Figure 10 and 11 show that increasing time of measurement results in increasing amounts of CO_2 adsorbed and in the broadening of the hysteresis loop. Maximum CO_2 adsorption capacities in Table 3 also markedly increase with increasing measurement time.

The CO_2 adsorption isotherms at 293 K under equilibrium time intervals of 5 and 300 s (Figure S10 and S11 in Supporting information and Table 3) show similar response to the lengthening time of measurements as
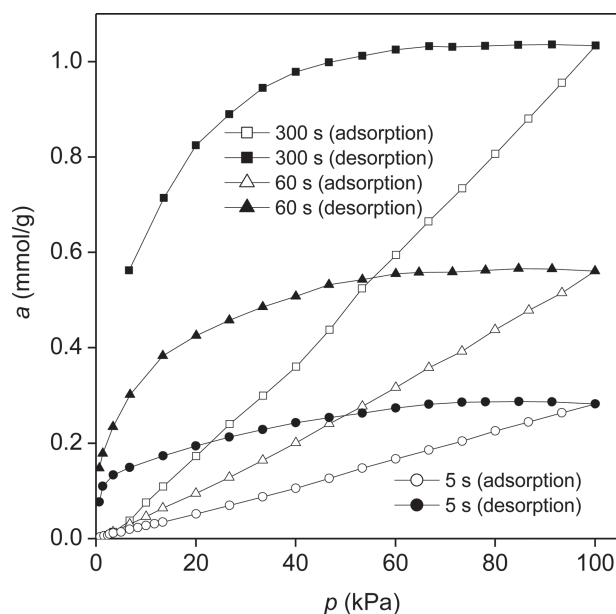

Figure 11. CO_2 isotherms on Pc(2,6-DEN) at 333 K collected using equilibration time intervals of 5, 60, and 300 s.

isotherms at 333 K. However, the influence of length of measurement time is less pronounced.

At temperatures applied for CO_2 adsorption the polycyclotrimers are softer than at 77 K applied for N_2 and H_2 measurement. We assume that the higher softness of Pc(1,4-DEB) and Pc(2,6-DEN) enhances their ability to dissolve CO_2 molecules. If lengthened time is given to the adsorption of carbon dioxide, an efficient utilization of dissolving ability of both polycyclotrimers takes place. The dissolving of CO_2 molecules and subsequent elastic deformation of polymer network may be the reason of the adsorption/desorption hysteresis similarly to the nitrogen adsorption/desorption. It follows from the inspection of Figure 10 and 11 that displayed isotherms have no tendency to approach some limit with prolongation of the measurement time.

In summary, it is necessary to state that hysteresis on carbon dioxide isotherms on siliceous mesoporous materials similar to the hysteresis on isotherms on polycyclotrimers were recently reported.[59] It appears that not only properties of the adsorbent but also properties of the carbon dioxide might be taken into consideration. Therefore, the mechanism of adsorption of carbon dioxide on the porous solids is worth of the further detailed study.

4. Conclusion

i. Hyperbranched partly cross-linked polyarylenes Pc(1,4-DEB), Pc(2,6-DEN), and Pc(2,6-DEA) were prepared in high or moderate yields by $TaCl_5/Ph_4Sn$ catalyzed polycyclotrimerization of corresponding diethynylarenes performed under mild conditions. The conversion of ethynyl groups and the relative content of branching points in prepared polymers decreased in the order Pc(1,4-DEB) > Pc(2,6-DEN) > Pc(2,6-DEA), that is, in parallel to the increasing number of condensed benzene rings in the arene core of monomers. The BET surface area and adsorption capacity were decreasing in the same order. The BET surface area attained 1299 m² g⁻¹ (micropore volume = 0.472 cm³ g⁻¹) for the sample Pc(1,4-DEB). The maximum hydrogen and CO_2 adsorption capacities of this sample were 1.26 wt% (100 kPa and 77 K) and 10.8 wt% (100 kPa and 273 K), respectively.

ii. Adsorption of nitrogen on Pc(1,4-DEB) and Pc(2,6-DEN) at 77 K was revealed to be a complex process that can be partly described by the dual-mode model in which Langmuir and Henry adsorption are assumed. Based on the nitrogen adsorption/desorption isotherms, it can be concluded that Pc(1,4-DEB) and Pc(2,6-DEN) contained permanent micropores. Besides the adsorption in permanent micropores, nitrogen penetrates through micropores into the polymer framework and dissolves in the polymer.

iii. The amount of CO_2 adsorbed on Pc(1,4-DEB) and Pc(2,6-DEN) at 293 or 333 K increased with increasing time

allotted to the experiment. We speculate that owing to the softness of the polymers at near to ambient temperature the enhanced dissolving ability can be assumed for Pc(1,4-DEB) and Pc(2,6-DEN). However, this ability can be efficiently utilized only if a prolonged time is provided to the adsorption process probably due to a slow penetration of CO_2 molecules into the polymers.

Supporting Information

Supporting Information is available from the Wiley Online Library or from the author.

[1] J. X. Jiang, A. I. Cooper, in *Functional Metal-Organic Frameworks: Gas Storage, Separation and Catalysis, Topics in Current Chemistry, Vol. 293* (Ed: M. Schroder), Springer, Berlin **2010**, p. 1.

[2] A. Thomas, P. Kuhn, J. Weber, M.-M. Titirici, M. Antonietti, *Macromol. Rapid. Commun.* **2009**, *30*, 221.

[3] F. Negri, N. Saendig, *Theor. Chem. Acc.* **2007**, *118*, 149.

[4] N. B. McKeown, P. M. Budd, D. Book, *Macromol. Rapid Commun.* **2007**, *28*, 995.

[5] J. Germain, F. Svec, J. M. J. Fréchet, *Chem. Mater.* **2008**, *20*, 7069.

[6] W. Lu, D. Yuan, D. Zhao, C. I. Schilling, O. Plietzsch, T. Muller, S. Bräse, J. Guenther, J. Blümel, R. Krishna, Z. Li, H.-C. Zhou, *Chem. Mater.* **2010**, *22*, 5964.

[7] H. Ren, T. Ben, E. Wang, X. Jing, M. Xue, B. Liu, Y. Cui, S. Qiu, G. Zhu, *Chem. Commun.* **2010**, *46*, 291.

[8] D. Yuan, W. Lu, D. Zhao, H.-C. Zhou, *Adv. Mater.* **2011**, *23*, 3723.

[9] R. Dawson, T. Ratvijitvech, M. Corker, A. Laybourn, Y. Z. Khimyak, A. I. Cooper, D. J. Adams, *Polym. Chem.* **2012**, *3*, 2034.

[10] D. Tan, W. Fan, W. Xiong, H. Sun, A. Li, W. Deng, C. Meng, *Eur. Polym. J.* **2012**, *48*, 705.

[11] Z. Xie, C. Wang, K. E. deKrafft, W. Lin, *J. Am. Chem. Soc.* **2011**, *133*, 2056.

[12] U. Stoeck, G. Nickerl, U. Burkhardt, I. Senkovska, S. Kaskel, *J. Am. Chem. Soc.* **2012**, *134*, 17335.

Materials
Views
www.MaterialsViews.com

Macromol. Chem. Phys. **2013**, *214*, 2016–2026
© 2013 WILEY-VCH Verlag GmbH & Co. KGaA, Weinheim

Macromolecular
Journals

2025

[13] J. Brandt, J. Schmidt, A. Thomas, J. D. Epping, J. Weber, *Polym. Chem.* **2011**, *2*, 1950.

[14] A. Patra, U. Scherf, *Chem. Eur. J.* **2012**, *18*, 10074.

[15] L. Chen, Y. Honsho, S. Seki, D. Jiang, *J. Am. Chem. Soc.* **2010**, *132*, 6742.

[16] W.-E. Lee, C.-L. Lee, T. Sakaguchi, M. Fujiki, G. Kwak, *Macromolecules* **2011**, *44*, 432.

[17] J.-Y. Lee, C. D. Wood, D. Bradshaw, M. J. Rosseinsky, A. I. Cooper, *Chem. Commun.* **2006**, 2670.

[18] N. B. McKeown, B. Ghanem, K. J. Msayib, P. M. Budd, C. E. Tattershall, K. Mahmood, S. Tan, D. Book, H. W. Langmi, A. Walton, *Angew. Chem. Int. Ed.* **2006**, *45*, 1804.

[19] J. Germain, J. Hradil, J. M. J. Fréchet, F. Svec, *Chem. Mater.* **2006**, *18*, 4430.

[20] J. Weber, M. Antonietti, A. Thomas, *Macromolecules* **2008**, *41*, 2880.

[21] S. Makhseed, J. Samuel, *Chem. Commun.* **2008**, 4342.

[22] Q. Chen, J.-X. Wang, F. Yang, D. Zhou, N. Bian, X.-J. Zhang, C.-G. Yan, B.-H. Han, *J. Mater. Chem.* **2011**, *21*, 13554.

[23] Q. Chen, J.-X. Wang, Q. Wang, N. Bian, Z.-H. Li, C.-G. Yan, B.-H. Han, *Macromolecules* **2011**, *44*, 7987.

[24] S. Makhseed, F. Ibrahim, J. Samuel, *Polymer* **2012**, *53*, 2964.

[25] J. R. Holst, E. Stöckel, D. J. Adams, A. I. Cooper, *Macromolecules* **2010**, *43*, 8531.

[26] Q. Chen, M. Luo, P. Hammershøj, D. Zhou, Y. Han, B. W. Laursen, C.-G. Yan, B.-H. Han, *J. Am. Chem. Soc.* **2012**, *134*, 6084.

[27] J.-X. Jiang, F. Su, H. Niu, H. C. D. Wood, N. L. Campbell, Y. Z. Khimyak, A. I. Cooper, *Chem. Commun.* **2008**, 486.

[28] X. Jiang, F. Su, A. Trewin, C. D. Wood, N. L. Campbell, H. Niu, C. Dickinson, A. Y. Ganin, M. J. Rosseinsky, Y. Z. Khimyak, A. I. Cooper, *Angew. Chem. Int. Ed.* **2007**, *46*, 8574.

[29] V. Hanková, E. Slováková, J. Zedník, J. Vohlídal, R. Sivkova, H. Balcar, A. Zukal, J. Brus, J. Sedláček, *Macromol. Rapid Commun.* **2012**, *33*, 158.

[30] S. Yuan, B. Dorney, D. White, S. Kirklin, P. Zapol, L. Yu, D.-J. Liu, *Chem. Commun.* **2010**, *46*, 4547.

[31] Z. Wang, S. Yuan, A. Mason, B. Reprogle, D.-J. Liu, L. Yu, *Macromolecules* **2012**, *45*, 7413.

[32] L. Ma, M. M. Wanderley, W. Lin, *ACS Catal.* **2011**, *1*, 691.

[33] S. Yuan, S. Kirklin, B. Dorney, D.-J. Liu, L. Yu, *Macromolecules* **2009**, *42*, 1554.

[34] K. Xu, H. Peng, Q. Sun, Y. Dong, F. Salhi, J. Luo, J. Chen, Y. Huang, D. Zhang, Z. Xu, B. Z. Tang, *Macromolecules* **2002**, *35*, 5821.

[35] M. Häußler, B. Z. Tang, *Adv. Polym. Sci.* **2007**, *209*, 1.

[36] T. Masuda, T. Higashimura, *Adv. Polym. Sci.* **1986**, *81*, 121.

[37] M. Shiotsuki, F. Sanda, T. Masuda, *Polym. Chem.* **2011**, *2*, 1044.

[38] K. Nagai, T. Masuda, T. Nakagawa, B. D. Freeman, I. Pinnau, *Prog. Polym. Sci.* **2001**, *26*, 721.

[39] Z. Duchoslavová, R. Sivkova, V. Hanková, J. Sedláček, J. Svoboda, J. Vohlídal, J. Zedník, *Macromol. Chem. Phys.* **2011**, *212*, 1802.

[40] T. Masuda, T. Mouri, T. Higashimura, *Bull. Chem. Soc. Jpn.* **1980**, *53*, 1152.

[41] P. Štěpnička, I. Císařová, J. Sedláček, J. Vohlídal, M. Polášek, *Collect. Czech. Chem. Commun.* **1997**, *62*, 1577.

[42] N. B. McKeown, P. M. Budd, *Chem. Soc. Rev.* **2006**, *35*, 675.

[43] A. V. Maffei, P. M. Budd, N. B. McKeown, *Langmuir* **2006**, *22*, 4225.

[44] J. Weber, Q. Su, M. Antonietti, A. Thomas, *Macromol. Rapid Commun.* **2007**, *28*, 1871.

[45] N. Ritter, M. Antonietti, A. Thomas, I. Senkovska, S. Kaskel, J. Weber, *Macromolecules* **2009**, *42*, 8017–8020.

[46] J. Jeromenok, W. Bölmann, M. Antonietti, J. Weber, *Macromol. Rapid Commun.* **2011**, *32*, 1846.

[47] N. Ritter, I. Senkovska, S. Kaskel, J. Weber, *Macromol. Rapid Commun.* **2011**, *32*, 438.

[48] N. Ritter, I. Senkovska, S. Kaskel, J. Weber, *Macromolecules* **2011**, *44*, 2025.

[49] J. Weber, J. Schmidt, A. Thomas, W. Böhlmann, *Langmuir* **2010**, *26*, 15650.

[50] Y. Tsujita, *Prog. Polym. Sci.* **2003**, *28*, 1377.

[51] J. Gao, T. A. Barbari, *Macromolecules* **2009**, *42*, 5700.

[52] B. Ghanem, N. McKeown, P. Budd, J. Selbie, D. Fritsch, *Adv. Mater.* **2008**, *20*, 2766.

[53] K. I. Sumiya, G. Kwak, F. Sanda, T Masuda, *J. Polym. Sci. Polym. Chem.* **2004**, *42*, 2774.

[54] Y. Sagara, S. Yamane, T. Mutai, K. Araki, T. Kato, *Adv. Funct. Mater.* **2009**, *19*, 1869.

[55] J. Brus, *Solid State Nucl. Magn. Reson.* **2000**, *16*, 151.

[56] Z. Dong, Z. Ye, *Macromolecules* **2012**, *45*, 5020.

[57] S. Lowell, J. E. Shields, M. A. Thomas, M. Thommes, *Characterization of Porous Solids and Powders: Surface Area, Pore Size and Density*, Kluwer, Dordrecht, The Netherlands **2004**, p. 121.

[58] L. Grajciar, J. Čejka, A. Zukal, C.O. Areán, G. T. Palomino, P. Nachtigall, *ChemSusChem* **2012**, *5*, 2011.

[59] H. Zhao, W. Yan, Z. Bian, J. Hu, H. Liu, *Solid State Sci.* **2012**, *14*, 250.

Supporting Information

Polycyclotrimers of 1,4-Diethynylbenzene, 2,6-
Diethynylnaphthalene, and 2,6-Diethynylanthracene:
Preparation and Gas Adsorption Properties
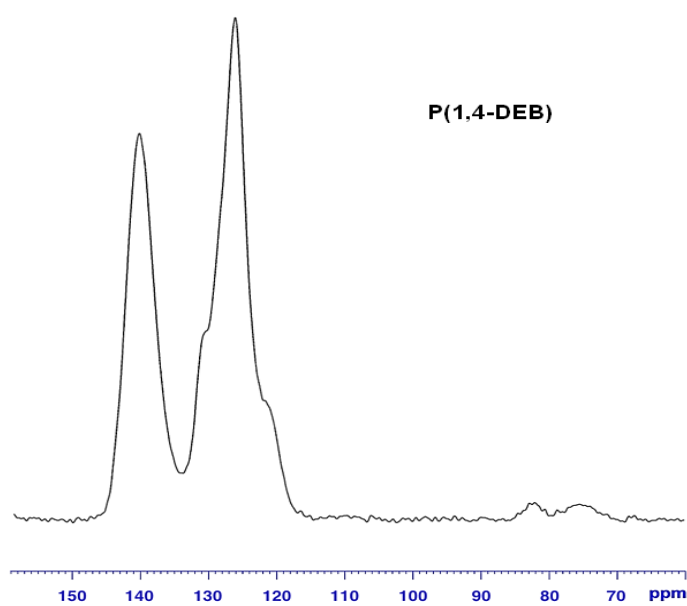
Arnošt Zukal,* Eva Slováková, Hynek Balcar, Jan Sedláček

Supporting Information

for *Macromol. Chem. Phys.* DOI: 10.1002/macp.201300317

Polycyclotrimers of 1,4-diethynylbenzene, 2,6-diethynylnaphthalene and 2,6-diethynylanthracene: preparation and gas adsorption properties

Arnošt Zukal[*], Eva Slováková, Hynek Balcar, Jan Sedláček

Figure S1. CP/MAS ^{13}C NMR spectrum of Pc(1,4-DEB).
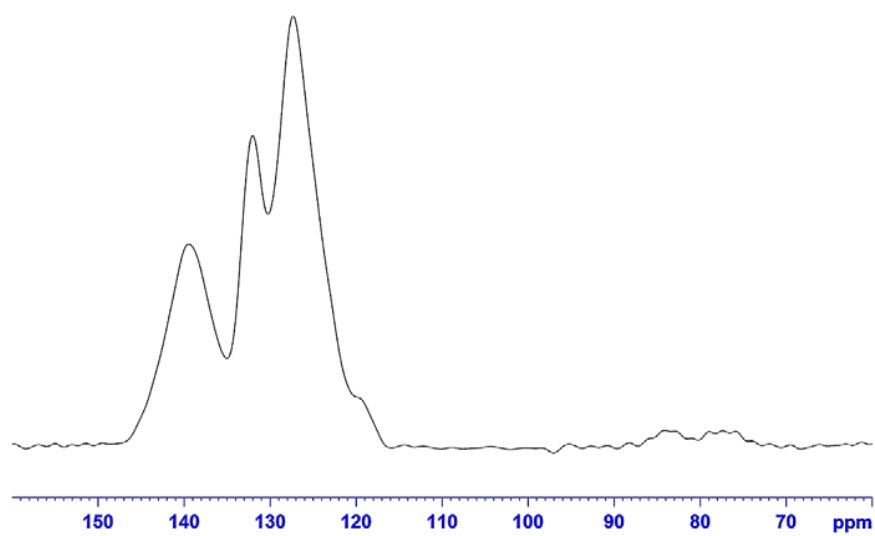
Figure S2. CP/MAS ^{13}C NMR spectrum of Pc(2,6-DEN).
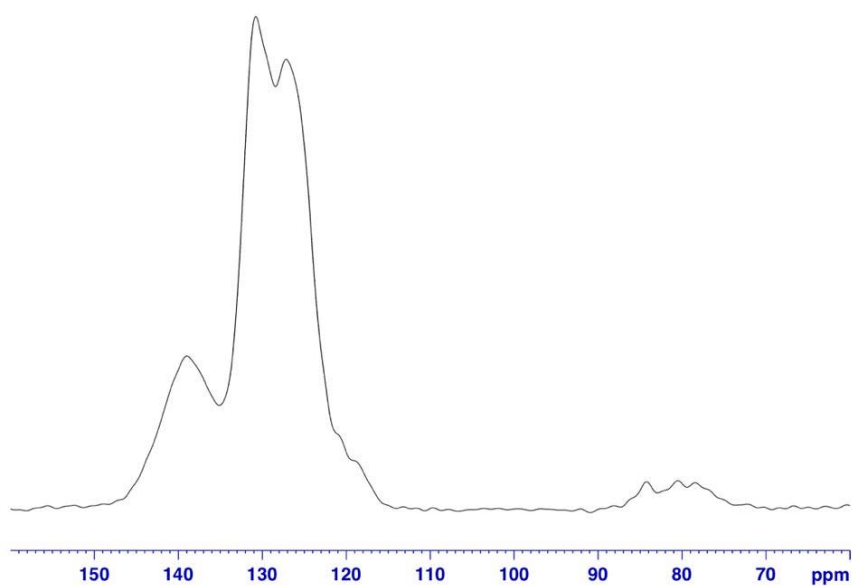
Figure S3. CP/MAS ^{13}C NMR spectrum of Pc(2,6-DEA).
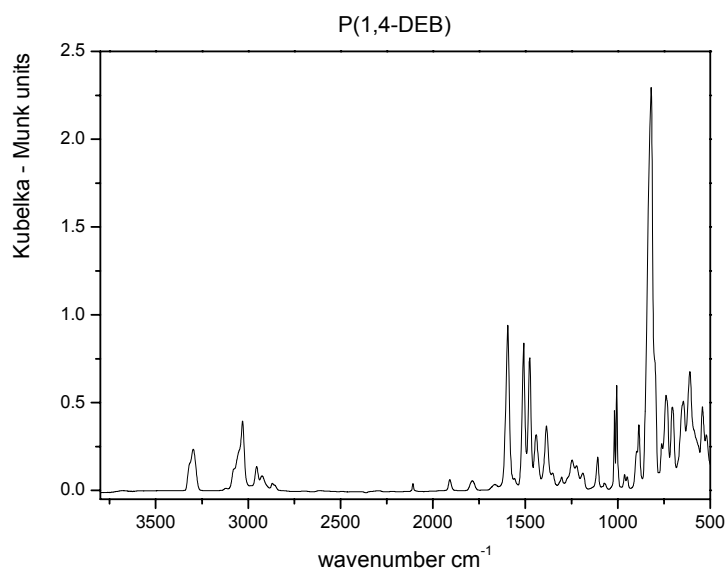
Figure S4. FTIR spectrum of Pc(1,4-DEB).
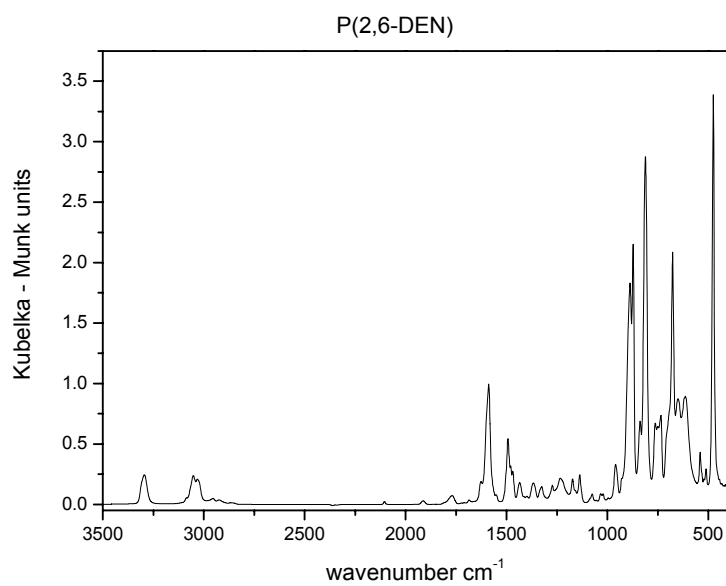
Figure S5. FTIR spectrum of Pc(2,6-DEN).
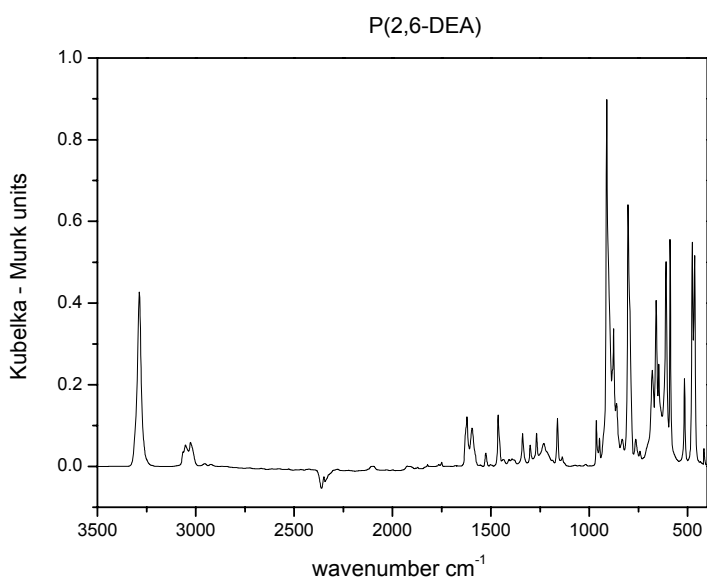
Figure S6. FTIR spectrum of Pc(2,6-DEA).

Derivation of Equation 1:

Derivation of the Equation 1 by which conversion of terminal ethynyls achieved due to the incorporation of diethynylarene molecules into polycyclotrimer (labeled as ξ) is calculated from ^{13}C CP/MAS NMR spectra of polycyclotrimers. The integral intensities of signals of sp^2 and sp carbons in ^{13}C CP/MAS NMR spectra of polycyclotrimers were labelled as A_{sp2} and A_{sp}, respectively. The average number of sp^2 carbons per one monomeric moiety inbuilt into the polycyclotrimer was labelled as N_{sp2}. The average number of remaining, i.e. non-transformed sp carbons per one monomeric moiety inbuilt into the polycyclotrimer was labelled as N_{sp}. The following relation exists between A_{sp2}, A_{sp}, N_{sp2} and N_{sp}.

$$N_{sp}/N_{sp2} = A_{sp}/A_{sp2} \qquad (S1)$$

There are two contributions to N_{sp2} value: (i) number of sp^2 carbons originally present in the monomer molecule and (ii) average number of sp^2 carbon newly formed from sp carbons by incorporation of a monomer molecule into polycyclotrimer. The first contribution was labelled as N_{ArM} and its values are as follows: $N_{ArM} = 6$ (for 1,4-DEB), $N_{ArM} = 10$ (for 2,6-DEN) and $N_{ArM} = 14$ (for 2,6-DEA). The second contribution is given by term: ($4-N_{sp}$). Number of 4 in the last term originated from the fact that each monomer molecule contained (before polycyclotrimerization) four sp carbons.
Thus, Equation S1 can be modified:

$$N_{sp}/(N_{ArM} + 4 - N_{sp}) = A_{sp}/A_{sp2} \qquad (S2)$$

N_{sp} is expressed from Equation S2 as follows:

$$N_{sp} = (A_{sp}N_{ArM} + 4A_{sp})/(A_{sp} + A_{sp2}) \qquad (S3)$$

- 6 -

Conversion of terminal ethynyls achieved due to the incorporation of a monomer molecule into polycyclotrimer, ξ, can be expressed as follows:

$$\xi = (4 - N_{sp})/4 \qquad (S4)$$

Substitution for N_{sp} from Equation S3 into Equation S4 gives ξ as a function of experimentally determined parameters A_{sp2} and A_{sp} and constant N_{ArM}:

$$\xi = (4A_{sp2} - A_{sp}N_{ArM})/(4A_{sp2} - + 4A_{sp}) \qquad (S5)$$

Equation S5 is given as Equation 1 in the main text.

Table S1. Degree of conversion of ethynyl groups in polycyclotrimerization of diethynylarenes into one hyperbranched polycyclotrimer macromolecule. Polycyclotrimerization proceeds entirely by E_P2E_M mode

Number of monomer molecules inbuilt in a polycyclotrimer macromolecule	Number of ethynyls in monomer molecules before polycyclotrimerization	Number of ethynyls converted during polycyclotrimerization	Number of nonreacted ethynyls present in a polycyclotrimer macromolecule	Degree of conversion of ethynyls - ξ
1	2	0	2	0
3	6	3	3	0.5
5	10	6	4	0.6
7	14	9	5	0.643
9	18	12	6	0.667
11	22	15	7	0.682
13	26	18	8	0.692
N	**2N**	**1.5(N-1)**	**0.5(N+3)**	**1.5(N-1)/2N**
→∞	→∞	→∞	→∞	**0.75**

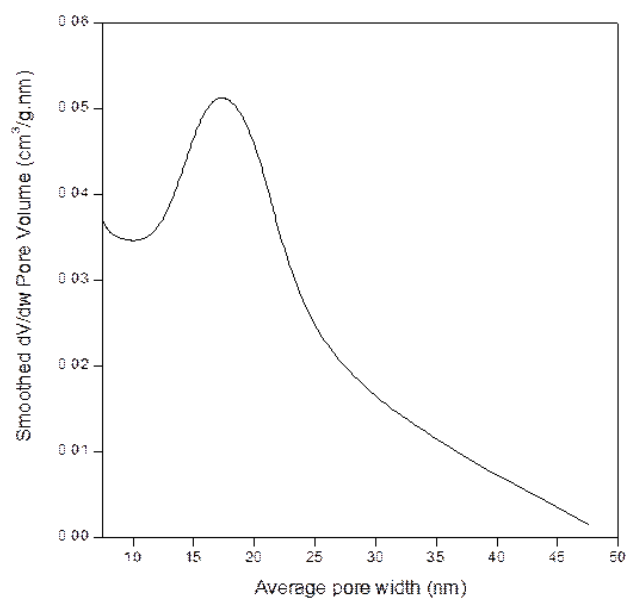Scheme S1. Growing modes in diethynylarenes polycyclotrimerization.
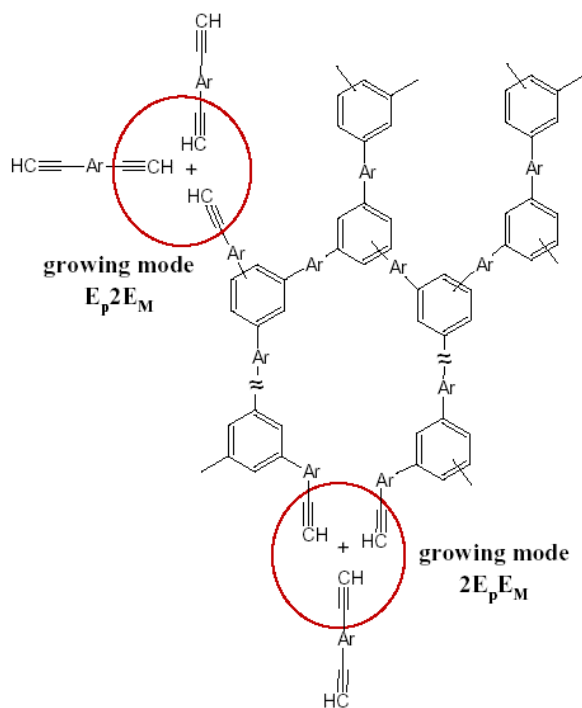
Figure S7. Mesopore size distribution of the sample Pc(1,4-DEB) calculated from the desorption branch of nitrogen isotherm. (The BJH method was used.)
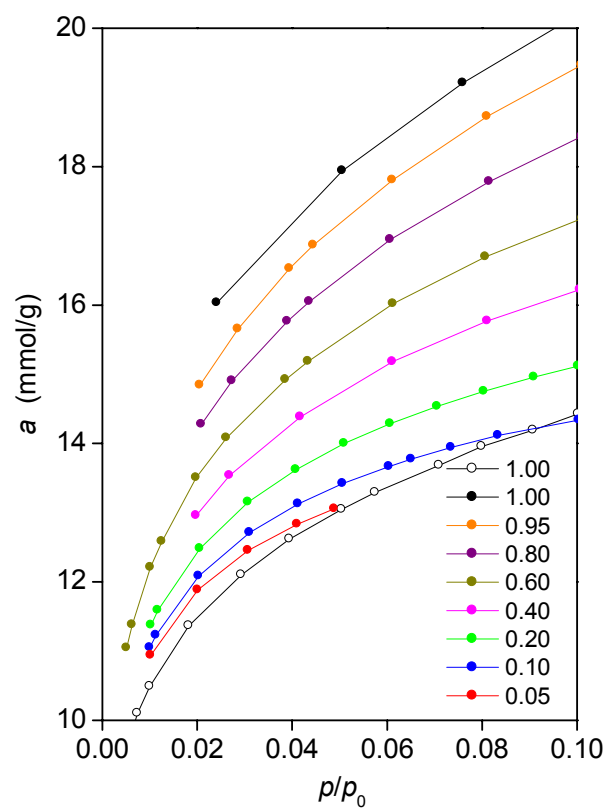
Figure S8. Low pressure region of nitrogen isotherm at 77 K and desorption scans (solid points) for Pc(1,4-DEB). The inset gives the pressures corresponding to the starting points of desorption scans.
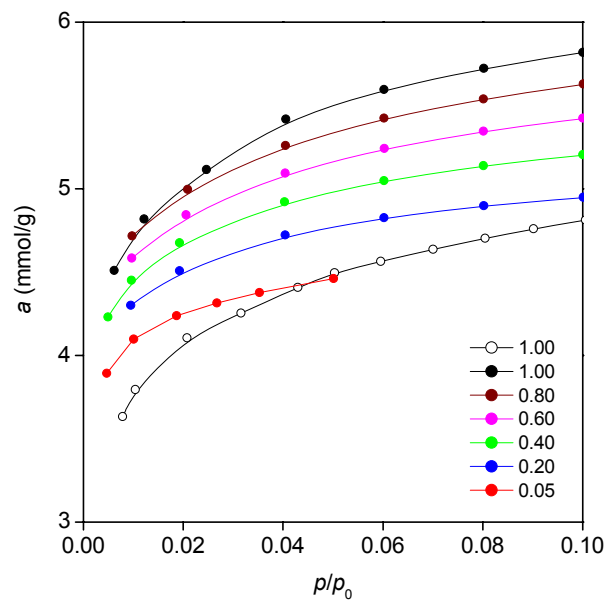
Figure S9. Low pressure region of nitrogen isotherm at 77 K and desorption scans (solid points) for Pc(2,6-DEN). The inset gives the pressures corresponding to the starting points of desorption scans.
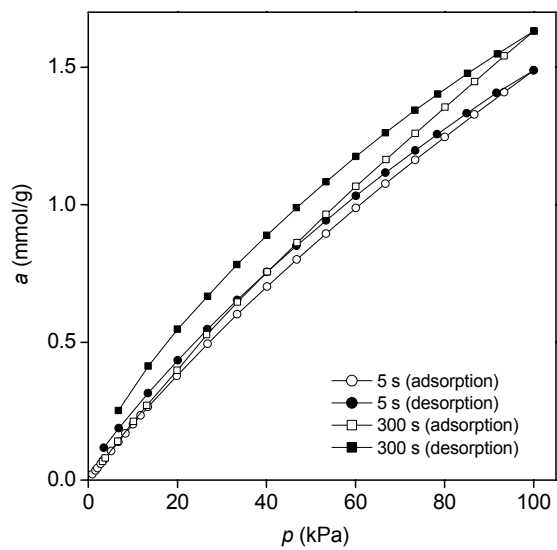
Figure S10. CO$_2$ isotherms on Pc(1,4-DEB) at 293 K collected using equilibration time intervals of 5 s and 300 s.
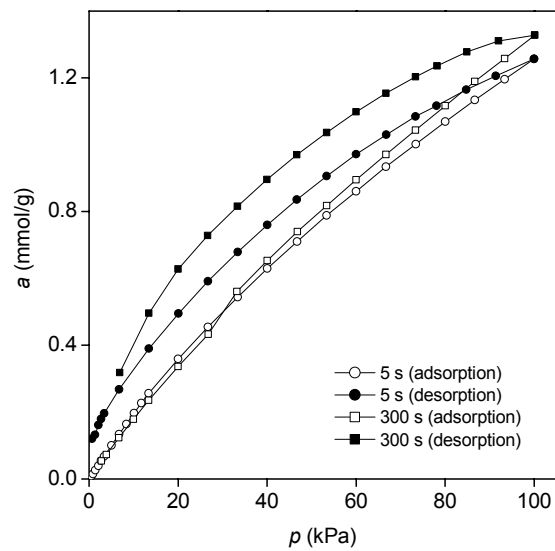
Figure S11. CO_2 isotherms on Pc(2,6-DEN) at 293 K collected using equilibration time intervals of 5 s and 300 s.